12-2015

Effects of Complex Formation of DNA with Positively Charged Polyamines and Polypeptides on the Products of Oxidative Damage to DNA 2-Deoxyribose by Hydroxyl Radicals

Modeste N. Tegomoh
East Tennessee State University

Effects of Complex Formation of DNA with Positively Charged Polyamines and Polypeptides on the Products of Oxidative Damage to DNA 2-Deoxyribose by Hydroxyl Radicals

---

A thesis

presented to

the Faculty of the Department of Chemistry

East Tennessee State University

In partial fulfillment

of the requirements for the degree

Master of Science in Chemistry

---

by

Modeste N'neckmdem Tegomoh

December 2015

Dr. Marina Roginskaya, Chair

Dr. Scott Kirkby

Dr. David Close

Keywords: DNA damage, oxidative stress, reactive oxygen species, hydroxyl radicals, DNA protection

ABSTRACT

Effects of Complex Formation of DNA with Positively Charged Polyamines and Polypeptides on the Products of Oxidative Damage to DNA 2-Deoxyribose by Hydroxyl Radicals

by

Modeste N'neckmdem Tegomoh

It is known that histones and other DNA-binding polycations protect DNA from radiation damage mediated by hydroxyl radicals. Until recently, this protection of DNA has mainly been attributed to compaction and aggregation. It was hypothesized that chemical repair of DNA sugar radicals by donation of hydrogen atom from polycations also significantly contributes to DNA protection. To test this hypothesis, the relative yields of low-molecular weight characteristic products of oxidation of DNA sugar were compared in X-irradiated samples of naked DNA and DNA complexes with a number of polycations by using an HPLC-based method of DNA damage product quantification. The variation in the percent contribution of the C1„ sugar damage product ongoing from free DNA to DNA-polycations complexes is in agreement with the hypothesis that chemical repair of DNA sugar radicals by donation of hydrogen atom from polycations contributes to the overall DNA protection against hydroxyl radical-mediated damage.

DEDICATION

To my mother, Emilia M. Forlemu, the rest of my family, and to the people in the world struggling to find a meaning in their life.

ACKNOWLEDMENTS

I am immensely grateful to my supervisor, Dr. Marina Roginskaya for accepting me into her research group and her unceasing guidance during this research project. I will also like to thank Dr. Scott Kirkby and Dr. David Close for being part of my advisory committee. My sincere gratitude goes to Dr. David Close and Dr. Yuriy Razskazovskiy for allowing me to use their lab space and to Dr. Yuriy Razskazovskiy for his great guidance during this research work.

Thank you to Dr. Scott Kirkby for making me see the best in me, inspiring me to be a better chemist, and for organizing the research scrum to build better confidence for better presentations in all the graduate students at the Chemistry Department at ETSU. Many thanks to all the faculty and staff of the Chemistry Department for sharing their wisdom with me. I will also like to thank Dr. Cassandra Eagle, Mr. Ryan Alexander, Ms. Jillian Quirante, Mr. Justin Pritchard and the International Office for their great advice and everything they did or do to help the Department of Chemistry run smoothly. Thanks to Mr. Josh Moore and Mr. Derrick Ampadu-Boateng for their great help as lab mates.

I will also thank all my family, friends, and all the students of the Chemistry Department for their great support.

TABLE OF CONTENTS

Page

LIST OF TABLES

Table Page

LIST OF FIGURES

Figures Page

LIST OF ABBREVIATIONS

5,„-Ald ..... 5,„-aldehyde

ARP ..... aldehyde-reactive probe

bp..... base pair

dL 2-deoxyribonolactone

DNA ..... deoxyribonucleic acid

FapyG 2,6-diamino-4-hydroxy-5-formamidopyrimidine

DSB..... double-strand break

dsDNA ..... double-stranded DNA

EA ..... ethanolamine

FBR ..... free base release

Fur..... furfural

GC-MS..... gas chromatograph –mass spectroscopy

Gy ..... gray

MDA ..... malondialdehyde

5-MF 5-methylenefuran-2-one

NCP..... nucleosome core particle

NHE ..... normal hydrogen electrode

Lac .....N-substituted 5-methylene-” ^{3}-pyrrolin-2-ones

ODC ..... ornithine decarboxylase

C4,„-OASC..... 4,„-oxidized abasic site

8oxoG 8-oxo-7,8-dihydroguanine

PCA..... positively charged polyamine

PCP ..... positively charged polypeptide

polyLys ..... poly-L-lysine

poly(Lys, Tyr) ..... polylysinetyrosine

PICA ..... positively charged polyamines induce compaction and aggregation

PDA ..... prominent diode array detector

SDP ..... sugar damage products

SSB ..... single strand break

ROS ..... reactive oxygen species

CHAPTER 1

INTRODUCTION

Oxidative Stress and DNA

In aerobic organisms, one of the most deleterious side effects of oxygenation is the oxidation of important macromolecules. To some level, the oxidation of these molecules is important to promote signaling processes which are necessary for the wellbeing of the organism. However, the over-production of species capable of oxidizing biomolecules can be defined as a stage of oxidative stress. This oxidative stress may occur as a result of exogenous and/or endogenous factors such as UV light[1], ionizing radiation[2,3], and environmental pollution.[4] The most common oxidizing species are the reactive oxygen species (ROS) which are usually free radical in nature. ROS including hydroxyl radicals ($^{\cdot}OH$), hydrogen peroxide (H_2O_2), superoxide radicals ($O_2^{\cdot -}$), peroxynitrite ($ONOO^-$), and nitric oxide (NO) have been shown to be implicated in a number of pathologies such as inflammatory diseases, ischemia and reperfusion[5,6], neurodegenerative diseases (like Huntington's disease[4] and Alzheimer's disease[4,7]), cancers[8], stroke[9], respiratory diseases[10], and aging processes.[8]

In this area of research, of all the biomolecules subjected to oxidative stress, deoxyribonucleic acid (DNA) as the major hereditary unit is the most widely studied. The interaction of DNA with ROS may lead to multitudes of oxidative modifications in DNA including damage to the deoxyribose moiety of the sugar-phosphate backbone of the DNA double helix, nucleobase modifications within the DNA sequence, single- and double-strand breaks (SSB and DSB, respectively), DNA interstrand crosslinks, and DNA-protein crosslinks.[8] These modifications in DNA are usually easily repaired by cells under normal metabolic

processes, but during oxidative stress, repair mechanisms are unable to cope with the volume of lesions and some are left unrepaired. Other types of DNA lesions such as clustered lesions are repaired slowly or irreparable. These types of DNA lesions usually consist of two or more closely spaced strand breaks, abasic sites, or oxidized bases on opposing strands. The accumulation of these leftover lesions and irreparable lesions (clustered DNA lesions) may lead to the development of the disease conditions listed above. For example, in the specific case of cancers, these unrepaired lesions in DNA are believed to be the precursor to oncogene activation and tumor-suppressor gene inactivation, resulting in uncontrolled cellular growth (tumorigenesis).[11]

Ionizing Radiation as an Important Source of Oxidative Stress

Radiation with a photon energy of more than 1216 kJ/mol (equal to the ionization of the water molecule) is, by definition, referred to as ionizing radiation. The two major events that usually occur when ionizing radiation interacts with matter are ionization and electronic excitation. When a molecule M is ionized, an electron is removed and as a result, a positively charged radical cation is formed:

$$M + h\nu \rightarrow M^{\cdot +} + e^{-} \qquad (1.1)$$

On the other hand, excitation is observed when ionizing radiation promotes an electron from an occupied orbital to an empty higher energy orbital:

$$M + h\nu \rightarrow M^{*} \qquad (1.2)$$

Ionizing radiation is one of the most important sources of oxidative stress in biological systems. The ionization of water molecules or biomolecules is capable of producing oxidative species including ROS which can induce oxidative damage in living cells[2]. Ionizing radiation has always

been a part of the human environment. In addition to natural radiation sources present in the Earth's crust, cosmic and solar radiation; man-made sources also contribute to our unceasing exposure to radiation.

Basic Mechanisms of Oxidative Damage to DNA by Ionizing Radiation

Traditionally, two types of radiation damage to DNA are recognized: the direct type of damage which involves the direct ionization of DNA by ionizing radiation or the transfer of electrons or holes to DNA from the DNA's solvation shell, and the indirect type of damage which involves the interaction of DNA with radicals produced by ionization of water molecules or biomolecules in the surrounding medium. In model systems of aqueous solutions of DNA, like the one we used in this research work, the DNA in solution is surrounded by water molecules and the indirect effect dominates significantly over the direct effect. Hydroxyl radicals, $^{\bullet}OH$, formed by water radiolysis are the major contributors to the indirect oxidative damage to DNA in aqueous solutions. However, in biological systems, the nucleus matrix is made of different organic molecules that are able to scavenge the hydroxyl radicals produced by ionizing radiation and therefore to reduce the indirect effect. Despite this scavenging effect, the indirect effect is estimated to contribute to about 60% of total DNA damage *in vivo*, with the direct effect contributing about 40%.[12]

Direct Type Damage

Direct damage of ionizing radiation to DNA has been studied in dry samples of DNA.[13-15] Dry DNA still contains some water molecules in its solvation shell. The solvation shell of DNA consists of about 22 water molecules per nucleotide. Approximately 2.5 water molecules per

DNA nucleotide are very tightly bound to DNA and are not removable even upon harsh conditions.[13] DNA hydration, Γ, is evaluated as the number of water molecules per DNA nucleotide. Basically, one cannot detect $^{\bullet}OH$ radicals at low DNA hydrations (Γ<8).[14] This means that in the first step of ionization, the hole produced in the DNA solvation shell transfers to DNA. It is not possible to distinguish the products of DNA damage resulting from hole transfer from the solvation shell and those resulting from the direct ionization of DNA. For that reason, the direct-type of damage is usually considered to arise from direct ionization of DNA or from the transfer of holes and electrons from the DNA solvation shell. It is therefore necessary to view DNA and its solvation shell as a single target. This general idea can be described by the equations below:

$$DNA + h\nu \rightarrow DNA^{\bullet +} + e^{-} \quad (1.3)$$

$$DNA + e^{-} \rightarrow DNA^{\bullet} \quad (1.4)$$

The direct-type of damage to DNA is not as widely studied as the indirect type damage partially due to the difficulties of creating adequate model systems.

Indirect Type Damage

Because water constitutes about 70-90% of tissues by weight, the indirect effect is generally described by the following equations:

$$H_2O + h\nu \rightarrow H_2O^{\bullet +} + e^{-} \text{ (ionization)} \quad (1.5)$$

$$H_2O + h\nu \rightarrow H_2O^{*} \text{ (excitation)} \quad (1.6)$$

$$H_2O^{\bullet +} + H_2O \rightarrow H_3O^{+} + {}^{\bullet}OH \quad (1.7)$$

$$H_2O^{*} \rightarrow H^{\bullet} + {}^{\bullet}OH \quad (1.8)$$

$${}^{\bullet}OH + {}^{\bullet}OH \rightarrow H_2O_2 \quad (1.9)$$

$$H^{\cdot} + O_2 \rightarrow HO_2^{\cdot} \quad (1.10)$$

$$HO_2^{\cdot} \rightarrow H^+ + O_2^{\cdot -} \quad (1.11)$$

The hydroxyl radicals, hydrogen peroxide (H_2O_2), and the superoxide radical anions ($O_2^{\cdot -}$) produced here all contribute to the oxidative stress of DNA and therefore constitute the indirect type of DNA damage by ionizing radiation. The electrons produced can interact with the DNA creating a one-electron-gain center. Actually, both direct and indirect effects of ionizing radiation produce a population of electron-gain (or one-electron reduced) and electron-loss (one electron-oxidized) centers that undergo rapid chemical transformation due to their instability and produce stable lesions. These stable lesions are further processed by cellular defense mechanisms. In this research study, hydroxyl radicals were used as the major oxidizing agent.

The Hydroxyl Radical

The hydroxyl radical is a very powerful oxidizing species, with the reduction potential of the couple $^{\cdot}OH, H^+/H_2O$ equal to 2.73 V.[16] As already stated above, this chemical species is generated through the radiolysis of water, which is initiated by the excitation or ionization of water (Reactions 1.5 and 1.6).[17]

The water radical cation ($H_2O^{\cdot +}$) is a strong acid and can therefore rapidly lose a proton to produce $^{\cdot}OH$ radical and the proton will be hydrated to form H_3O^+ (Reaction 1.8). The excited water molecule may undergo a homolytic bond cleavage to yield $H^{\cdot}$ and $^{\cdot}OH$ radicals (Reaction 1.9). The hydroxyl radicals once produced, can react immidiately with species located in close proximity to their zone of production, with the rate of difusion being the rate limiting step in most cases. The rate constant for the reaction of hydroxyl radicals with the sugar

molecule, glucose, has been determined to be 1.5 x 10^9 $M^{-1}s^{-1}$ at pH 7.5[18], which approaches the generally accepted average diffusion rate constant of 10^{10} $M^{-1}s^{-1}$, confirming the idea that this radical is so reactive that it will react with species immediately upon coming into contact with them. Three major reaction types for ·OH are known:[17]

1. The first type of reaction is addition to double bonds: The ·OH is electrophilic and can undergo addition reactions with unsaturated bonds, including C=C and C=N. In the specific case of DNA, the addition reactions of hydroxyl radicals occur primarily with unsaturated double bonds of the nucleobases. An example of such a reaction is that culminating in the formation of 8-oxo-7-8-dihydroguanine (8-oxoG) which will be discussed in detail below. A general reaction scheme illustrating the addition reaction of ·OH with a double bond is shown in Figure 1.

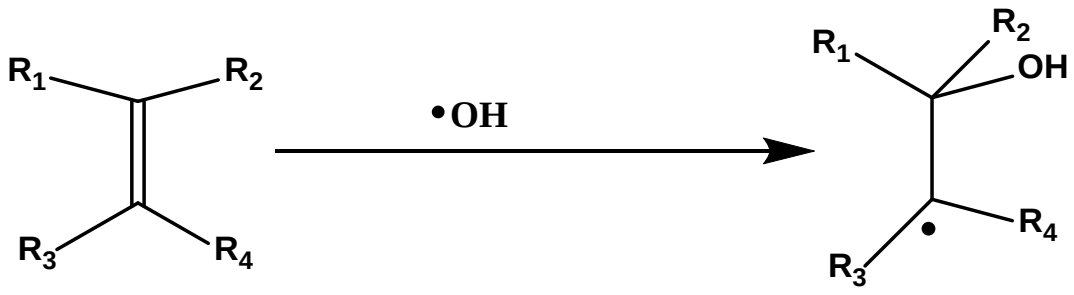

Figure 1: Electrophilic addition reaction of ·OH to a double bond

This reaction is the most preferred reaction path of ·OH due to its electrophilic nature.

2. The second reaction type of ·OH is hydrogen abstraction: This is the second most important type of reaction involving ·OH. This is the abstraction of a H-atom from a given species to form water, this process is very thermodynamically favorable because of strong O-H bonds in the water molecule. For the specific case of DNA, the H-atom is abstracted from the 2-deoxyribose, creating a 2-deoxyribosyl radical in

DNA. This reaction type of $^{\cdot}OH$ with DNA is the focus of this research and will be discussed further in subsequent sections. The general reaction scheme illustrating the H-abstraction mechanism of $^{\cdot}OH$ with any given species is shown in Figure 2.

Figure 2: The mechanism of H-abstraction by $^{\cdot}OH$

3. The last type of reaction $^{\cdot}OH$ can undergo is electron transfer: despite its high reduction potential ($E[^{\cdot}OH, H^{+}/H_2O] = 2.79$ V[16]), direct electron transfer is rarely observed in $^{\cdot}OH$-reactions, and where it does occurs, intermediate complexes are likely to be involved. Therefore, in most $^{\cdot}OH$-induced oxidations, short-lived adducts must be considered as intermediates. In the specific case of DNA, this involves the oxidation of nucleobases (specifically guanine). It is therefore evident that $^{\cdot}OH$ cannot be directly used for the study of one-electron oxidation reactions.

Types of Oxidative Damage to DNA: Sugar and Base Damage

The interaction of DNA with ROS can cause damage in DNA at the level of the 2-deoxyribose moiety (sugar damage) or at the level of the nucleobase moiety (base damage). It is commonly believed that sugar damage contributes for about 1/3 of the total DNA damage while the base damage contributes the remaining 2/3 of the total damage.[19] Sugar damage is usually related to SSBs and DSBs, and these types of damage have been generally accepted as important biomarkers for cellular DNA damage[8]. SSBs and DSBs are also considered to be mutagenic in

nature due to the possibility of base deletion, which can easily happen during natural repair processes like non-homologous recombination[8,9].

DNA Base Damage

Nucleobases are more prone to oxidative damage compared to the 2-deoxyribose moiety due to their lower reduction potential. These oxidative base lesions can occur through the direct and/or indirect effect of ionizing radiation, and whatever pathway taken, guanine is the most affected due to its lowest reduction potential. The table below summarizes the standard reduction potentials of DNA nucleosides, reported by Steenken *et al.*[20] where E^0 values are reported at pH 7 versus the normal hydrogen electrode (NHE).[20]

Table 1: The Standard Reduction Potentials for DNA Nucleosides[20]

DNA nucleosides	**E^0, V**
Adenosine	1.42
Guanosine	1.29
Thymidine	1.7
Cytosine	1.6

As follows from the table above, oxidative base lesion occurs primarily on guanosine, leading to a one-electron oxidation intermediate guanosine radical cation ($Gua^{Ï\,+}$ or $G^{Ï\,+}$) and the positive

charges introduced in DNA by this process are commonly referred to as holes.[22] The $G^{\ddot{I}+}$ is a stronger acid (pKa = 3.9, experimental; and 3.6, calculated[23]) than G itself (pKa= 9.5[24]) and at physiological pH, it quickly ($k \sim 2.0 \times 10^6\ s^{-1}$ [25]) undergoes deprotonation to form $G(N_1\text{-}H)^{\ddot{I}}$ or simply $G^{\ddot{I}}$. The $G^{\ddot{I}}$ radical is so unstable that it has not been detected at room temperature[24] and it decays rapidly in the 120-230 K temperature range.[26] It is therefore hypothesized that $G^{\ddot{I}}$ undergoes a second one-electron oxidation to form the carbocation $G(N_1\text{-}H)^+$. [23,24] The resulting carbocation can undergo a nucleophilic addition reaction with water to produce 8-oxoG. Another proposed idea is that, $G^{\ddot{I}+}$ can react with water to form $G(OH)^{\ddot{I}}$ radical and that this radical can proceed down one of two pathways: a second one-electron oxidation to form 8-oxoG[27,28] or a one-electron reduction to form 2,6-diamino-4-hydroxy-5-formamidopyrimidine (FapyG).[29,30] A summary of these oxidation processes may be seen in Figure 3.

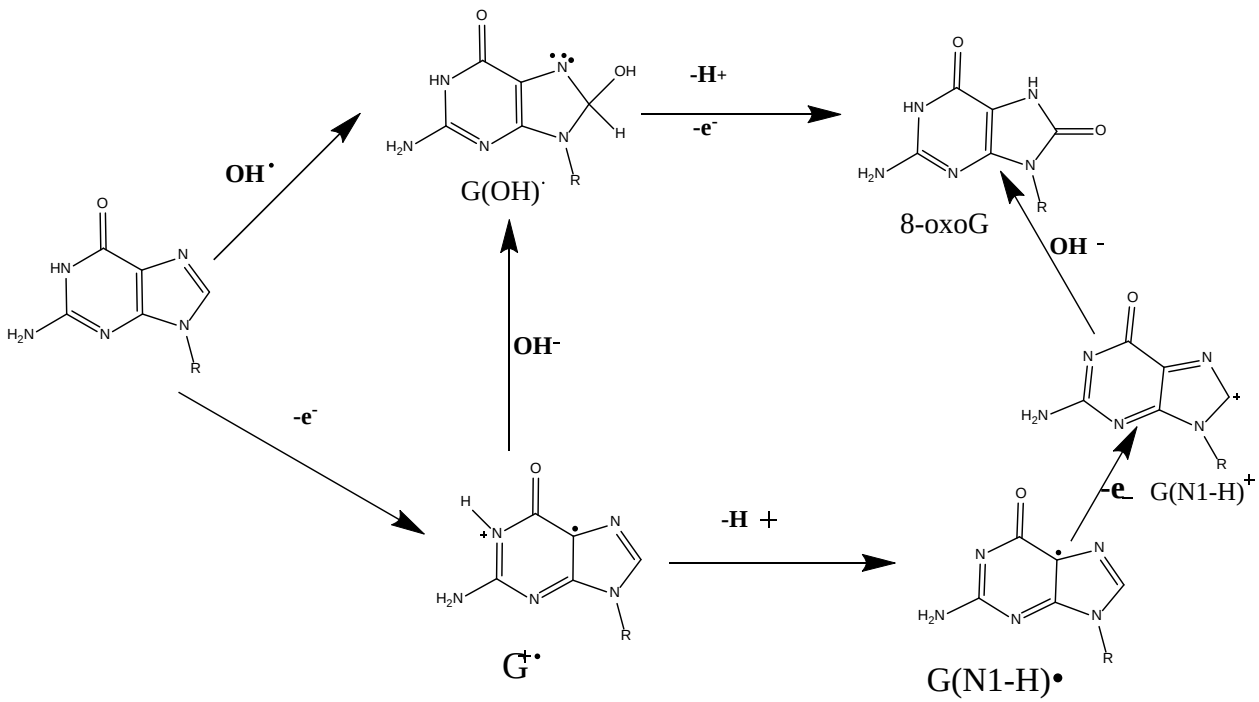

Figure 3: Reactions and products of guanine oxidation. This scheme is adapted from a similar scheme found in Close *et al*.[24]

8-oxoG is commonly used as a biomarker for oxidative stress *in vivo*.[31-33] Elevated levels have been found in a number of tissues, such as in the lung[34,35] of those working or living in areas with high doses of oxidative stressors, like asbestos fibers[36,37], exhaust from diesel engines[38] and environmental pollution.[39] Some other oxidative stressors include heavy metals and metalloids[40], polycyclic aromatic hydrocarbons[41-43], and benzene, styrene, and organoarsenic.[38]

The standard reduction potential of 8-oxoG (0.74 V versus NHE[44]) is even lower than that of the parent G making it easily oxidizable compared to the DNA nucleobases. For this reason, some research groups have used a number of oxidizers such as peroxynitrite, iridium hexachloride anion ($[IrCl_6]^-$), singlet oxygen ($^1O_2$), and the dichromate anion ($[Cr_2O_7]^{2-}$)[45] in

order to identify other species that can be used in combination with 8-oxoG as biomarkers of oxidative stress in cell. The products of this further oxidation of 8-oxoG have been identified *in vitro,*[45] and due to its low reduction potential, oxidizers that are even less potent than $^{\cdot}OH$, including carbonate radicals (E^0=1.59 V[46]), and organic radicals such as alkylhydroperoxyradicals (E^0=0.9 V) are all capable of oxidizing this G adduct yielding different compounds. Some of these oxidized products of 8oxoG include imidazalone (2,5-diamino-4H-imidazol-4-one), oxazalone (2,2,4-triamino-1,3-oxazol-5-one), cyanuric acid[45], and 1,3,5-triazepane-2,4,6,7-tetrone.[47,48] Their structures are shown in Figure 4.

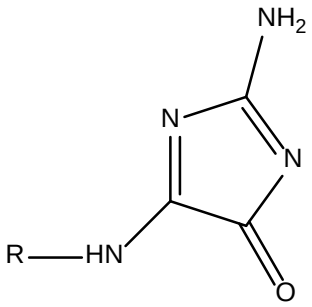

imidazalone

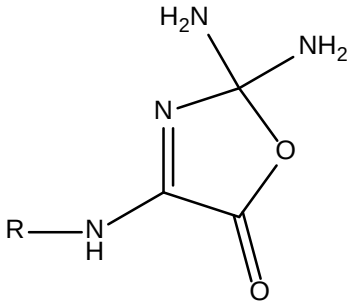

oxazalone

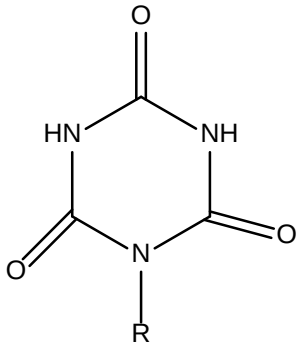

cyanuric acid

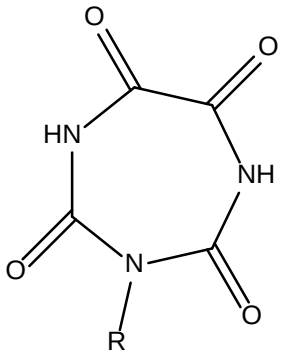

1,3,5-triazepane-2,4,6,7-tetrone

Figure 4: Some oxidation products of 8-oxo-7,8-dihydroguanine (8-oxoG)[45,47,48]

DNA Sugar Damage

2-deoxyribose (Figure 5) is a 5-member ring structure which, together with phosphodiester groups, forms the backbone of the DNA macromolecule. Upon reaction with the 2-deoxyribose moiety of DNA, ROS in general and $^{\cdot}OH$ in particular, can abstract hydrogen from the five carbon positions present, leading to the formation of a 2-deoxyribosyl radical. Sugar lesions occur predominantly at the C1´, C4´, and C5´ positions with an insignificant contribution from the C2´ and C3´ positions likely due to the lesser stability of the 2-

deoxyribosyl radicals formed upon hydrogen abstraction from these positions.[49] The relative stability of the radicals formed was computed by Colson and Sevilla at the ROHF/3-21G level of theory and gave the following trend: $^{\ddot{I}}$C1´> $^{\ddot{I}}$C4´ > $^{\ddot{I}}$C5´ ~ $^{\ddot{I}}$C3´ > $^{\ddot{I}}$C2´. The stability of the C1´ and C4´ are very important due to their involvement in base release and strand breaks, respectively.[50] Structures of the possible radicals formed by hydrogen abstraction from 2-deoxyribose are shown in Figure 5.

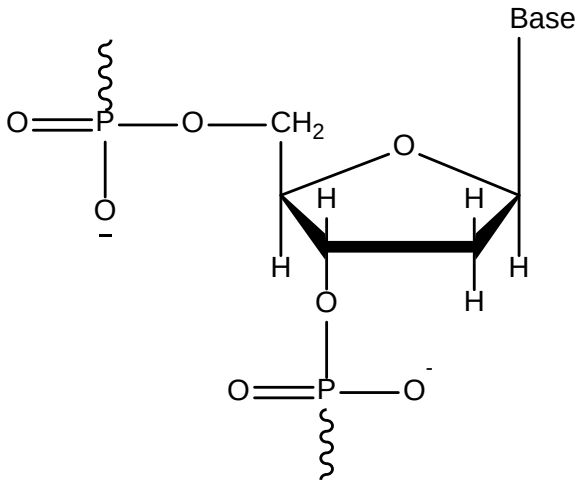

Figure 5: Structure of the 2-deoxyribose of the sugar-phosphate backbone of DNA

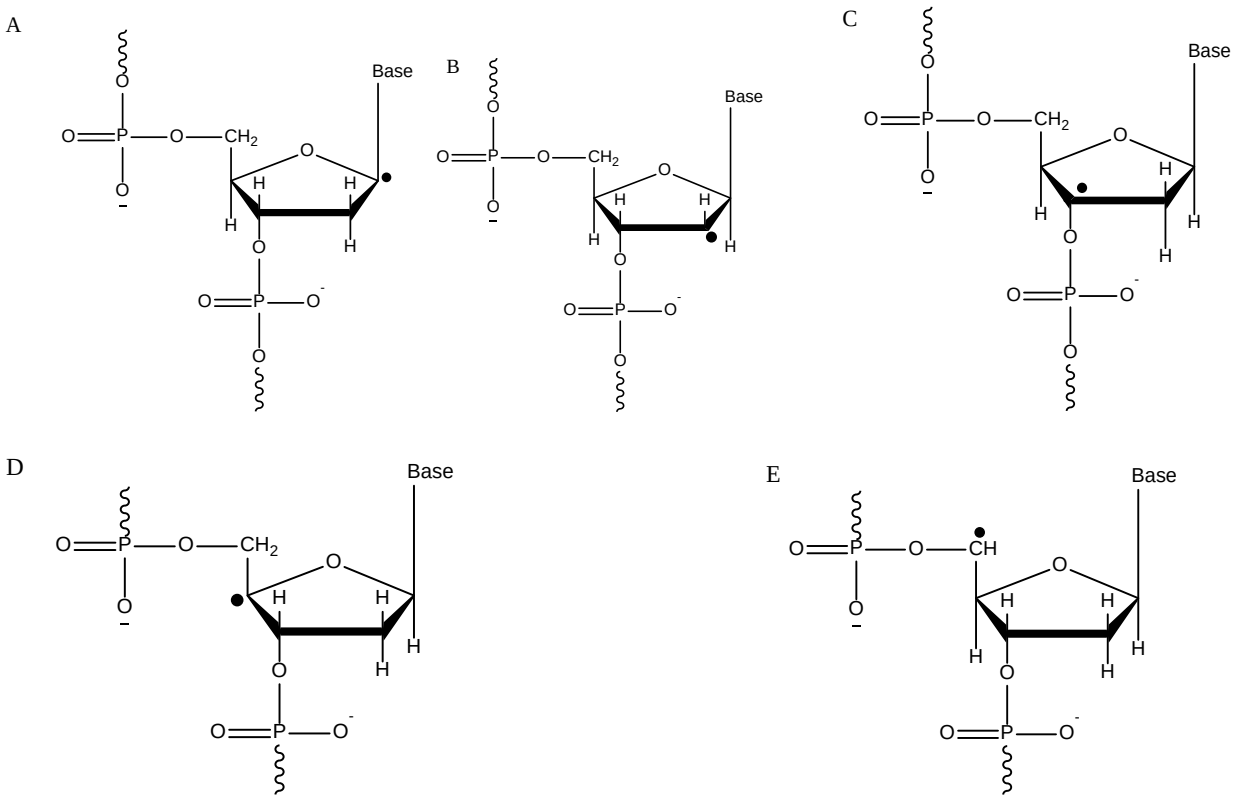

Figure 6: The structures of deoxyribosyl radicals formed via hydrogen abstraction. The radicals are arranged in increasing numerical order: A) C1„-radical; B) C2„-radical; C) C3„-radical; D) C4„-radical; and E) C5„-radical

The studies of DNA damage by ROS rely much on the question of which DNA sugar hydrogen is preferentially abstracted, and a lot has been done by the Roginskaya group[51-54] and other research groups on the subject. As in many research areas, a lot of controversy exists with this subject, but the most important thing to note is that the nature of DNA oxidative lesions depends strongly on the position where hydrogen abstraction occurs on the 2-deoxyribose.

Based on the large amount of work that has been done on this field, it is commonly thought that DNA sugar damage occurs through the combination of three major routes: C1´, C4´, and C5´

sugar hydrogen abstraction by ROS. Water constitutes the highest percentage by weight of our body and as a result, hydroxyl radicals are considered the most important ROS in biological systems; This radical preferentially oxidizes the DNA sugar in the specific order: C4´ > C1´ > C5´ >> C2´ ~ C3´.[51-55] The question of which pathway dominates over the other is governed by the combination of thermodynamic and kinetic parameters: the thermodynamic preference of hydrogen abstraction from each position of the 2-deoxyribose follows the order C1´ > C4´ > C2´ > C3´ > C5´[50,56] and the kinetic preference, which is governed by the solvent accessibility, follows the order C5´ > C4´ > C3´ ~ C2´ ~ C1´. This kinetic preference or solvent accessibility parallels the interaction of the corresponding hydrogen with hydroxyl radicals.[49]

C1´ Pathway. This pathway is involved when a radical is created on the C1´-carbon of the parent sugar due to the abstraction of the corresponding hydrogen by hydroxyl radicals. As already stated above, the C1´ hydrogen is not very accessible, primarily due to the fact that it is deeply buried in the DNA minor groove, so that solvent accessibility and therefore hydroxyl radical accessibility is limited in this area.[49] The accessibility of the C1´ hydrogen becomes even more critical when minor groove-binding molecules bind to DNA. The formation of the C1´ deoxyribosyl radical is followed by oxidation to form a carbocation or a peroxyl radical, which then undergoes fragmentation to produce a superoxide radical anion and a carbocation at the C1´ position. The carbocation produced by either of the two pathways then undergoes a nucleophilic addition reaction with water and the reaction is accompanied by the release of an unaltered nucleobase (termed free base release and denoted FBR). The resulting intermediate, 2-deoxyribonolactone (dL), is relatively unstable and will undergo ² - and ´-elimination of 5„-

phosphate and the 3„-phosphate upon heating or at basic pH to form 5-methylenefuran-2-one (5-MF). This reaction scheme is summarized in Figure 7.

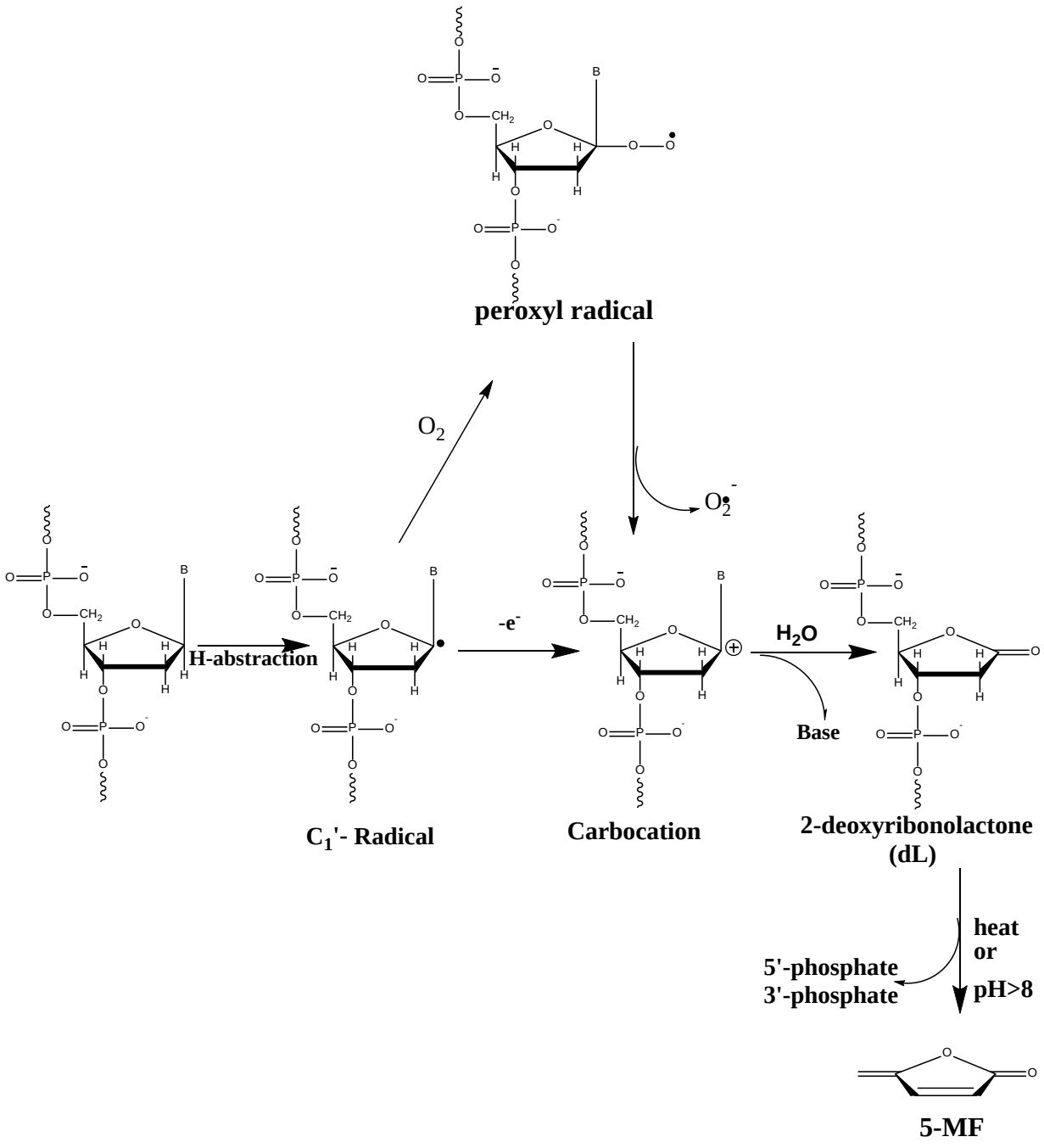

Figure 7: The formation of 5-MF from a C1„ radical and dL precursor lesion[55]

C5´ Pathway. This pathway is involved when a radical is created on the C5´-carbon of the parent sugar moiety due to hydrogen abstraction at this corresponding position. This position is highly accessible to attack from the bulk, and the two hydrogen atoms attached to the C5´-carbon are very vulnerable to hydrogen abstraction by hydroxyl radicals. Although these two hydrogen atoms are accessible from the minor groove of the DNA double helix, one of them is more accessible to solvent molecules due to its orientation away from the groove toward the solvent,[49] which is the reason why this hydrogen is the primary target of hydrogen abstraction by hydroxyl radicals at this position. Pathways involving the abstraction of hydrogen from the 5„-position have been proposed for DNA scission mediated by enediyne antibiotics, Fenton-generated hydroxyl radicals, gamma radiolysis, cationic metal porphyrins, and the hydroperoxyl radical (•OOH).[49]

After the abstraction of the 5´-hydrogen by a hydroxyl radical, the resulting C5´-deoxyribosyl radical can undergo a second one-electron oxidation to yield an intermediate carbocation, which can undergo a nucleophilic addition reaction with water to produce a hydroxylated C5´position. The hydroxylated C5„-position then undergoes 5„-phosphate elimination to yield an oligonucleotide of 5„-aldehyde (5„-Ald), which can then undergo FBR and 3´-phosphate elimination to generate furfural (Fur). The reaction scheme of this process is summarized in Figure 8.

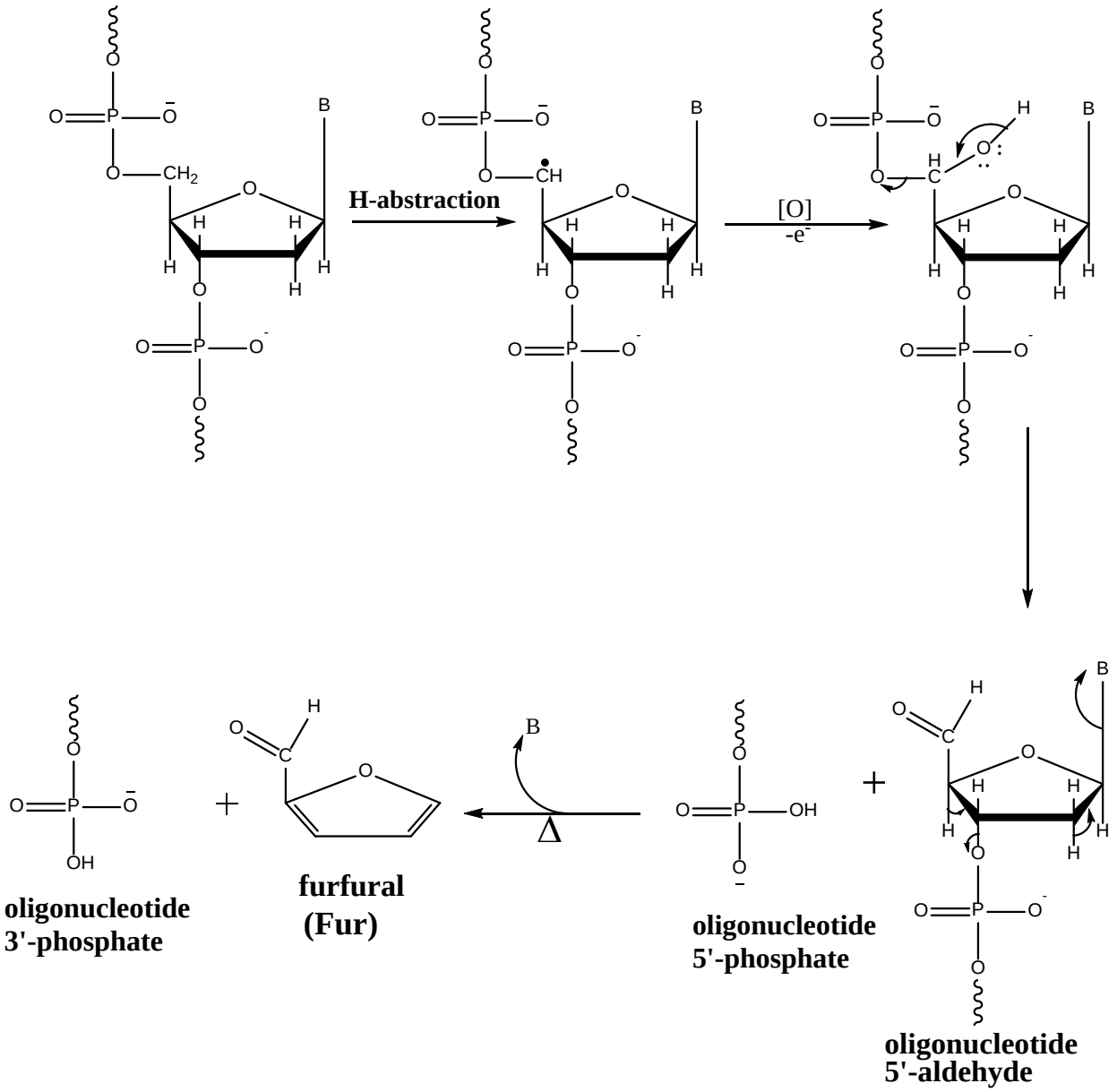

Figure 8: The formation of 5,-aldehyde (5,-Ald) from the precursor C5,-deoxyribosyl radical. This radical undergoes base and phosphate elimination reactions to generate furfural (Fur)[55]

C4„ Pathway. This pathway involves the abstraction of hydrogen from the C4´-carbon of the 2-deoxyribose of the DNA, leaving behind a C4„-deoxyribosyl radical. The relatively high accessibility of this site makes it a potential target for DNA-cleaving molecules.[49] Systems involving ionizing radiation, methidiumpropyl(EDTA)•Fe(II), Fenton-generated hydroxyl radicals, and several drugs (including bleomycin, calicheamicin, neocarzinostatin, elsamicin A, and C1027) have been proposed to undergo 4„-hydrogen abstraction to yield DNA damage.[49]

A mechanism relying on the alkyl phosphate and ribose 5´-phosphate chemistry, and independent of the presence of oxygen was proposed by the von Sonntag research group.[57] Based on this proposed mechanism, an alkyl radical created adjacent to a phosphate ester undergoes a nucleophilic addition reaction with water followed by β-elimination of phosphate.[49] On DNA model systems, von Sonntag *et al.* extrapolated this proposed mechanism and hypothesized a C4´ radical was formed followed by elimination of one or both phosphate group(s).[49,57] In addition to this model, a radical cation intermediate is formed followed by hydrolysis and release of a proton.[49,58,59] The lone pair of electrons on the oxygen atom in the ring is believed to stabilize this radical.[49,59] This proposed mechanism was also observed in model systems by Giese *et al.*,[60] where the final product formed is dependent on whether the nucleophilic addition reaction with water occurs at the carbocation center or the carbon-centered radical.

The C4´ pathway is commonly accepted as the main contributor to DNA immediate strand breaks caused by radiation-induced hydroxyl radical formation. This pathway is assumed to contribute about 50% of all immediate strand breaks in aqueous solution of DNA,[61] as opposed to the ~20% initially proposed by Balasubramanian *et al.*[62] This pathway may be divided into two pathways: malondialdehyde formation (not included in this research study) and formation of a C4´-oxidized abasic site (C4´-OAS).

Although it was first identified in c-irradiated aqueous solution of DNA[63,64], C4´-OAS has also been identified as a product of bleomycin-facilitated anaerobic DNA cleavage.[65-71] The formation of this lesion has been shown to induce DNA-DNA cross-linking reactions[72-74], and the result of this cross-linking is the blocking of DNA replication and repair[75,76], which increases the mutagenic potential for the C4´-OAS.

Fluorimetric assays performed by Dhar *et al.*[77] found the yield of C4„-OAS in DNA to be 27.5% of all radioinduced aldehyde-reactive probe (ARP) carbonyl groups, while gas chromatography-mass spectrometry (GC-MS) techniques used by Chen *et al.*[78] found the C4„-OAS to be only 3% of all 2-deoxyribose damage. The controversy observed in these two data sets is informative on how much is still not known concerning the role of C4´-OAS in radiation induced oxidative damage to DNA. The procedures used by these two research groups rely on multiple calibration curves, and require calibration using well-characterized authentic oligonucleotides containing chemically incorporated C4„-oxidized abasic sites.[54]

A proposed mechanism for the formation of a C4´-OAS shown in Figure 9 was suggested by the Roginskaya[54] research group. A C4´-deoxyribosyl radical can undergo a nucleophilic addition reaction with oxygen to produce a peroxyl radical, which proceeds through an unknown mechanism to give C4´-OAS. It is also possible for the peroxyl radical to undergo elimination of a superoxide radical to form a C4´-deoxyribosyl carbocation that can undergo an elimination reaction in the presence of water to form the C4´-OAS.

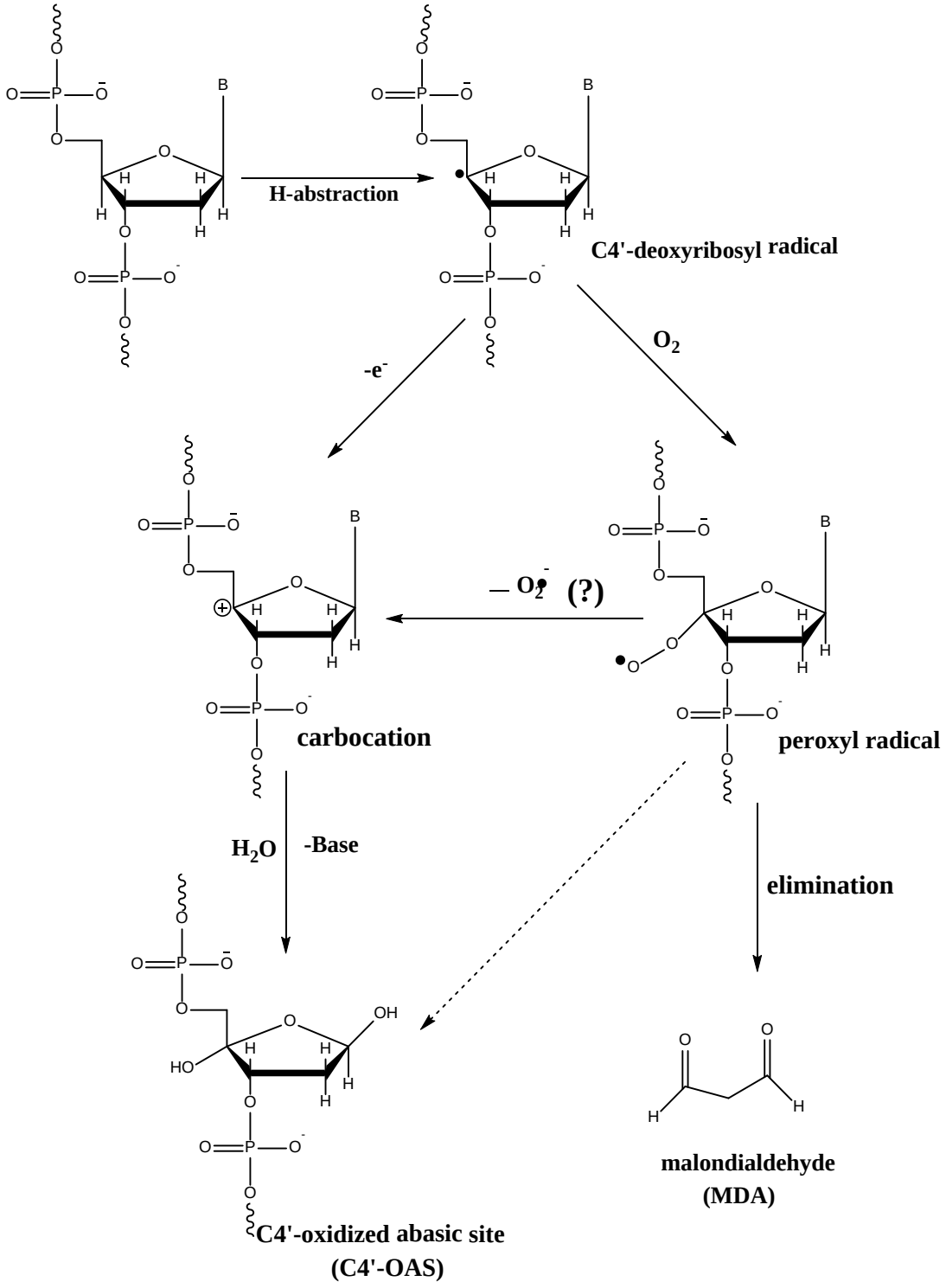

Figure 9: The C4„-pathway chemistry under aerobic and anoxic conditions, leading to the formation of C4„-OAS and MDA sugar damage products. Modified from a similar scheme in Roginskaya *et al.*[54]

Quantification of the DNA Sugar Damage Products Using HPLC

An HPLC-based method of qualitative and quantitative analysis of DNA sugar damage products was earlier developed by the Roginskaya research group.[51-54] The methodology is based on the idea that the oxidized DNA lesions can undergo fragmentation of the 2-deoxyribose ring by catalytic and/or heat treatment to give characteristic low-molecular weight products that may be identified and quantified using HPLC. These characteristic low-molecular weight products are unique to the precursor 2-deoxyribose lesion, and the strand break resulting from this fragmentation is usually accompanied by a release of an unaltered free DNA base.

Characteristic Low-Molecular Weight Products Resulting from the C1´ and C5´ Precursor Lesions

The reaction that leads to the formation of C1´ and C5´ products from precursor lesions, as shown in Figures 7 and 8 respectively, is catalyzed by species with Lewis acid properties (in this work, spermine, polylysine (polyLys), poly(lysine, tyrosine) (poly(Lys, Tyr)), or polyarginine (polyArg)). This reaction condition was optimized by the Roginskaya research group[51-53] and steady state concentrations of both 5-MF and Fur were obtained after 25-30 min of heating in the presence of a cationic form of polyamine/polypeptide. These species, with Lewis acid properties, are necessary to stabilize the negative charge on the phosphodiester groups of the DNA backbone in other to facilitate the fragmentation process and cause the elimination of these aforementioned groups. The reaction for the formation of 5-MF from (dL) is shown in Figure 10 and the reaction that leads to the formation of Fur from 5´-Ald is shown in Figure 11.

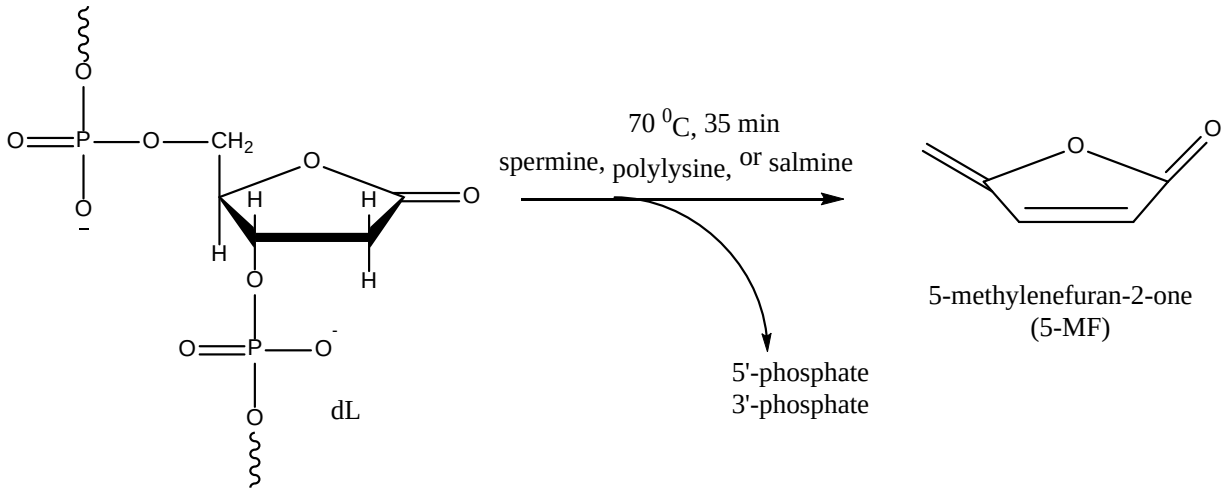

Figure 10: The reaction leading to the formation of 5-methylenefuran-2-one from 2-deoxyribonolactone

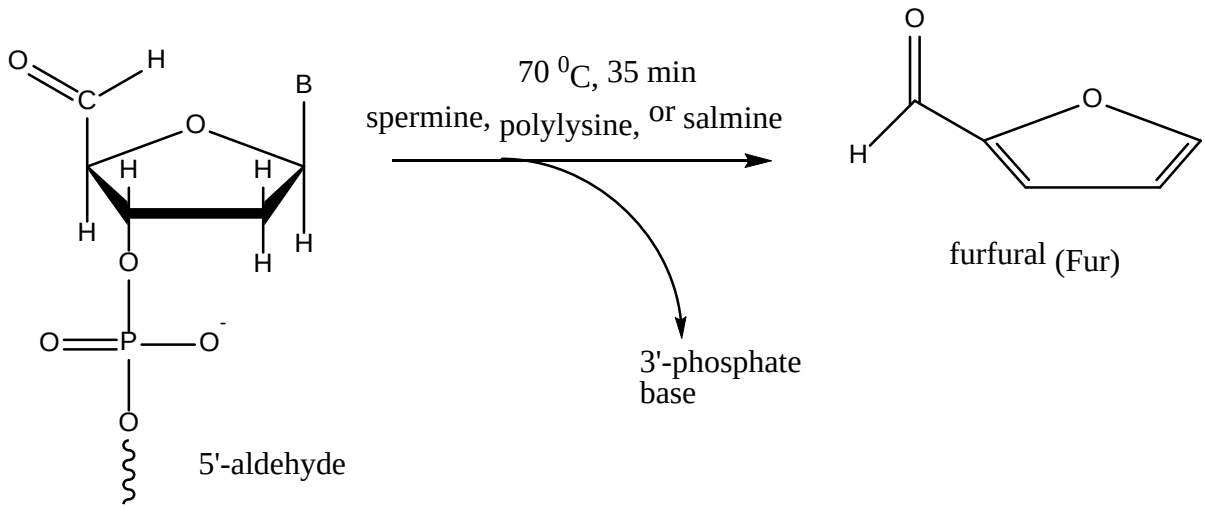

Figure 11: The reaction leading to the formation of furfural from 5´-aldehyde

Characteristic Low-Molecular Weight Product Resulting from the C4´ Precursor Lesion

Lac Formation. The C4´-OAS DNA lesion can undergo a nucleophilic substitution reaction with a primary amine under neutral or slightly acidic conditions to produce N-substituted 5-methylene-" ^{3}-pyrrolin-2-ones (which is referred to in this work as simply Lactam or Lac). The exact structure of the product form is specific to the primary amine used in this reaction. Depending on the primary amine used, the yields have been shown to be greater than 75%[79-81], and the resulting lactams are easily quantified using HPLC equipped with a UV detector, due to their relatively strong absorption below 350 nm.[79,82]

The measurement of Lac allows us to give a rough estimate of the contribution of the C4´-pathway in radiation damage to DNA. The primary amines that were used in this work include: glycine, putrescine, and ethanolamine. In addition to their small and hydrophilic nature, these amines are not retained in reverse-phase separation conditions. They also create a slightly acidic condition optimal for the derivatization process. The choice of these amines was based on the problem at hand, and also, due to the close similarities in their structures, there is no significant variation in the extinction coefficient of the lactams formed. The reaction between C4´-OAS and a primary amine is shown in Figure 12.

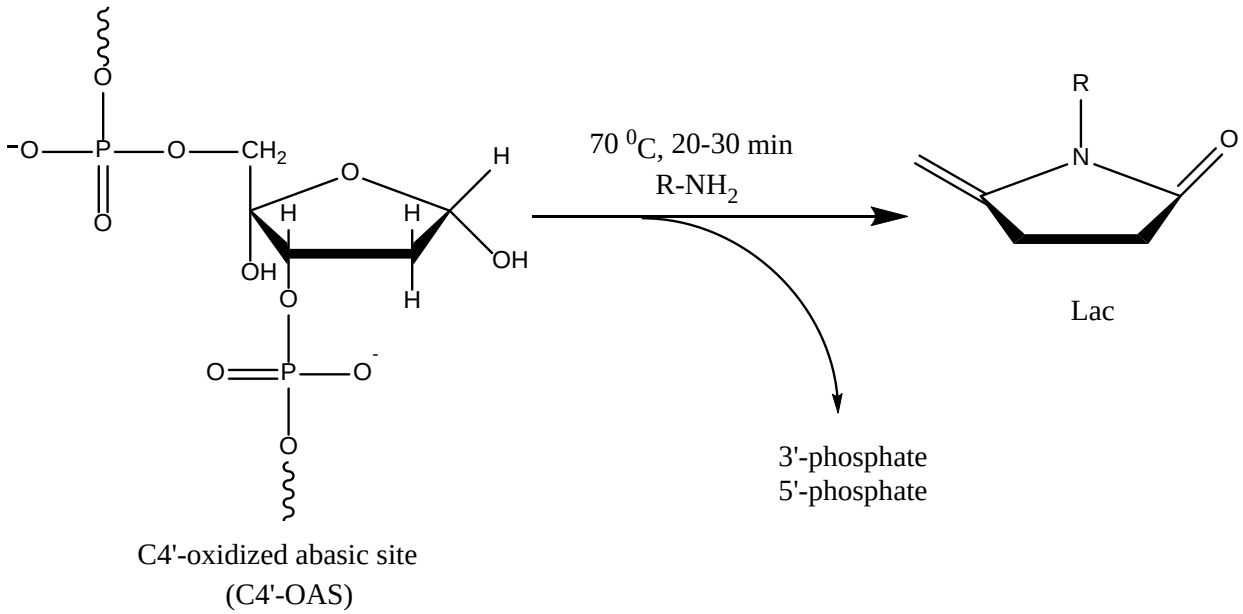

Figure 12: Lactam (Lac) formation from C4´-OAS

DNA in Biological Systems

The DNA in somatic cell nuclei is tightly packaged by histones and a large variety of non-histone proteins to form a complex structure called chromatin. It is commonly thought that these proteins confer about 10,000-fold compaction of DNA in chromatin compared to free DNA.[83] This compaction of DNA in chromatin starts by the formation of a nucleosome core particle (NCP). NCPs have been well characterized structurally through X-ray crystallography[84] and various additional thermodynamic and biophysical methodologies.[85,86] A NCP consists of 146-147 base pair (bp) of DNA wrapped 1.75 turns around an octamer built from two copies each of histones H2A, H2B, H3, and H4[84-86] (this structure is commonly described as “beads on a string”). The H1 histone, called the linker-histone, lies between each NCP on a chromosome

linker region of DNA between 20 and 100 bp in length. This description of chromatin can be seen in Figure 13 below.

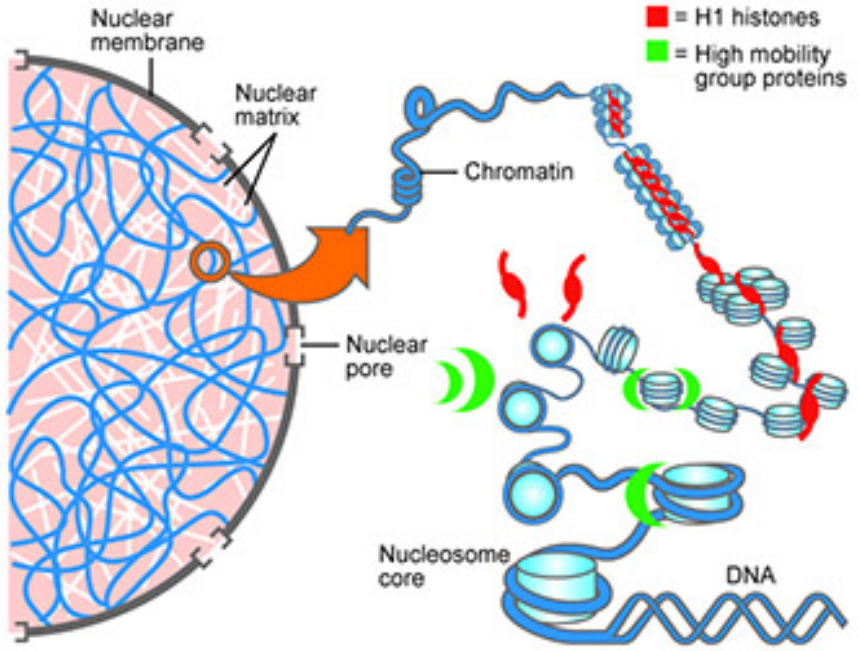

Figure 13: Structural features of DNA-histones and non-histones proteins complex.[87] Used with permission from Jeanne Kelly, Aardvark Designs, and the National Cancer Institute.

During vertebrate spermiogenesis, however, the majority of the histone and other non-histone proteins associated with DNA are replaced by arginine-rich oligopeptides called protamine.[88] This protamine-association of DNA allows for its tighter condensation and makes the DNA resistant to nuclease digestion and other DNA-altering agents.[89] Some mammalian sperm cells contain two different types of protamine, usually referred to as protamine I and II. Protamine I has a relatively conserved amino acid sequence among mammals, and is present in

all mammalian sperm cells. The protamines of other vertebrates, such as fish, are similar to the protamine I of mammals. Protamine II is less conserved and is found only in some mammals including humans.[89] Protamines from fish and mammalian protamine I are the focus of most studies regarding DNA condensation by protamines, primarily due to the fact that protamine I is more widely distributed than protamine II and also because organisms from which sperm cells are commercially available do not contain protamine II (examples include salmon).

In DNA-protamine complexes, positively charged arginine residues in protamine interact with the negatively charged phosphodiester backbone of the DNA. Such interaction minimizes the repulsion within the DNA backbone, making it possible for this macromolecule to double pack and fold up on itself and therefore creating the highly compact and tightly bound toroids.[89] Although it is not doubted that the interaction between protamine and DNA is electrostatic, there is no published structure which would give a clue as to precisely how the positively charged basic residues in protamine are aligned with the negatively charged phosphate groups in DNA. Nevertheless, mammalian sperm chromatin may be divided into three major structural domains: (I) the vast majority of sperm DNA is coiled into toroids by protamines[90], (II) a much smaller percent remains bound to histones[91-95], and (III) the DNA is attached to the sperm nuclear matrix at matrix attachment region (MARs).[96,97] Figure 14 shows the replacement process and the plausible DNA-protamine complex.

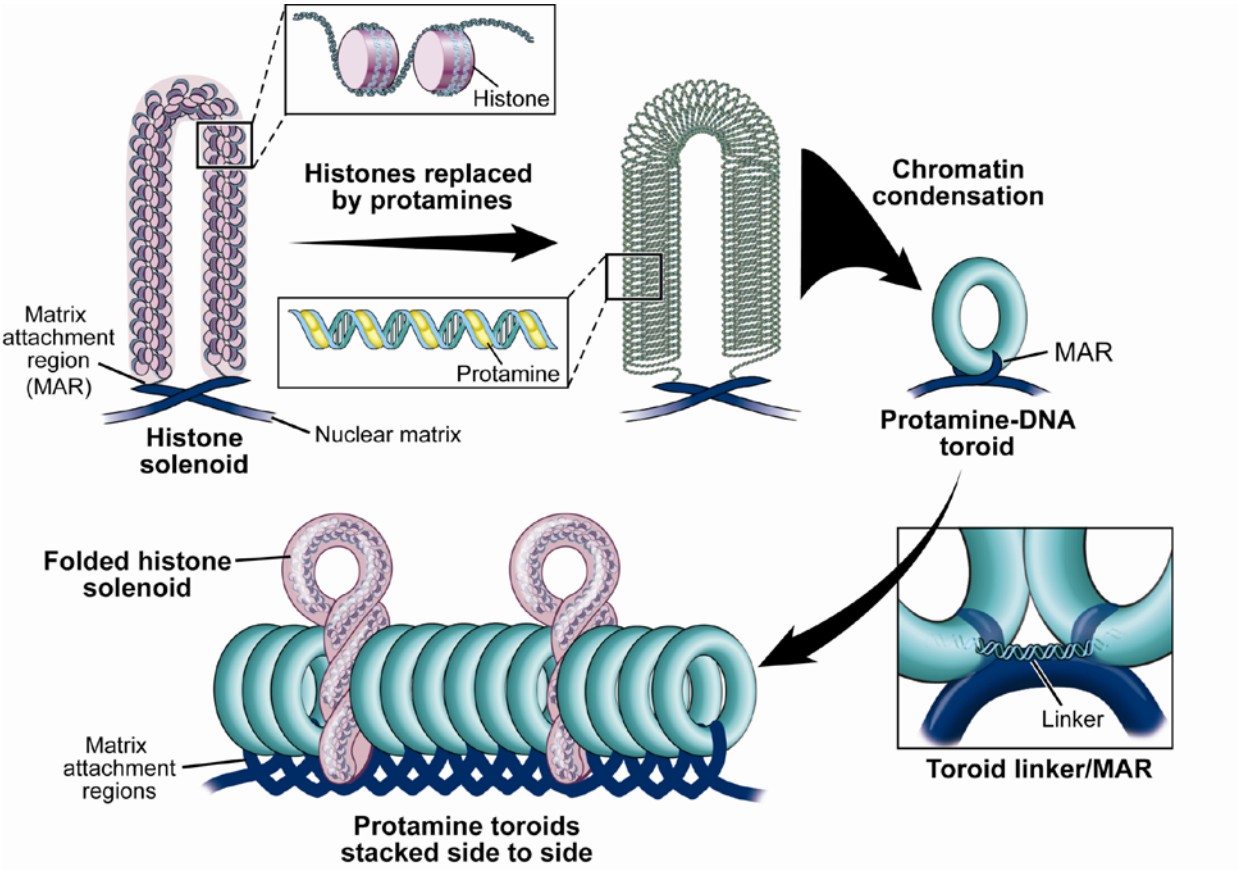

Figure 14: Mature sperm DNA organization and its most important features.[98] Creative Commons License

Other plausible DNA condensers include positively charged polyamines (PCAs), namely spermine, spermidine, and putrescine (structures are shown in Figure 15). These are small organic cations present in the nucleus of all eukaryotic cells in millimolar concentration ranges.[99] They are biosynthesized by enzymatic decarboxylation of the amino acids ornithine and arginine by the enzyme ornithine decarboxylase (ODC).[100] It has been hypothesized that due to their high affinity with the anionic sites of nucleic acids, the polyamine's primary role is to stabilize and condense DNA.[101] This idea is based on the fact that during DNA replication (DNA

is free of histones or protamines during this process), ODC is synthesized in a burst at the end of the G_1 phase, just before the S (synthesis) phase, and then is rapidly degraded[102], indicating the crucial role of these polyamines during this process. They have also been found to participate in several essential metabolic processes such as regulation of RNA transcription, specific gene expression, and the progression of the cell cycle.[100]

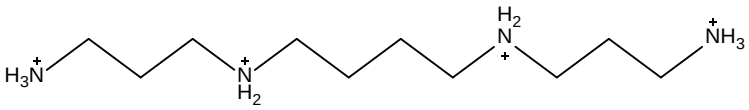

Spermine

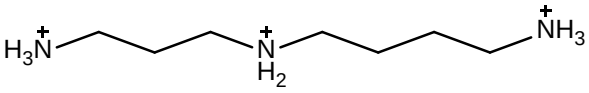

Spermidine

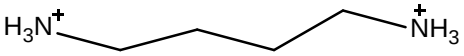

Putrescine

Figure 15: Structures of biologically important polyamines

Radioprotection of DNA by Histones, Positively Charged Polypeptides, and PCAs

The idea of DNA radioprotection was brought up a long time ago in combination with the recognition that DNA, as the major hereditary unit of the cell, is the critical target of ionizing radiation. Knowing the mechanism of this protection is critical, especially for clinical radiation therapy, since it is necessary to reduce damage to the normal tissues while causing maximum damage to cancerous cells.[103]

Radiosensitivity of DNA, estimated as the yield of double strand breaks (DSBs) was shown to increase on going from intact cells to isolated DNA with partially stripped chromatin being intermediate in this order.[104,105] The removal of histones from cellular chromatin leads to a 40-80-fold increase in the yield of DNA strand breaks produced upon irradiation, suggesting that the association of histones with DNA to form nucleosomes and higher-order chromatin structures plays an important role in the radioprotection of DNA.[106-108]

Positively charged oligopeptides such as oligolysines[109] and PCAs[105,110-112] which mimic histones in the mode of DNA binding, have also been shown to protect DNA in completely or partially dehistonized chromatin. Incubation with the polyamine spermine has been shown to protect viral DNA from the induction of strand breaks at levels comparable to those provided by the organization of DNA into compact nuclear chromatin.[110,113,114] The mechanism of protection of DNA by these DNA-binding proteins and/or PCA remains poorly studied.

Protection Against the Direct Effect of Ionizing Radiation

The direct-type damage results from the direct ionization of DNA or transfer of electrons or holes to DNA from its solvation shell. Although a significant amount of information exists concerning the direct-type damage of DNA, very little is known about the protection effect of

histones and non-histone proteins against. A paper published in 2006 by Roginskaya *et al.*,[15] plausible mechanism of radio-protection of DNA from the direct damage by histone-mimicking PCP complexes using such PCP's as polyLys, polyArg, and polylysinetyrosine (poly(Lys,Tyr)) was proposed. Approximately a 2.5-fold, 2.3-fold, and 1.8-fold average protection of DNA in dry films ($\Gamma = 2.5$) from the direct-damage by polyLys, poly(Lys,Tyr), and polyArg, respectively was observed. They attributed this DNA radioprotection to the conformational changes of DNA secondary structure induced by PCPs and/or to the repair of DNA by hydrogen atom transfer from PCPs to DNA.

Protection Against the Indirect Effect of Ionizing Radiation

The attack of DNA by radicals produced in the surrounding milieu by ionizing radiation constitutes the indirect effect of ionizing radiation on DNA. The hydroxyl radical produced by the radiolysis of water was the radical of interest in this research study. A lot of work has been done to understand the plausible mechanism of protection of DNA by proteins and soluble nuclear components against $^{\cdot}$OH induced damage. Various mechanisms have been proposed to explain the protection afforded by DNA-binding proteins and soluble nuclear components against $^{\cdot}$OH-induced DNA damage. At least four mechanisms are known: 1) $^{\cdot}$OH scavenging, 2) positively charged polypeptides and/or polyamines induced compaction and aggregation (the PICA effect), 3) repair of DNA by electron transfer, and 4) repair of DNA by hydrogen atom transfer. While most of research has been focused on the first two mechanisms, several research groups reported some evidence of the third mechanism. The fourth type of radioprotection has been neglected in publications.

$^{\cdot}$OH Scavenging. Since the oxidative damage to DNA from the indirect effect of ionizing radiation occurs predominantly from $^{\cdot}$OH, scavenging of this radical by proteins and/or soluble nuclear components is important for DNA radioprotection. Because of the very high reactivity of hydroxyl radicals as hydrogen abstractors, they will react indiscriminately with H-donors at diffusion-controlled rates.[61,115] For this reason, hydroxyl radicals travel very short distances before reacting with their targets. Therefore DNA in biological systems appears to be significantly protected from the damage by $^{\cdot}$OH by a large variety of soluble bioorganic molecules (sugars, amino acids, and thiols) present in the nucleus in millimolar concentrations. This type of scavenging of $^{\cdot}$OH by soluble bioorganic molecules is termed “scavenging in the bulk”. The term is usually used to refer to the process by which molecules scavenging $^{\cdot}$OH are not tightly associated with DNA (they have low binding affinity to DNA). Scavenging efficiency of $^{\cdot}$OH by soluble organic components in this case is therefore highly dependent on the scavenging capacity and on the concentration of these scavengers in the bulk solution.[116]

The other type of $^{\cdot}$OH scavenging process is scavenging by molecules that are tightly associated with DNA (molecules with relatively high binding affinity to DNA). These molecules include histones and non-histones proteins, PCPs, protamine (both I and II), and such PCAs as spermine, putrescine, and spermidine. These molecules not only protect DNA by reducing its surface accessibility to $^{\cdot}$OH due to DNA condensation, but also afford DNA radioprotection by scavenging $^{\cdot}$OH radicals in close proximity to DNA.

PICA Effect. It was mentioned in a review by Pogozelski and Tullius,[49] that the efficiency of $^{\cdot}$OH-induced damage to DNA correlates with the accessibility of this species to DNA.[49] In other words, DNA in its condensed form (like in chromatin) is less likely to be damaged by $^{\cdot}$OH due to reduced accessibility of the attack sites in the condensed structure.[117] It is also well documented that DNA aggregation (multiple DNA molecules are bound together) occurs when about 90% of the phosphate groups are neutralized.[118] This aggregation can also lead to reduced accessibility of some attack sites in DNA. All these correlate with the findings by Newton *et al.,*[114] where they performed an experiment with PCAs including putrescine and spermine with the hope of extrapolating the results of their findings to histones and non-histone proteins. They found that at physiological ionic strength, and polyamine concentrations below 1 mM, the protection afforded to DNA by spermine or putrescine was equivalent. Protection of DNA in this concentration range was attributed to the capacity of both polyamines to scavenge radiation-induced radicals. At concentrations above 1 mM, spermine provided significantly greater protection of DNA than putrescine. Since within this concentration range polycationic polyamines such as spermine condense DNA[119-121], the enhanced protection of DNA in this higher concentration range was attributed to the capacity of spermine to bind to and to aggregate DNA. Thus polyamine-induced compaction and aggregation of DNA (the PICA effect) protects DNA from damage by reducing the surface accessibility of DNA to radiation-induced radicals.

Newton *et al.*[109] extended their research to oligolysines, with the intention of using systems that are structurally more closely related than other ligands to naturally occurring DNA condensing agents such as histone proteins. The result of their experiment suggests that oligolysines, such as trilysine, with a total charge of +3, do not condense DNA, and as a result, behave similarly to putrescine with radical scavenging being the predominant mechanism of

protection of DNA. Also, as the chain of the oligolysine was increased, DNA protection was enhanced[109]. This enhanced protection was attributed to the PICA effect.

DNA Radioprotection by Electron Transfer from Proteins to DNA. Oxidative damage to DNA can lead to the removal of a single electron from a nucleobase resulting in the formation of an electron-deficient site, or hole. A hole generated in DNA is expected to quickly localize at the nearest purine bases, guanine (G) or adenine (A), which have lower oxidation potentials than pyrimidine bases.[122] Thus, the radical cation state $G^{\ddot{I}+}$ or (less likely) $A^{\ddot{I}+}$ is generated. As the rate of irreversible trapping of the hole due to its reaction with polyamines[123], water, oxygen, and other species is relatively slow[122,124], the hole migrates within DNA using G and A nucleobases.[125] In protein-DNA complexes, an amino acid residues, X, that has a lower oxidation potential than G and A, can act as electron donor (or equivalently hole acceptor) retrieving the native state of a nucleobase B from its radical cation.[126]

$$B^{\ddot{I}+} + X' \quad B + X^{\ddot{I}+} \tag{1.13}$$

This possible electron transfer reaction should prevent possible damage to DNA. The low standard reduction potentials of tryptophan (1.0 V)[127] and of tyrosine (0.9 V)[128] make the repair of $G^{\ddot{I}+}$ (1.3 V)[127] feasible as has been observed for different systems in aqueous solution,[129-131] and for DNA-tripeptide complexes.[132-134] Furthermore, the charge transfer in DNA-tripeptide (Lys-Tyr-Lys) complex was probed using flash-quench experiments, and the transient absorption spectroscopy gave a spectrum with a sharp maximum at 405 nm assigned to the tyrosine radical.[132] It was suggested that this radical was formed through charge transfer from a guanine

radical in DNA, since the increase of the 405 nm signal occurred with the same kinetics as the decrease of the guanine radical peak, as monitored at 510 nm.[132]

The influx of electrons and efflux of holes from protein to DNA in dry or hydrated chromatin X-irradiated at 77 K was observed by Weiland and Hüttermann.[135] An approximately two-fold net increase in radical concentration in DNA in dry chromatin was observed as compared to DNA alone, with an increased contribution of electron-gain centers (pyrimidine radical anions) and reduction in electron-loss centers ($G^{Ï+}$) in DNA in dry chromatin[135]. These findings support the hypothesis that chromatin components protect DNA from oxidative damage.

DNA Radioprotection by Hydrogen Transfer from Proteins to DNA. The hypothesis of repair of DNA deoxyribosyl radicals by hydrogen transfer from protein in DNA complexes with histones and histone-like polycations has been mentioned in Roginskaya earlier work[15] as one of the plausible mechanisms of DNA radioprotection by PCPs against direct radiation damage. To the best of our knowledge, this hypothesis has never been examined experimentally. The plausibility of such repair is based on the difference in enthalpies of bond formation for the deoxyribose C-H bonds and the protein C-H, N-H, and O-H bonds. According to theoretical calculations, the ±-C-H bond energy in peptides is as low as ~345 kJ/mol.[136] This is significantly lower than the weakest of all C-H deoxyribose bonds, the C1´-H bond, which is ~376 kJ/mol according to the theoretical calculations performed by Miaskiewicz and Osman[137]. Thus, the mechanism of ±-hydrogen transfer from peptide to a DNA sugar radical in a DNA-peptide complex is thermodynamically favorable. Evidence for the formation of ±-carbon radicals in X-irradiated chromatin at 77 K has been obtained by Weiland and Hüttermann[135], though the mechanism of formation of these radicals remains unclear.

The bond energy of a secondary C-H bond is ~390 kJ/mol[138], which is higher than that of the C1´-H bond, but is close to that of the C4´-H (389 kJ/mol[50]) and C5´-H (>390 kJ/mol[50]) bonds, respectively. This suggests a plausible hydrogen transfer from PCAs and PCPs side chains to DNA.

In addition, tyrosine residues of histones may play a special role in DNA protection against oxidative damage. Histone octamer contains as many as 20 tyrosines.[139] The enthalpy of the O-H bond of the phenolic ring of tyrosine is estimated at ~371 kJ/mol based on the theoretically calculated enthalpy of the O-H bond in phenol[140], which means that tyrosine side chains can also contribute to the repair of DNA deoxyribosyl radical by hydrogen donation.

We therefore hypothesize that DNA complex formation with PCPs or PCAs results in the modification of pathways of DNA sugar damage by hydroxyl radicals because of the chemical repair of deoxyribosyl radicals in DNA by hydrogen atom donation from PCPs or PCAs to DNA deoxyribosyl radicals. This process will favor the repair of the C5´-deoxyribosyl radical first, since this radical is the most surface-exposed and the energy of the C5´-H bond is the highest, plausibly followed by the repair of the C4´-sugar radical, and lastly, by the repair of the C1´-sugar radical, which is buried in the minor groove in dsDNA, with the energy of the C1´-H bond being the lowest. As a result, the relative ratios of characteristic products of DNA sugar damage by hydroxyl radicals are expected to be different in DNA-PCP or DNA-PCA complexes as compared to naked DNA. We expect the relative yield of the characteristic product of the C1´ sugar damage, 5-MF, to dominate over the others in complexes of DNA with PCPs due to the higher stability and lower accessibility of the C1´ sugar radical, which results in a less efficient repair of the C1´ sugar radical by hydrogen donation from the peptide or polyamine chain.

Specific Aims

The objectives of this work were:

1. To design an optimal system to study the effect of DNA complex formation with polycations on the relative yield of products of DNA sugar damage by hydroxyl radicals using HPLC-based analysis. Requirements for such a system included the ease of sample preparation, manipulation, and reasonable reproducibility of the results. Different forms of the complexes were tested including dilute solutions, concentrated solutions prepared by hydration of dry films, and suspensions.

2. To test the hypothesis that DNA complex formation with polycations results in the modification of pathways of DNA sugar damage by hydroxyl radicals. The ratios of DNA sugar damage products 5-MF, Lac, and Fur as well as FBR were compared for naked DNA and for DNA complexes with a number of polycations (see Aim 3).

3. To test the hypothesis that DNA complex formation with polycations results in the modification of pathways of DNA sugar damage by hydroxyl radicals because of the chemical repair of deoxyribosyl radicals in DNA by hydrogen atom donation from polycations to deoxyribosyl radicals.

CHAPTER 2

EXPERIMENTAL METHODS

Instrumentation, Glassware, and Other Materials

Instrumentation

A Shimadzu High Performance Liquid Chromatograph (from Shimadzu) supplied with an autosampler, degasser, column oven, photodiode array (PDA) detector composed of a tungsten lamp and a deuterium lamp, and analytical column (Phenomenex Gemini^{TM}, C18, reversed phase 250 mm x 4.6 mm, 5µm) was used as the major analytical instrument for data analysis. A Cary 100 UV-visible spectrophotometer (from Agilent) was used to determine the concentration of prepared samples. A Phillips X-ray machine from Dr. David Close's laboratory (Department of Physics and Astronomy, ETSU) equipped with a tungsten anode was used to generate the X-ray radiation. A vacuum set composed of Labconco Centrivap Concentrator, Labconco Rotary Vane Electric Pump, and a pressure gauge was used for concentrating samples. Other instrumentation used in this research included a laboratory analytical balance, an oven, a microprocessor-controlled hot water bath, and a vortex mixer (all from Fisher Scientific).

Glassware and Other Materials

Other important glassware and materials used in this research included beakers, Erlenmeyer flasks, volumetric flasks, measuring cylinders, glass vials, Wheaton Ampoules, graduated pipettes, mechanical pipettes with appropriate tips, disposable pipettes, graduated plastic vials (1.5 mL), centrifuge tubes (50 mL and 15 mL), magnetic stirring bar, HPLC inserts (200µL), and matched quartz cell cuvettes. Dialysis tubes (from Sigma) with a pore size of 25 Å were also used for the procedures utilized for preparation of complexes of DNA with polypeptides.

Reagents

Deoxyribonucleic Acid

The sodium salt of salmon testes DNA was purchased from Sigma-Aldrich Chemical Company.

Salmon Sperm Nuclei

Salmon sperm nuclei, used for the preparation of DNA-protamine solution and suspension were purchased from Sigma-Aldrich.

Other Reagents

Glycine, spermine tetrahydrochloride, putrescine dihydrocloride, ethanolamine hydrochloride, protamine sulfate, poly-L-lysine (polyLys) hydrochloride (MW per one lysine hydrochloride = 149.45 g/mol, total MW > 30,000), 1:1 copolymer of lysine and tyrosine (poly(Lys, Tyr)) hydrobromide (average MW per lysine-tyrosine hydrobromide = 185.95 g/mol, total MW = 72 000) were purchased from Sigma-Aldrich. Sodium hydroxide (NaOH) pellets (from Sigma Aldrich) was also used in this research as a desiccating agent for preparation of films.

HPLC Solvents

80% (v/v) acetonitrile (CH_3COCN) made from HPLC-grade acetonitrile (from VWR) and HPLC-grade water (from Fisher) and 40 mM aqueous ammonium acetate made from a 4 M stock solution of ammonium acetate (ACS reagent grade from Fisher) in HPLC-grade water were both used for HPLC separation and analysis.

Buffers and Solutions

Stock solutions were prepared using HPLC-grade water. A 1 M stock solution of phosphate buffer, pH = 6.9 was made by mixing an equal volumes of 1 M stock solutions of potassium monobasic phosphate (KH_2PO_4) and potassium dibasic phosphate (K_2HPO_4) (all from Sigma). The 1 M phosphate buffer was then diluted to make a 10 mM phosphate buffer stock solution with the same pH. This 10 mM phosphate buffer solution was used in nearly all experimental procedures to maintain near-physiological pH. A 5 M stock solution of sodium chloride (in HPLC-water) was used to adjust the ionic strength of some solutions when needed.

Preparation of DNA Solutions

10 mM DNA solutions (the DNA concentration here and elsewhere in this text is expressed per DNA nucleotide) were prepared by mixing 36 mg salmon testes DNA (average MW per nucleotide = 360 g/mol) with 10 mL of 10 mM phosphate buffer, pH = 6.9. This mixture was allowed to stand overnight at 4^oC so as to allow enough time for DNA to dissolve. The next day, the solution was stirred gently for about 30 minutes to ensure homogeneity.

15 mM DNA solutions were also made following the procedure above, but this time with corresponding amounts of DNA and phosphate buffer, and the concentrations were determined spectrophotometrically. These higher concentrations of DNA solutions were used for the preparation of DNA complexes with polypeptides or polyamines.

Other Stock Solutions

A 2 M glycine stock solution (in HPLC water) and a stock solution containing 2 M ethanolamine hydrochloride and 1 M sodium acetate, pH = 6.9, were used to catalyze the formation of Lac, a stable product of the C4´ pathway DNA sugar damage. The following stock solutions were also prepared in HPLC-grade water: 2 M putrescine dihydrochloride, 100 mM

spermine tetrahydrochloride, 100 mM polyLys, and 100 mM poly(Lys, Tyr) hydrobromide. These were used for preparation of complexes of these polycations with DNA. A saturated stock solution of salmon protamine sulfate (salmine) was prepared for the precipitation of DNA. All these solutions were stored at 4^{o}C.

Fricke Dosimetry

Fricke Dosimetry is based on the chemical conversion of Fe^{2+} to Fe^{3+} by hydroxyl radicals produced by radiolysis of aqueous solutions. Fe^{3+} shows a characteristic absorption maximum at 303 nm while Fe^{2+} also has some residual absorption at this wavelength. For this reason, the difference of molar absorptivities of these two ions is required; " [= 2201 M^{-1} cm^{-1}. When Fricke solutions are X-irradiated, Fe^{3+} accumulates linearly with dose when doses are in the range of 0 to ~400 gray (Gy), so that the slope of the plot of optical density at 303 nm vs. time (d[OD_{303}]/dt), is proportional to the dose rate (dD/dt), where D is the irradiation dose delivered to the solution.

100 μL of 1 mM $FeSO_4$ in 0.4 M H_2SO_4 was placed into 2 mL Wheaton ampoules and X-irradiated during time periods of 0 (control), 10, 20, 30, 40, 50, and 60 s. Each of these seven samples was analyzed using the Cary 100 UV-vis spectrophotometer between 250 nm to 450 nm for the accumulation of Fe^{3+}, and the optical density of the samples was plotted as a function of irradiation time. The regression line obtained was then used to evaluate the dose of the X-ray instrument using Equation 2.6.The derivation of Equation 2.6 is shown below.

Applying the Lambert-Beer law, the absorbance of the Fe^{3+} cation may be evaluated as shown in Equation 2.1.

$$OD_{303} = \varepsilon_{303} \times l \times [Fe^{3+}] \quad (2.1)$$

Equation 2.1 can then be differentiated with respect to time to yield Equation 2.2

$$\frac{\partial OD_{303}}{\partial t} = \varepsilon_{303} \times l \times \frac{[Fe^{3+}]}{\partial t} \quad (2.2)$$

where $\partial OD_{303}/\partial t$ is the rate of change of absorbance with time, which stands for the slope of the regression line obtained by plotting OD_{303} vs. time, while $\partial[Fe^{3+}]/\partial t$ is the rate of accumulation of Fe^{3+} with time.

The rate of accumulation of Fe^{3+} may be written as the product of the density of the mixture, the radiation chemical yield of Fe^{3+} ($G(Fe^{3+})$), and the rate of change of dose with respect to time, $\partial D/\partial t$:

$$\frac{[Fe^{3+}]}{\partial t} = \rho \times G(Fe^{3+}) \times \frac{\partial D}{\partial t} \quad (2.3)$$

At 298.15 K and atmospheric pressure, the density of a standard Fricke solution may be approximated to 1 kg L^{-1}, which is approximately the same as that of water, while the radiation chemical yield of Fe^{3+} is known to be equal to 1.5 x 10^{-6} mol J^{-1}.[141] Substituting these values in Equation 2.3, we obtain:

$$\frac{[Fe^{3+}]}{\partial t} = 1kg\ L^{-1} \times 1.5 \times 10^{-6} mol\ J^{-1} \times \frac{\partial D}{\partial t} \quad (2.4)$$

Substituting Equation 2.4 in Equation 2.2, we obtain:

$$\frac{\partial OD_{303}}{\partial t} = \varepsilon_{303} \times l \times 1kg\ L^{-1} \times 1.5 \times 10^{-6} mol\ J^{-1} \frac{\partial D}{\partial t} \quad (2.5)$$

Substituting for ε_{303}, l, and solving for $\partial D/\partial t$ yields

$$\frac{\partial D}{\partial t} = 302.89\ J\ kg^{-1} \times \frac{\partial OD_{303}}{\partial t} \quad (2.6)$$

Where the units J kg^{-1} are equivalent to gray.

The data from the X-ray Fricke dosimetry were plotted, and the resulting regression line (OD_{303} = 0.0359t + 0.2852) was used to evaluate the dose rate of the X-ray

instrument using Equation 2.6. The data and plot for OD_{303} vs. time can be seen in Table 2 and Figure 16, respectively.

Table 2: Optical Density of the Irradiated Solution as a Function of Irradiation Time

Irradiation time, s	OD_{303}
0	0.216
10	0.681
20	1.062
30	1.351
40	1.759
50	2.022

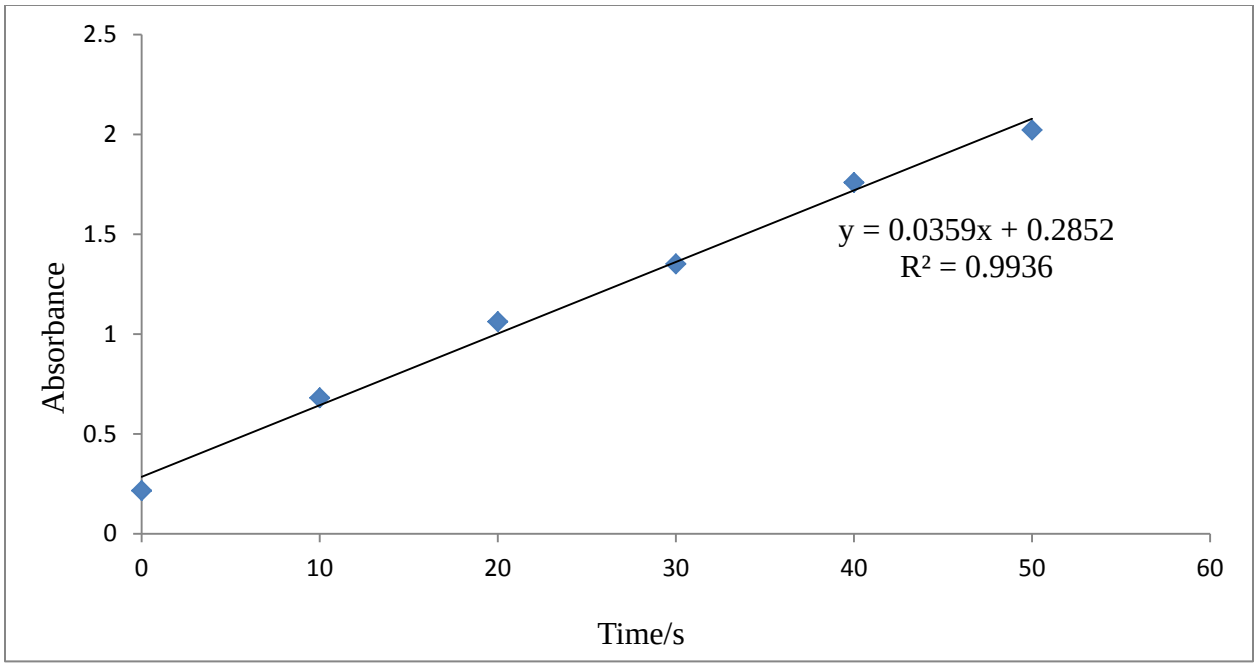

Figure 16: The Fricke dosimetry dose-response curve

Sample Preparation and X-Irradiation Procedures

Dilute Solutions Preparation and X-Irradiation Procedures

DNA Dilute Solution. A 200 µL of 10 mM DNA stock solution was placed into a 2 mL flat-bottom Wheaton ampoule. The samples were X-irradiated at room temperature from the bottom using an X-ray Philips tube with a tungsten anode. The tube was operated at 55 kV and 20 mA that produced a dose rate of 10.87 Gy/s (measured by Fricke dosimetry). Dilute solutions were X-irradiated at doses from 0 Gy to 0.65 kGy.

DNA-Putrescine Dilute Solution. A 6.70 mL of 15 mM DNA, 30 µL of 2 M putrescine dihydrochloride, and 3.27 mL of HPLC-grade water were mixed to make 10 mL final solution containing 10 mM of DNA and 5 mM of putrescine dihydrochloride. The mixture was briefly vortexed to ensure homogeneity, and neither precipitation nor cloudiness was observed. The final

solution was a mixture of 1:1 charge ratio of DNA/putrescine dihydrochloride. The solution was stored at 4^{o}C or kept on ice when needed.

DNA or DNA-Putrescine Viscous Solution Preparation and X-Irradiation

A 200 µL of DNA stock solution (10 mM) or DNA-putrescine stock solution in phosphate buffer, pH 6.9, were added into 2 mL flat bottom Wheaton ampoules and placed in a mini-desiccator containing sodium hydroxide pellets. The system was placed under vacuum for about 30 min and left overnight at 4^{o}C for the DNA solutions to dry into films. The following day, 20 µL of HPLC-grade water was added to the dry samples and left overnight at 4^{o}C for the samples to equilibrate. The following day, homogeneous viscous solutions were formed.

The samples were X-irradiated from the bottom at room temperature. DNA viscous solutions were irradiated at doses from 0 Gy to 2.6 kGy.

DNA-Polycations Suspensions Preparation and X-Irradiation Procedures

DNA-Protamine Suspension Preparation. A 330 g of salmon testes sperm nuclei were crushed in a mortar using a pestle, with a stepwise addition of 2 M sodium chloride solution. A total volume 30 mL of 2 M sodium chloride solution was added. The mixture was transferred into a 50 mL centrifuge tube and left for two days at 4^{o}C to soak. On the third day, the sample was filtered using a glass microfiber filter (from Whatman) to remove undissolved cell components. The filtrate was transferred into a dialysis tube and dialyzed overnight in a cold room (Department of Biological Sciences, ETSU) against 1 M sodium chloride in phosphate buffer, pH 6.9. The next day, the solution was still clear, and the 1 M sodium chloride in phosphate buffer was replaced by 800 mM sodium chloride solution in phosphate buffer, pH 6.9,

and again dialyzed overnight in the cold room. The following day, the solution was still clear and the 800 mM sodium chloride was replaced by a 400 mM sodium chloride solution in phosphate buffer, pH 6.9, and the dialysis was left overnight in the cold room. The following day, the solution in the dialysis tube was cloudy. It was then transferred into a 50 mL centrifuge tube and 10 mL of 10 mM phosphate buffer was slowly added. Formation of a fine precipitate was observed. The sample was then centrifuged with a Labconco Centrivap Concentrator and the supernatant was discarded. 1 mL of 10 mM phosphate buffer solution, pH 6.9, was added to the precipitate and briefly vortexed. As a result, 1 mL of DNA-protamine suspension was obtained. The amino acid composition of salmine is shown in Table 3.

Table 3: Structural Composition of Salmine[142]

Amino Acids	Percent composition	Number of residues
Isoleusine	0.44	1
Alanine	0.45	1
Valine	1.40	3
Glycine	1.80	4
Serine	3.12	7
Proline	2.70	6
Arginine	89.80	50
Total	99.71	72

DNA-PolyLys Suspension Preparation. A 5 mL of 15 mM DNA stock solution was placed into a 15 mL centrifuge tube and 800 µL stock solution of polyLys hydrochloride was added dropwise, with the mixture being vortexed after each addition. A fibrous precipitate of DNA-polyLys was observed. 4.2 mL of stock solution of 5 M sodium chloride was added for the final concentration of sodium chloride in the mixture equal to 2.1 M. The precipitate was dissolved and a clear solution obtained due to the increased ionic strength. The mixture was transferred into a dialysis tube and dialyzed against 0.7 M sodium chloride solution in 10 mM phosphate buffer for 6 hours at room temperature. Formation of a fine precipitate was observed. The mixture was transferred into a 15 mL centrifuge tube, centrifuged and the supernatant was discarded.1 mL stock solution of 10 mM phosphate buffer was added and the sample was briefly vortexed.1 mL DNA-polyLys suspension was thus obtained. The structure of polyLys HCl is shown in Figure 17.

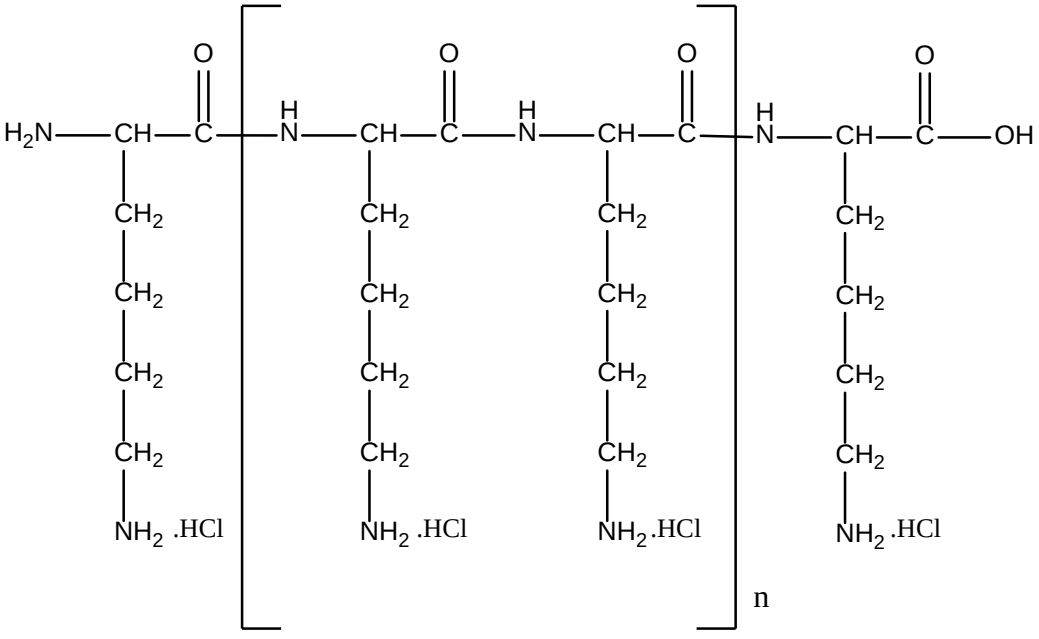

Figure 17: Structure of polyLys hydrochloride

Measuring the Concentration of DNA in the Suspensions. A 10 µL of the DNA-protamine/DNA-polyLys suspension was placed in a 15 mL centrifuge tube and diluted 500-fold with a 2 M sodium chloride solution. The suspensions became clear; the precipitate dissolved since the increase in the ionic strength of the solution decreased DNA-protamine/DNA-polyLys electrostatic interactions. The optical density of DNA was measured spectrophotometrically. Approximately 1 mL DNA-protamine/DNA-polyLys suspension was then diluted to make a 10 mM (in DNA nucleotides) stock solution of DNA-protamine/DNA-polyLys suspension. The suspensions were stored at 4^{o}C and/or on ice until needed.

DNA- Poly(Lys, Tyr) Suspension Preparation. A 5 mL of 5 M sodium chloride stock solution was placed in a 15 mL centrifuge tube. 300 µL stock solution of 100 mM poly(Lys, Tyr) hydrobromide was added to the sodium chloride solution and briefly vortexed. The solution turned cloudy due to the poor solubility of poly(Lys, Tyr) hydrobromide in solutions with high concentrations of inorganic salts. 3 mL of stock solution of 10 mM DNA was added to the mixture and the sample was briefly vortexed to ensure homogeneity. The mixture remained cloudy after addition of the DNA solution. The overall mixture was then transferred into a dialysis tube and dialyzed overnight against a 10 mM stock solution of phosphate buffer at room temperature. The next day, the mixture was centrifuged and the supernatant discarded. The precipitate was washed with 10 mL phosphate buffer to remove any unbound poly(Lys, Tyr). The mixture was again centrifuged and the supernatant discarded. 1 mL of 10 mM phosphate buffer stock solution was then added to the precipitate and the sample was briefly vortexed. The suspension was stored at 4^{o}C and/or on ice until needed. The structure of poly(Lys, Tyr) is shown in Figure 18.

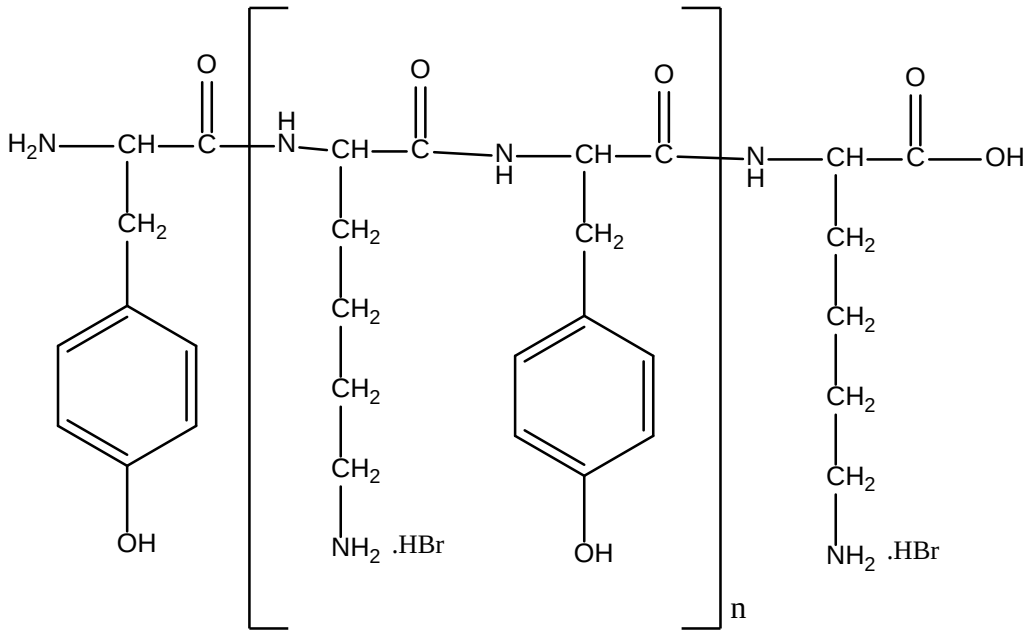

Figure 18: Structure of the alternating copolymer (Lys, Tyr)

Measuring the Concentration of DNA in the Suspension. Because this suspension was not soluble in 5 M sodium chloride, a 2 M stock solution of ethanolamine hydrochloride was used instead of sodium chloride solution. 10 µL of the suspension was placed into a 15 mL centrifuge tube and diluted 500-fold with a 2 M stock solution of ethanolamine hydrochloride. The mixture was briefly vortexed to ensure homogeneity, and the mixture became clear (all visible precipitate dissolved). The concentration of DNA was measured spectrophotometrically and approximately 1 mL of the suspension was diluted to make a 10 mM (in DNA nucleotides) poly(Lys, Tyr) suspension. The stock suspension was stored at 4^{o}C and/or on ice until needed. The suspension was briefly vortexed each time before use.

DNA-Spermine Suspension Preparation. A 100 µL of 10 mM DNA stock solution was placed into a 15-mL centrifuge tube and 10 µL of 100 mM spermine tetrahydrochloride stock

solution was added into the tube. Formation of a fibrous precipitate was observed. 60 µL of 1 M sodium chloride solution was added to the mixture. The precipitate dissolved completely and a clear solution was obtained. A total of 570 µL of 10 mM phosphate buffer stock solution was gradually added to the mixture in small aliquots. First, 15 x 20 µL aliquots were added followed by vortexing each time. The solution became cloudy, and finally 3 x 90 µL aliquots were added with vortexing; the solution remained cloudy. The sample was left for about 40 min at room temperature and a fine precipitate was formed. The sample was centrifuged and the supernatant discarded. 200 µL of 10 mM phosphate buffer solution was added to the sample followed by brief vortexing. The sample was again centrifuged and the supernatant discarded. 100 µL of 10 mM phosphate buffer solution was added to the washed precipitate and the sample was placed on ice prior to irradiation.

Irradiation Procedure. The suspensions were briefly vortexed when needed. 100 µL of the suspension was X-irradiated at doses up to 2.6 kGy.

Post-Irradiation Sample Treatments

After X-irradiation, samples were subjected to post-irradiation heat treatments at 70 ^{o}C in the presence (when required) of spermine, glycine, or ethanolamine to yield HPLC-detectable low molecular weight sugar damage products (SDP) of ^{Ï}OH -damage to DNA. Spermine treatment was used for naked DNA samples or for soluble DNA-polypeptide or polyamine for quantification of the C1´ and C5´ pathways based on the analysis of the yields of 5-MF and Fur, respectively. For suspensions, samples were heated without addition of spermine since positively charged groups in these complexes are Lewis acids and thereby serve as catalysts for 5-MF and Fur release. Glycine or ethanolamine treatments were used for quantification of the C4´ pathway.

Glycine was used for naked DNA samples or for soluble DNA- polypeptide or polyamine samples. For suspensions, ethanolamine was used for quantification of the C4´ pathway instead of glycine. The production of low molecular weight sugar damage products was also accompanied by release of free unaltered bases.

Quantification of C1´ and C5´ Pathways

Heat Treatment with Spermine. After irradiation, an aliquot from each sample was placed in a labeled plastic tube and a required volume of 100 mM spermine + 40 µL uracil (used as an HPLC internal standard) was added to yield a final concentration of spermine equal to 10 mM. The samples were briefly vortexed and precipitates formed. The samples were then heated for 35 min in a 70^{o}C water bath. Following heating, the samples were incubated on ice for 1 min and 10 µL saturated protamine sulfate solution was added to precipitate any unbound DNA. The samples were again left on ice for 10 min to allow for complete precipitation. Following complete precipitation, the samples were centrifuged for about 2 min, and the supernatant (typically 150 µL) was transferred to HPLC vials with plastic inserts for the 5-MF, Fur, and FBR analysis.

Heat Treatment Without Spermine. Following irradiation, samples were heated for 35 min in a 70^{o}C water bath. 10 µL stock solution of 50 µM uracil was added to the samples after heating and briefly vortexed to ensure homogeneity. After incubation on ice for about 2 min, 7 µL of saturated protamine sulfate was added to precipitate, remaining (if any) unbound DNA in the suspension. The samples were incubated on ice for 10 min to allow complete precipitation of DNA. Following complete precipitation, the samples were centrifuged for about 2 min and the supernatant was transferred to HPLC vials with plastic inserts for 5-MF, Fur, and FBR analysis.

Quantification of the C4´ Pathway

Heat Treatment with Glycine. After irradiation, an aliquot from each sample was placed into a labeled plastic tube and 10% of the final volume of the stock solution of 2 M glycine + 40 µM uracil was added. The samples were briefly vortexed to ensure homogeneity and heated for 20 min in 70^{o}C water bath. Following heating, the samples were incubated on ice for 2 min and 20 µL of saturated protamine sulfate solution was added to precipitate the DNA. The samples were again left on ice for 10 min to allow complete precipitation of DNA. Following complete precipitation, the samples were centrifuged for 2 min and the supernatant was transferred into HPLC vials with plastic inserts for Lac analysis.

Heat Treatment with Ethanolamine. After irradiation, an aliquot from each sample was placed into a labeled plastic tube and 50 µL of the stock solution of 2 M ethanolamine was added. The samples were briefly vortexed and a clear solution was obtained (precipitates dissolved due to the increased ionic strength). The samples were then heated for 30 min at 70^{o}C. Following heating, the samples were incubated on ice for 2 min and 20 µL stock solution of 50 µM uracil was added. 40 µL of saturated protamine sulfate was added, samples were briefly vortexed, and left on ice for 10 min to allow complete precipitation of DNA. Following complete precipitation, the samples were centrifuged for 2 min and the supernatant was transferred into HPLC vials with plastic inserts for Lac analysis.

HPLC Analysis

A two-solvent system was used for all HPLC analysis programs consisting of 40 mM aqueous ammonium acetate buffer (aqueous mobile phase) and 80% v/v aqueous acetonitrile (organic mobile phase). A linear acetonitrile gradient was used to elute the products at a flow rate of 1 mL/min, with the column temperature set at 30^{o}C. Samples in an autosampler tray were

incubated at 4^{o}C. The HPLC was equipped with a two-lamp photodiode array detector (PDA) composed of a deuterium lamp for the UV wavelength range and a tungsten filament lamp for visible wavelength.

Separation and Analysis of Lac, 5-MF, Fur, and FBR using HPLC

For HPLC separation and analysis, 70-150 µL of supernatant was usually transferred into a labeled HPLC vial containing a 200 µL plastic insert. The injection volumes were usually in the range of 50-100 µL. The HPLC column was equilibrated for about 40 min with 40 mM ammonium acetate buffer. A single conditioning run (no sample injection) was performed immediately after equilibrating the column.

A linear gradient of 80% v/v aqueous acetonitrile from 0% to 20% over 15 min was applied to elute all the low-molecular weight products of interest. The concentration of the organic mobile phase was then increased to 40% to wash the column for 2 min, and then the column was equilibrated with 40 mM ammonium acetate for 10 min. This gradient is shown in Figure 19. These products were identified based on the comparison of their UV-vis spectra and retention time with authentic samples.

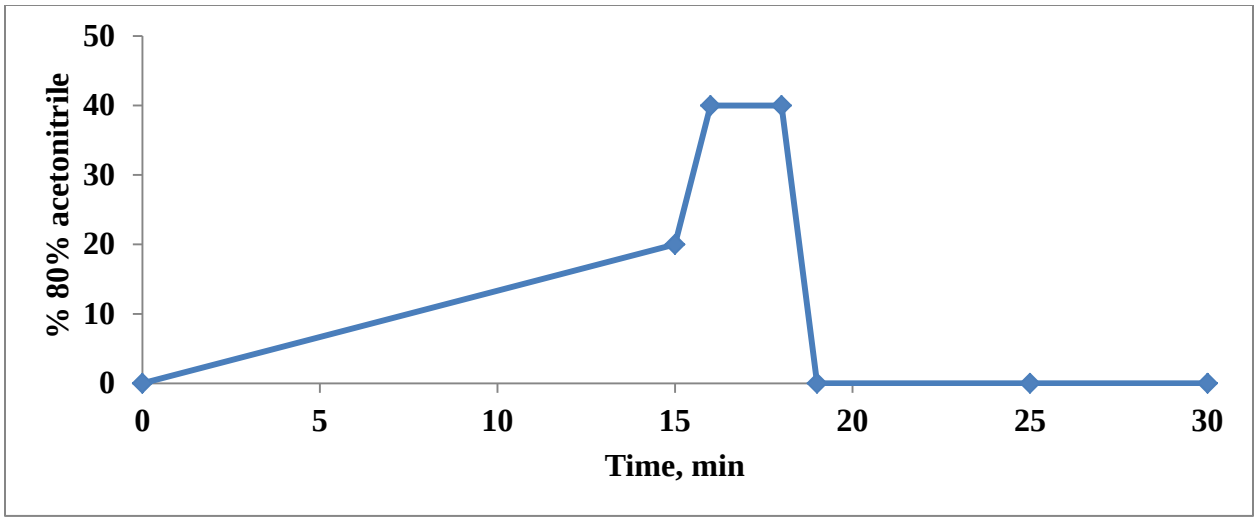

Figure 19: Gradient used to elute all the low-molecular weight products of interest

Analysis of HPLC Chromatograms. Uracil was used as an internal standard due to its absence in DNA. With a known concentration of uracil in each sample, the peak areas of SDP and FBR from HPLC chromatograms could be converted into concentrations using Equation 2.7 derived from the Lambert-Beer law.

$$\frac{A_X}{A_U} = \varepsilon_{X,254\,nm} \times l \times \frac{[X]}{\varepsilon_{U,254\,nm} \times l \times [U]} = \varepsilon_{X,254\,nm} \times \frac{[X]}{\varepsilon_{U,254\,nm} \times [U]} \qquad (2.7)$$

where A_X is the area under the assigned chromatographic peak of compound X, ε is the extinction coefficient, and [X] is the concentration of compound X. Equation 2.7 can be rearranged to solve for [X] as shown in Equation 2.8.

$$[X] = [U] \times \frac{A_X}{A_U} \times \frac{\varepsilon_{U,254\,nm}}{\varepsilon_{X,254\,nm}} \qquad (2.8)$$

Extinction coefficients for each of these low-molecular weight products were determined by the Roginskaya research group in 40 mM ammonium acetate, pH 6.9, and they are summarized in Tables 4 and 5.

Table 4: Molar Extinction Coefficients of DNA Sugar Damage Products (SDP) in 40 mM Ammonium Acetate, pH 6.9

SDP	Molar Extinction Coefficient at 254 nm, $M^{-1}cm^{-1}$
Fur	5500
Lac	8700
5-MF	10830

Table 5: Molar Extinction Coefficients of Native DNA Bases and Uracil in 40 mM Ammonium Acetate, pH 6.9

Bases	Molar Extinction Coefficients at 254 nm, $M^{-1}cm^{-1}$
Adenine	11990
Cytosine	5070
Guanine	9280
Thymine	6690
Uracil	7950

CHAPTER 3

RESULTS AND DISCUSSION

Dilute Solutions of DNA and DNA-Putrescine

Putrescine exists as a dication in the pH range used in this research (pH 6.9). The 1:1 charge ratio of 10 mM DNA-putrescine stock solution prepared, as described in Chapter 2, was based on the assumption that putrescine binds to DNA using the two terminal positively charged protonated amine groups. The interaction between DNA and putrescine is believed to be purely electrostatic, though the exact structure of this complex is not known.[143] No precipitate was observed when putrescine was added to DNA due to the low binding affinity of putrescine to DNA ($K_b \sim 1 \times 10^{-3}$ M^{-1} [143]).

Hydroxyl radicals were used as the oxidant in this research. They are generated from water with a radiation chemical yield of 0.265 μmol/J[17] by radiolysis of aqueous solutions. Aliquots of 10 mM DNA (control) and 10 mM (in DNA nucleotides) of 1:1 charge ratio of DNA-putrescine dilute solutions were prepared and X-irradiated at doses from 0 to 0.65 kGy (see protocol in Chapter 2). After irradiation, samples were divided into two aliquots, and one was heat treated in the presence of spermine to catalyze the formation of 5-MF and Fur (see Figures 10 and 11, respectively). The other aliquot was heat treated in the presence of glycine to derivatize C4´-OAS to Lac (see Figure 12). The resulting low-molecular weight sugar damage products (SDP), in addition to the four unaltered nucleobases and uracil were analyzed using reverse phase HPLC. Labeled representative chromatograms are shown in Figure 20 and 21. The control chromatograms (no irradiation, panels A and D) show the uracil peak only as expected.

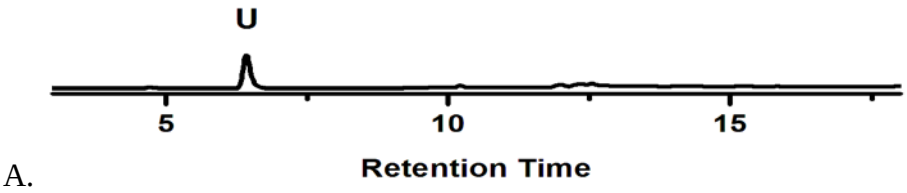

A.

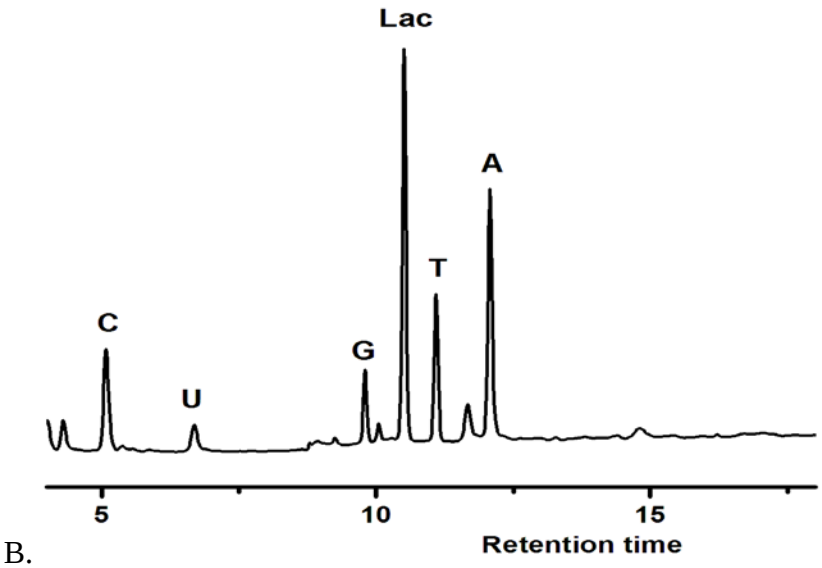

B.

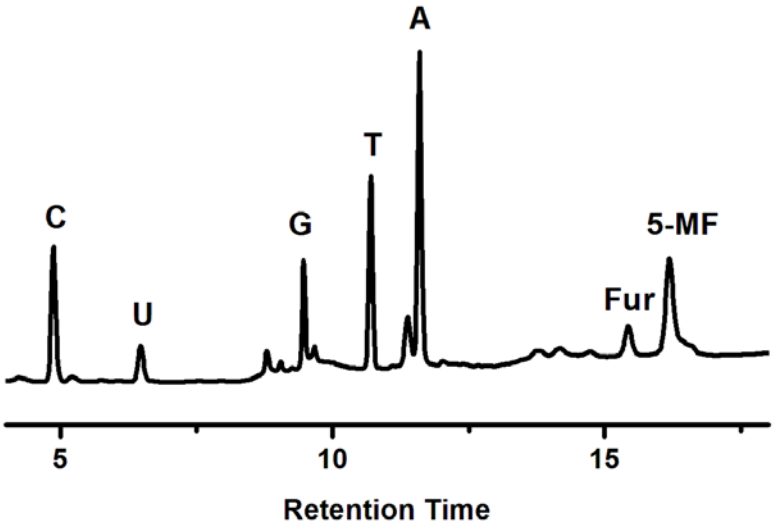

C.

Figure 20: HPLC representative chromagrams of X-irradiated samples of 10 mM dilute DNA. A) catalytic heat treatment after 0 Gy of X-irradiation (control), B) glycine heat treatment after 0.65 kGy of irradiation, and C) spermine heat treatment after 0.65 kGy of irradiation.

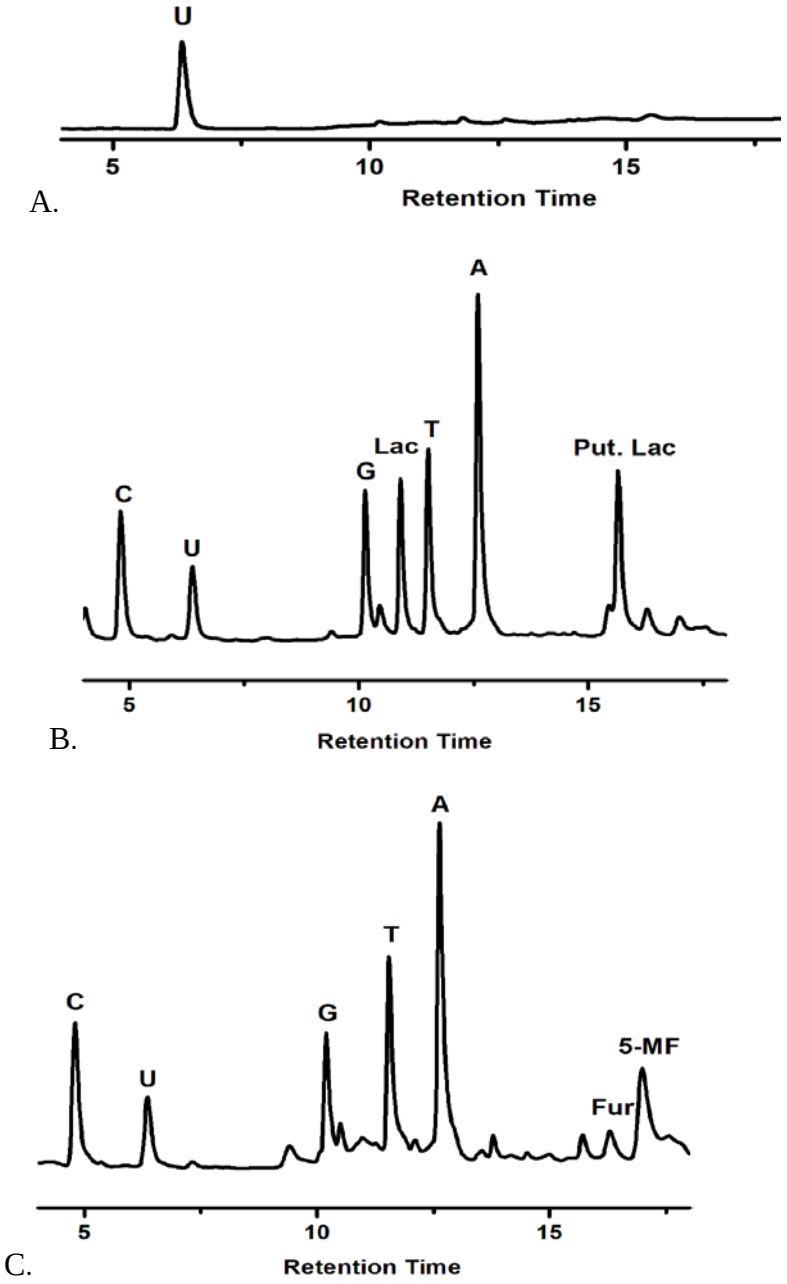

Figure 21: DNA-putrescine representative chromatograms. (A) glycine heat treatment after 0 Gy of irradiation, (B) glycine heat treatment after 0.65 kGy of irradiation, and (C) spermine heat treatment after 0.65 kGy of irradiation.

In addition to the four nucleobases, uracil, and Lac, the chromatogram in panel E (which represents solutions of DNA-putrescine X-irradiated and then heat treated with glycine) shows an additional peak labeled “Put-Lac”. This “Put-Lac” stands for putrescine Lac, which is the Lac that is formed by derivatizing C4´-OAS to Lac using putrescine. This is possible because putrescine has two primary amine groups that bind with low affinity to DNA as judged by the fact that no precipitate was observed after addition of putrescine to DNA. The low binding affinity of putrescine to DNA can also be seen in chromatogram E since the peaks of 5-MF and Fur are very low compared to their peaks in chromatogram F with the same irradiation dose. This evidence confirms that putrescine does not bind to DNA strongly enough to be used as a catalyst for 5-MF and Fur release (unlike spermine). We can therefore conclude that putrescine in the DNA-putrescine compexes remains mostly in solution in its free form. This is the reason why putrescine contributes significantly as a derivatizing agent to convert C4´-OAS into Lac.

The peaks of the individual SDP (Lac, 5-MF, and Fur), the individual FBR (adenine, cytosine, guanine, and thymine), and uracil were integrated and the areas under the peaks were converted into concentrations using Equation 2.8 (see Chapter 2). Several replicates were performed (duplicates or triplicates) using the same experimental conditions for the analysis of the yields of individual SDP, total SDP, individual FBR, and total FBR. Total SDP in this research refers to the sum of Lac, 5-MF, and Fur, as opposed to the total SDP which also include malondialdehyde (MDA)[54] which was not quantified in this research. The resulting data were statistically analyzed and the average concentrations of the individual SDP, the total SDP, and total FBR were plotted against the radiation dose. The peak areas of Lac from glycine and Lac from putrescine were summed up and converted into the total concentration of Lac using the extinction coefficient of Lac from glycine. This summation was based on the assumption that

since both types of lactams contain the same aromatic ring, which is mainly responsible for the absorption of light, it is reasonable to assume that both products have nearly the same extinction coefficients.

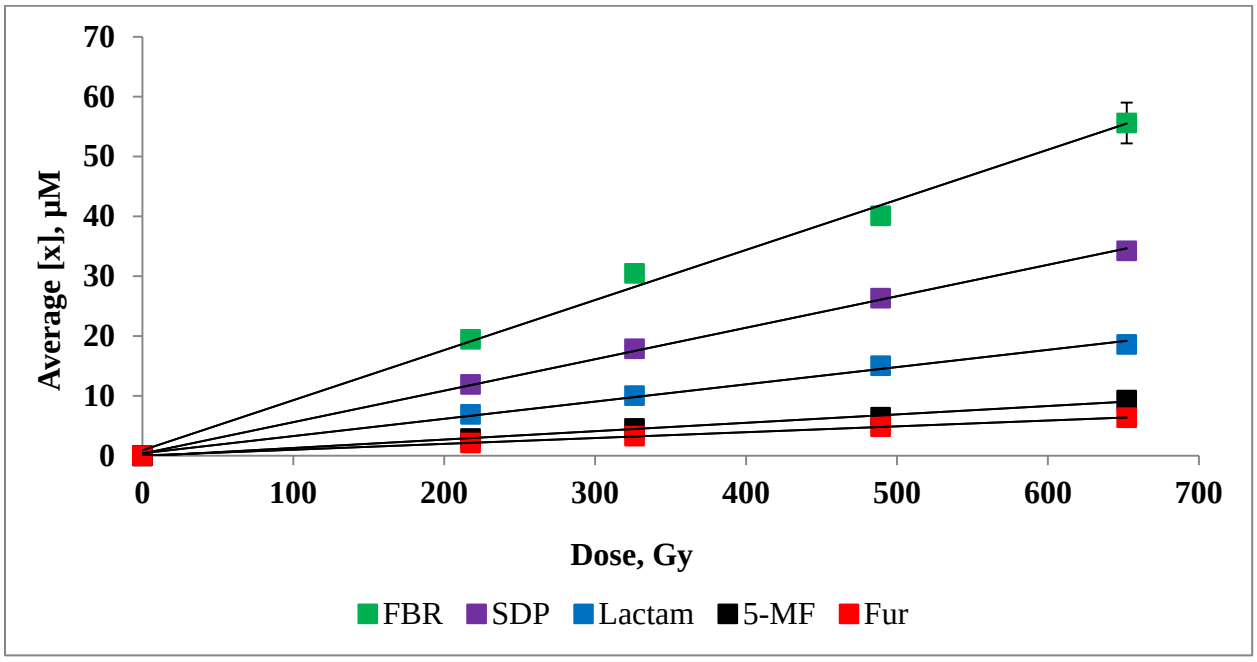

A.

Figure 22 (continued on the next page)

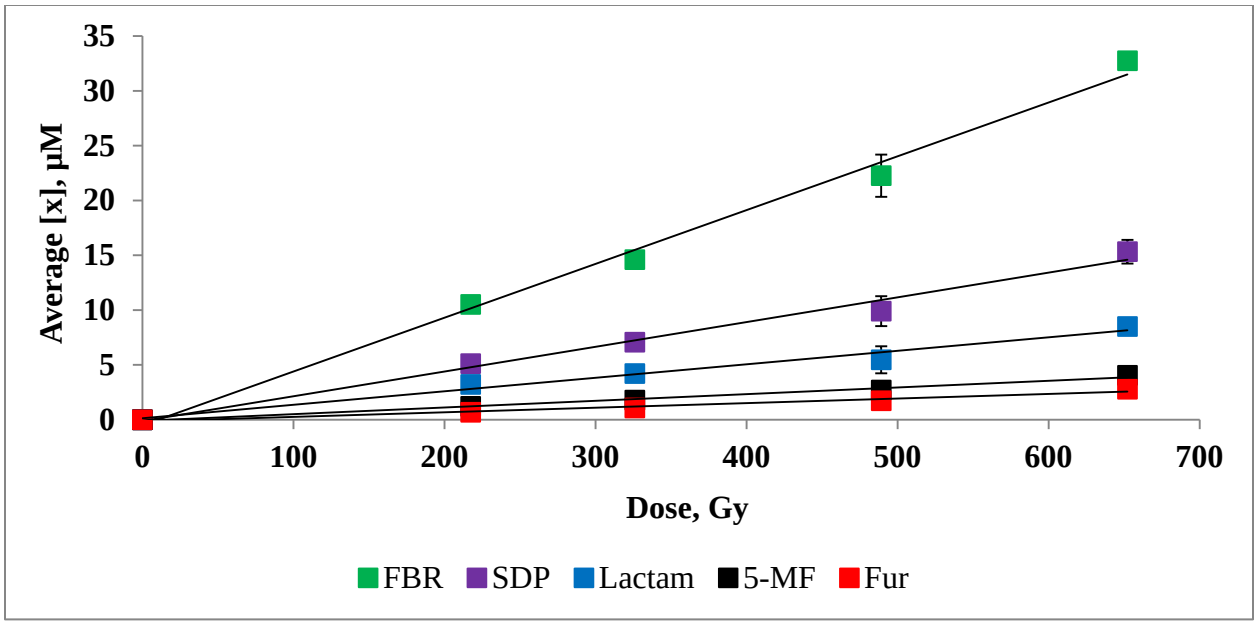

B.Figure 22: A plot of average concentrations of individual SDP, total SDP, and FBR as a function of X-irradiation dose. (A) DNA dilute solution (control), (B) DNA-putrescine dilute solution.

As can be observed in the plots in Figure 22, there is linear accumulation of FBR, of individual SDP, and consequently of total SDP as a function of X-irradiation dose when the dose does not exceed 650 Gy. In each case where the error bars are not visible, it means they are smaller than the symbol used. The radiation chemical yields (in nmol/J) were calculated from the slopes of the regression lines in Figure 22 by approximating the density of the solutions to that of water (1 g/mL). The relative contribution of each SDP analyzed in this research was calculated as the percent ratio of the radiation chemical yield of each individual SDP and the radiation chemical yield of the total SDP. The ratios obtained were therefore intepreted as the percent contribution of each sugar damage pathway. Radiation chemical yields and percent contributions of each characteristic product of sugar damage are summarized in Table 6.

Table 6: Radiation Chemical Yields and Percent Contributions of Individual SDP in DNA (control) and DNA-Putrescine Dilute Solutions

	Radiation chemical yield (nmol/J)		Percent contribution (%)	
DNA damage products	DNA (control)	DNA-putrescine	DNA (control)	DNA-putrescine
Lac	29.0	12.0	54.7	54.5
5-MF	14.0	6.0	26.4	27.3
Fur	10.0	4.0	18.4	18.2
SDP	53.0	22.0	N/A	N/A
FBR	84.0	49.0	N/A	N/A

The yields of FBR are usually used as an internal benchmark of DNA strand breaks due to the fact that the majority of free radical-initiated damages to the DNA sugar backbone are capable of destabilizing the glycosidic bond[49] and cause the release of an unaltered free base and a damaged DNA sugar, which later can be converted into a strand break.[49,54] It is therefore understandable that the yield of FBR should be greater than the yield of total SDP measured in this research since not all DNA sugar damage products were analyzed in the present work (for example, MDA).

There is a significant decrease in the radiation chemical yield of total SDP (22 nmol/J) and FBR (49 nmol/J) in DNA-putrescine samples compared to that observed with free DNA samples (53 nmol/J for SDP and 84 nmol/J for FBR). The latter values are in good agreement with earlier published radiation chemical yields on individual products in solutions of naked DNA.[54] The yield of total SDP in DNA-putrescine samples is about 2.3-fold lower than the yield

in free DNA samples, which indicates that putrescine does protect DNA from the attack of hydroxyl radicals.

The percent contributions of individual SDP to the total SDP were plotted as column bars (Figure 23).

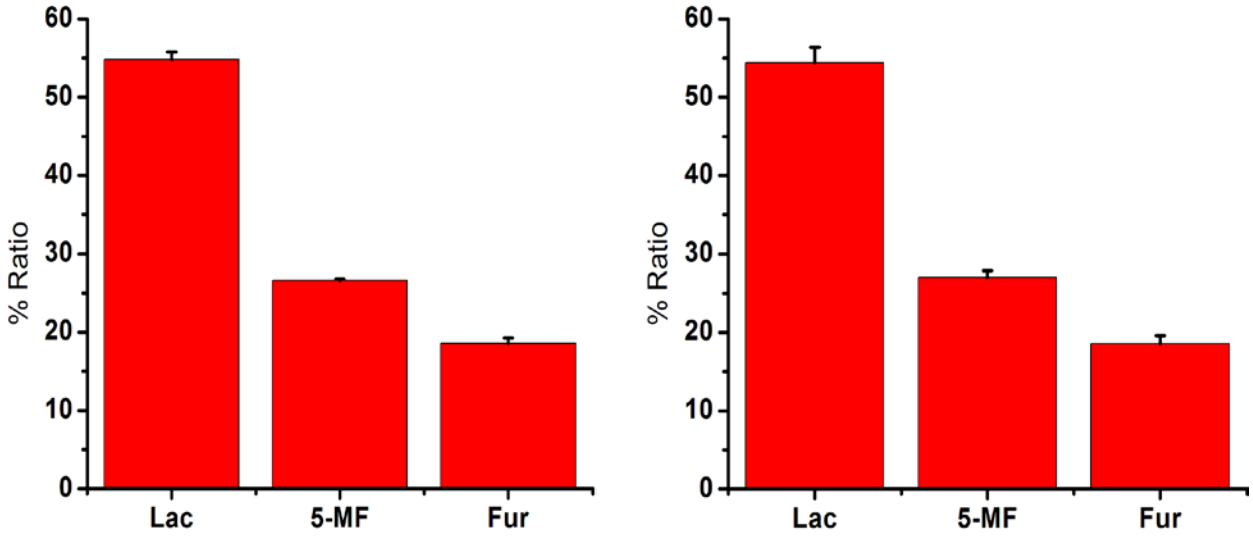

A. G(SDP) = 53 nmol/J **B.** G(SDP) = 22.6 nmol/J

Figure 23: Bar plots of the percent contributions of individual SDP to the total SDP in (A) DNA (control) and (B) DNA-putrescine

It is obvious that production of Lac dominates in these systems, followed by 5-MF, and lastly Fur. These results match the order for the preferential site for hydrogen abstraction, C4´> C1´>C5´, as observed in experiments with X-ray-generated hydroxyl radicals performed by Roginskaya's research group.[54] The percent contributions of individual SDP in free DNA solutions and in DNA-putrescine solutions are very similar, though the radiation chemical yield of the total SDP in DNA-putrescine complex (22.6 nmol/J) is more than 2-fold lower compared to that observed with naked DNA (53 nmol/J). Due to the reported inability of putrescine to efficiently bind and compact DNA[114], the protection of DNA in this case is solely attributed to

scavenging of hydroxyl radicals by putrescine in the bulk. This results in a decrease of the steady-state concentration of hydroxyl radicals. Modification of individual pathways of DNA sugar damage is therefore not expected.

In summary, with the decrease in the yields of total SDP and no variation in percent contribution of individual sugar damage pathways on going from free DNA to DNA-putrescine solutions, the protection of DNA in this system can be attributed to hydroxyl radical scavenging by putrescine in the bulk.

DNA and DNA-Putrescine Concentrated Solutions

DNA and DNA-putrescine concentrated solutions were prepared as described in the protocol in Chapter 2. Concentrated solutions contain very low amount of water (compared to dilute solutions), and therefore higher doses of irradiation were required. Concentrated solutions were X-rayed at doses from 0 Gy to 2.6 kGy. Chromatograms were similar to those of DNA and DNA-putrescine dilute solutions. The average concentrations of individual SDP, total SDP, and FBR were plotted as a function of irradiation dose and the plots are shown in Figure 24.

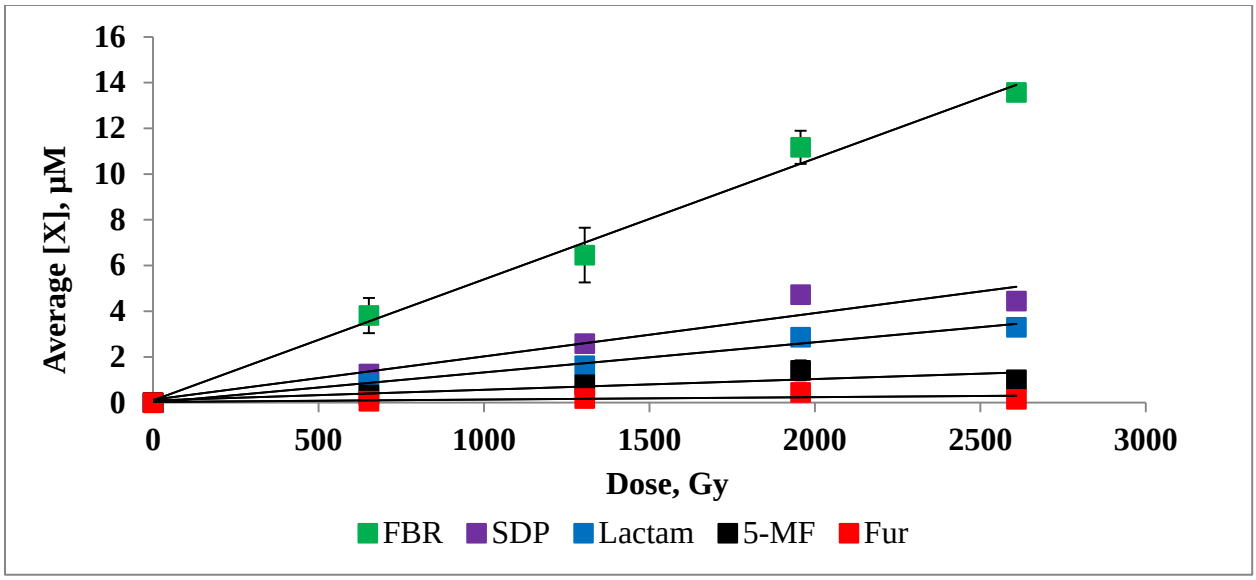

A.

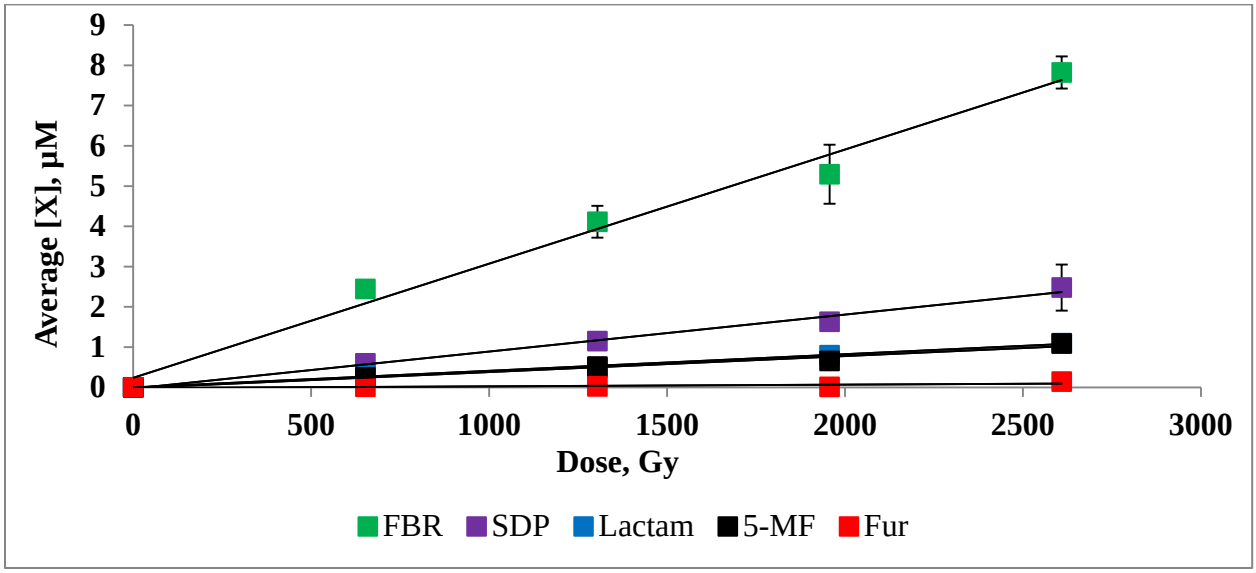

B.

Figure 24: Plots of average concentrations of individual SDP, total SDP, and FBR for (A) concentrated solution of DNA (control) and (B) concentrated solution of DNA-putrescine

The obsarance of error bars in some series means that the size of error bars are smaller than the size of the symbol used. All plots in Figure 24 show that there is a linear dose dependence of the yields of individual SDP, total SDP, and FBR for the irradiation doses up to 2.6 kGy. The slopes of the regression lines were not converted into radiation chemical yields for concentrated solutions since the density of the concentrated solution could not be approximated to that of water. The percent contributions were then calculated as the percent ratios of the slope of the corresponding SDP and the slope of the total SDP. The slopes of the regression lines and percent contributions of each individual SDP to the total SDP are summarized in Table 7.

Table 7: The Slopes of Individual SDP, Total SDP, and FBR and Percent Contributions of each SDP to the Total SDP in Concentrated Solutions

	Slope (μM/Gy)		Percent contribution (%)	
DNA damage products	DNA	DNA-putrescine	DNA	DNA-putrescine
Lac	1.3×10^{-3}	4×10^{-4}	68.4	44.9
5-MF	5.0×10^{-3}	4×10^{-4}	26.3	44.9
Fur	10×10^{-4}	9×10^{-5}	5.30	10.1
SDP	1.9×10^{-3}	8.9×10^{-4}	N/A	N/A
FBR	5.3×10^{-3}	2.8×10^{-3}	N/A	N/A

The percent contributions of each individual SDP to the total SDP are plotted Figure 25.

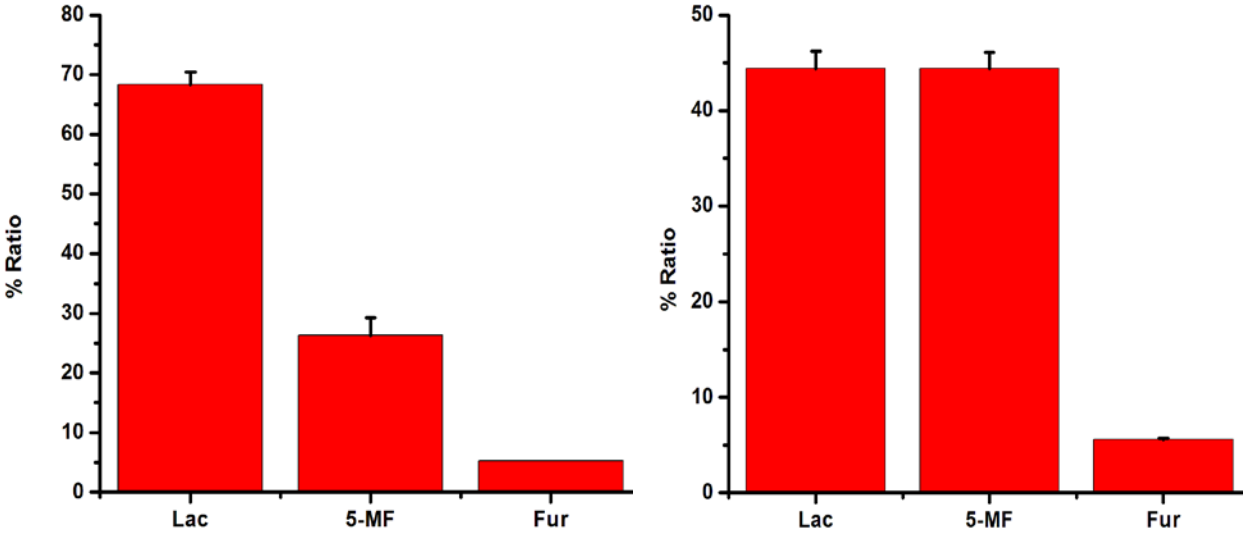

A. **B.**

Figure 25: Bar plots of the percent contribution of individual SDP to the total SDP in (A) DNA concentrated solutions (control), and (B) DNA-putrescine concentrated solutions

Comparison of the percent contribution of individual SDP to the total SDP in dilute DNA solutions and concentrated solutions shows that there is a shift of relative roles of individual pathways of SDP. While the percent contribution of the C1´ pathway remains essentially the same (based on the comparison of the percent yields of 5-MF), there is a pronounced decrease in the percent contribution of the C5´ pathway (based on the comparison of the percent yields of Fur), from 18.4% in dilute solutions to 5.3% in concentrated solutions by the expense of the increase in the percent contribution of the C4´ pathway (based on the comparison of the percent yields of Lac), from 54.7% in dilute solutions to 68.4 % in concentrated solutions.

DNA aggregation can be considered as one of plausible mechanisms of protection of the most surface-exposed C5´ position of the DNA deoxyribose ring. It is generally accepted that DNA aggregation occurs when about 90% of the phosphate groups are neutralized.[118] This

neutralization of DNA negative charges by cations such as sodium ions minimizes the repulsion force between the DNA molecules and allows them to come together to form aggregates. Aggregation of DNA, limits the number of attack sites available to hydroxyl radicals due to reduced surface accessibility and therefore constitutes the DNA “self-protection mechanism”. We can also hypothesize that in aggregated forms of DNA, the C4,-position of one DNA molecule is close enough to the C5,-position of another DNA molecule to allow the C4,-hydrogen to be transferred to the C5,-radical, which is a thermodynamically favorable process since the enthalpy of the C-H bond at the C5, is the highest among other C-H bonds in DNA deoxyribose.[50]

Also, the misbalance between the yields of FBR and total SDP becomes more pronounced in concentrated DNA solutions, with FBR/SDP ratio of ~ 1.6 in dilute solutions and ~ 2.8 in concentrated DNA solutions. This means that the assumed stoichiometric ratio of the 1:1 for free base:SDP product is distorted even more upon concentrating the DNA solutions. This can occur when low-molecular SDP (5-MF, Lac, and Fur) or their DNA-bound precursors (dL, C4´-OAS, or 5-Ald) participate in some side reactions, which decrease the effective concentrations of these sugar damage end products or their intermediates. We can hypothesize that in X-irradiated DNA aggregates formed in concentrated DNA solutions, aldehyde and ketone groups of oxidized DNA lesions can undergo Schiff reactions with amino groups of purines or cytosine of neighboring DNA to form intramolecular crosslinks. Alternatively, free low-molecular SDP can react via the same mechanism. Reaction of Fur with adenines in DNA to form N^6-furfuryladenine, commonly known as kinetin, a hormone with cytokinin acitivity and antiaging effects, is well-known.[144]

The results with DNA-putrescine concentrated solutions show about 2-fold decrease in the yields of total SDP (8.9×10^{-4}) as compared to that observed with naked DNA (1.9×10^{-3}) concentrated solutions. As in dilute solutions, this protection effect is most likely attributed to hydroxyl radical scavenging by putrescine molecules in the bulk. In addition, the percent contribution of individual SDP in DNA-putrescine concentrated solution is different from that observed with dilute solutions and DNA concentrated solution. There is a pronounced growth of the contribution of the C1„ pathway in DNA-putrescine concentrated solutions (based on the relative percent yield of 5-MF), so that the percent contributions of Lac and 5-MF become equal. This significant increase of the relative contribution of 5-MF, led us to the conclusion that there must be an additional DNA protection mechanism involved in concentrated solutions of DNA-putrescine other than the DNA self-protection through aggregation and hydroxyl radical scavenging mechanisms.

The bond energy of a secondary C-H bond is ~390 kJ/mol[138], which is higher than that of the C1´-H bond (~376 kJ/mol), but is close to that of the C4´-H (389 kJ/mol) and C5´-H (>390 kJ/mol) bonds.[50] This suggests a plausible hydrogen transfer from putrescine C-H groups to DNA 2-deoxyribosyl radicals. This hydrogen transfer process will be inefficient for the C1´radical due to the low accessibility of the C1´ position (deeply buried into the DNA minor groove) and the lower energy bond of the C1´-H bond. The C5´ and C4´ radicals will consequently be preferentially repaired by this hydrogen transfer process . It is interesting that the relative role of the C5´ damage pathway (based on the yields of Fur) has somewhat increased in DNA-putrescine concentrated solutions compared to DNA concentrated solutions. It is possible that in the absence of putrescine, DNA “self-protects” its C5´ positions more efficiently. Again, this can be attributed to the C4´ to C5´ intermolecular hydrogen transfer mechanism.

With putrescine shielding DNA molecules and hence decreasing their intermolecular interaction, this intermolecular hydrogen transfer process is suppressed.

The question why this hydrogen transfer process is not observed in DNA-putrescine dilute solutions may be answered by considering increased concentrations of putrescine and DNA in concentrated solutions as compared to dilute solutions, which favors formation of DNA-putrescine complexes. For the repair mechanism to be efficient, hydrogen transfer needs to occur faster than oxygen addition to the 2-deoxyribosyl radicals. Otherwise, oxygen addition will result in formation of more permanent DNA sugar lesions (see Figures 7, 8, and 9 in Chapter 1).

To summarize, hydrogen transfer from putrescine to DNA 2-deoxyribosyl radicals has been demonstrated experimentally for the first time as a plausible DNA repair mechanism in DNA-putrescine concentrated solutions. It was therefore necessary to perform more experiments with positively charged polycations to confirm this assertion. Effective distance between DNA and polycations seems to be a very important factor to consider in this hydrogen transfer process. It is therefore necessary to explore other DNA-polycations preparation methods, that will maximize this parameter.

DNA-Polycation Suspensions

Natural and synthetic polyamines and synthetic polymers (for example, polyLys) have been widely used to condense DNA into nanoparticles for DNA delivery in gene therapy.[145] It is well known that these species condense DNA into nanoparticles in dilute solution.[146-148] This efficient condensation of DNA by these polycations shows the strong interaction of DNA and these polycations. The DNA-polycation suspensions prepared in this research can therefore be considered as nanoparticles suspended in aqueous solution.

Spermine (see Figure 15) is a stronger binder to DNA than putrescine with an approximate binding constant of 3×10^{-2} M^{-1} compared to 1×10^{-3} M^{-1} for putrescine.[143] Spermine exists as a quaternary cation in the range of pH 6.9, used in this research. DNA-spermine suspension was prepared by mixing 10 mM DNA with an excess of spermine (10 mM) to form a precipitate. The precipitate was then dissolved by increasing the ionic strength of the mixture and then the samples were gradually diluted to decrease ionic strength of the solutions until DNA-spermine suspensions were formed (see Chapter 2 for details).

DNA-protamine suspensions were prepared by extraction from salmon sperm nuclei, followed by a series of dialysis as described by the protocol in Chapter 2. Salmon protamine, generally known as salmine, is an oligopeptide made of 72 amino acids with 89.8% being arginine residues (see Table 3 in Chapter 2). So protamine can be visualized as a chain of positively charged arginine groups that can interact with the negatively charged phosphodiester groups of the DNA backbone by electrostatic interactions. It is well known that protamine replaces histones during spermiogenesis and compacts DNA more than histones proteins.[89] It is therefore understandable that at low ionic strength and high enough concentration of protamine (1:1 charge ratio of DNA/arginine), precipitation of the DNA-protamine complex should be observed.[149] Precipitation of DNA was also observed with PolyLys at a 1:1 charge ratio[149] which is the reason why DNA and polyLys were mixed in a 1:1 charge ratio to prepare the suspension in this research. The ionic strength of the mixture was increased using a 5 M sodium chloride solution to dissolve the precipitate, followed by dialysis against 0.7 M sodium chloride solution to make the suspension.

DNA-poly(Lys, Tyr) suspensions were prepared by mixing 1:2 mole ratio of DNA/amino acid residues (Lys, Tyr) in a 5 M sodium chloride solution. This 1:2 mole ratio was selected

based on the work done by Santella *et al.*[150] They reported that the complex is completely soluble until the input ratio reaches 2 amino acids residues per DNA nucleotide and precipitation occurs. At this ratio there is one Lys and one Tyr per DNA nucleotide, so there is 1:1 charge ratio. Since the poly(Lys, Tyr) copolymer is not soluble in 5 M sodium chloride solution, it was first added to 5 M sodium chloride solution and formation of a suspension was observed. The DNA solution was then added to the suspension and the mixture was dialyzed against 10 mM phosphate buffer solution. The idea was that as sodium chloride diffuses out of the dialysis membrane, the copolymer will become soluble and will bind to DNA to form the DNA-poly(Lys, Tyr) suspension.

DNA-spermine, DNA-protamine, DNA-polyL, and DNA-poly(Lys, Tyr) suspensions were X-irradiated at doses from 0 Gy to 2.6 kGy. Following irradiation, samples used for the analysis of 5-MF and Fur were directly heated, without addition of spermine (since the polycations bound to DNA in these suspensions serve as catalysts of 5-MF and Fur release), while the samples used for the analysis of Lac were heat treated with appropriate amount of ethanolamine hydrochloride (see Chapter 2) to derivatize C4„-OAS into Lac. Ethanolamine hydrochloride was used as a derivatizing agent instead of glycine in these experiments since, unlike zwitterionic glycine, ethanolamine forms a positively charged ion in solution, so it binds DNA more efficiently than glycine and hence can more efficiently compete for DNA with a polycation complexed with DNA. The yield of Lac using ethanolamine as a derivatizing agent is similar to that observed with glycine[54], which made ethanolamine the reagent of choice for the derivatization of C4„-OAS to Lac for DNA-polycations suspensions. The resulting preparations were analyzed by HPLC. Representative chromatograms are shown in Figure 26.

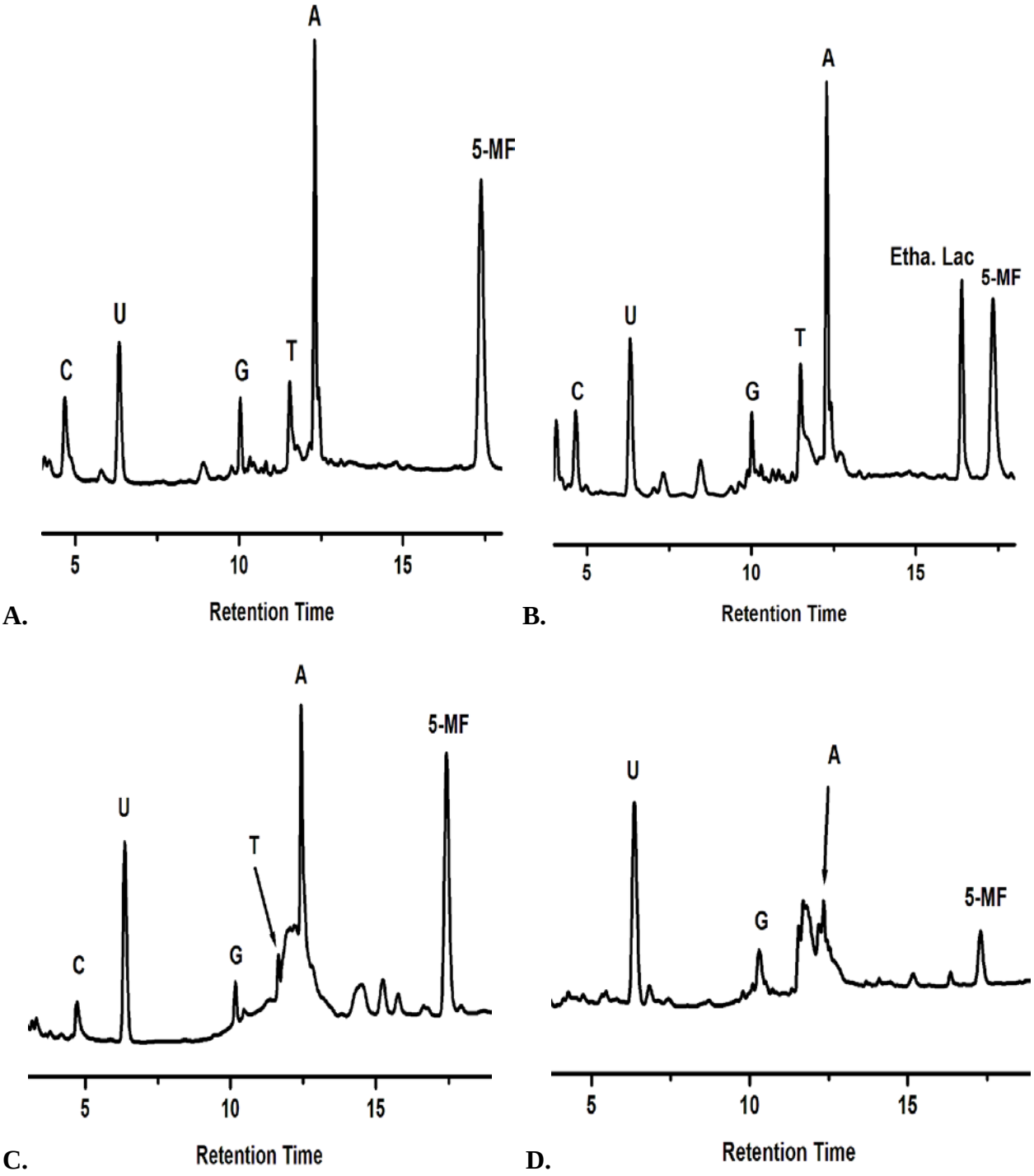

Figure 26: Representative HPLC chromatograms for DNA-spermine and DNA-poly(Lys, Tyr) suspensions. (A) DNA-spermine, (B) DNA-spermine ethanolamine, (C) DNA-poly(Lys, Tyr), and (D) DNA-poly(Lys, Tyr) ethanolamine. All heat treated after 3 min of X-irradiation.

Panels A and B in Figure 26 were obtained with DNA-spermine suspension. Chromatograms for DNA-protamine and DNA-polyLys suspensions look similar to those of DNA-spermine (not shown). The Lac formed from ethanolamine (EA Lac, Figure 26, panel B) elutes with retention time close to Fur.[54] Fur is completely absent in these samples of DNA-polycation suspensions as can be seen in chromatograms A and C, so that the EA Lac peak is not interfered by Fur. It is remarkable that Lac is completely absent in the sample of DNA-poly(Lys, Tyr) as can be observed in chromatogram D, so that 5-MF is the only SDP produced in DNA-poly(Lys, Tyr) suspensions. Release of free bases is also reduced in in DNA-poly(Lys, Tyr) suspensions.

Chromatographic peaks were integrated and the peak areas were converted into concentration using Equation 2.8. The average concentrations of individual SDP, total SDP, and FBR were plotted as a function of irradiation dose and the results are shown in Figure 27. For clarity purposes, the plots of total SDP and FBR are shown separately from those of individual SDP, with the exception of DNA-poly(Lys, Tyr), since 5-MF is the only SDP produced in this system.

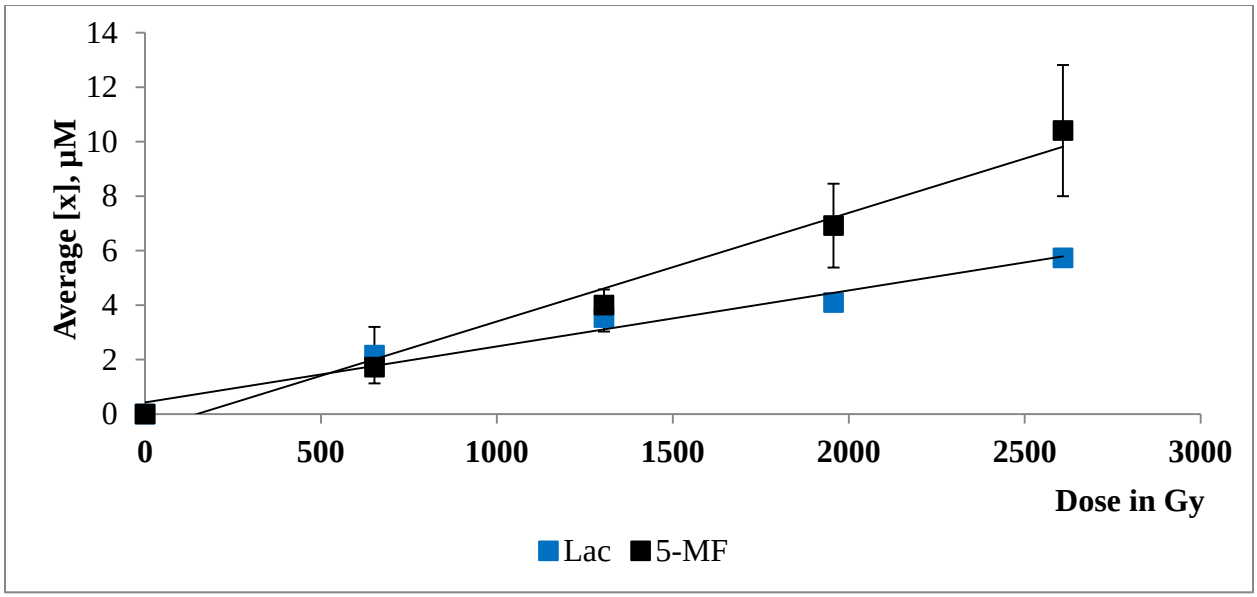

A.

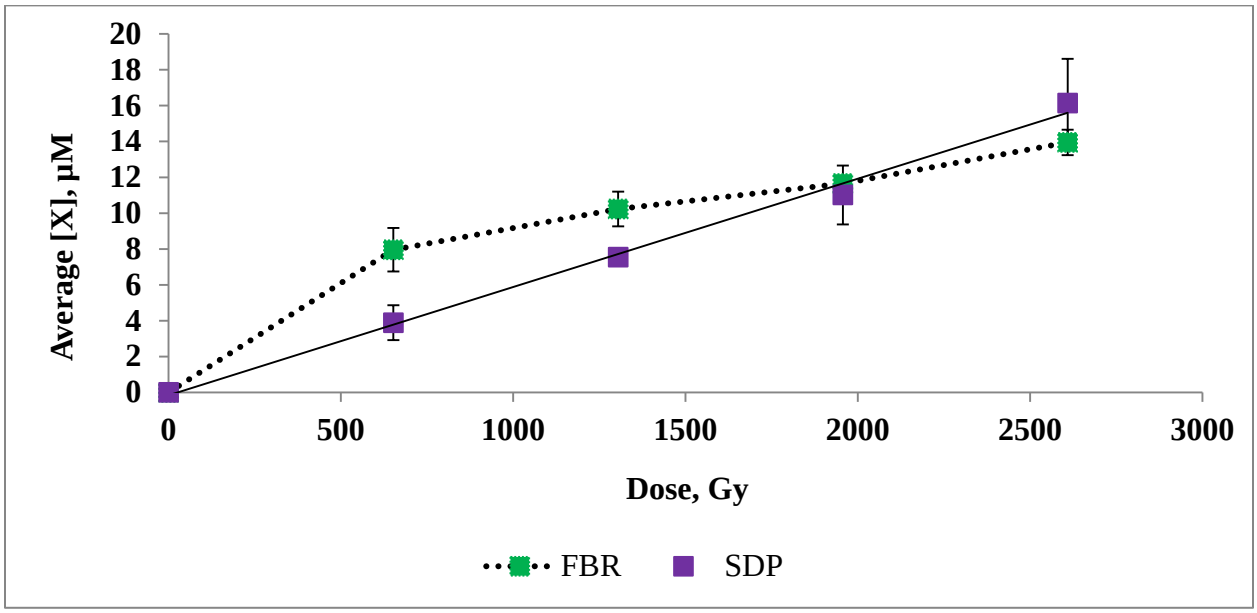

B.

Figure 27 (continued on the next page)

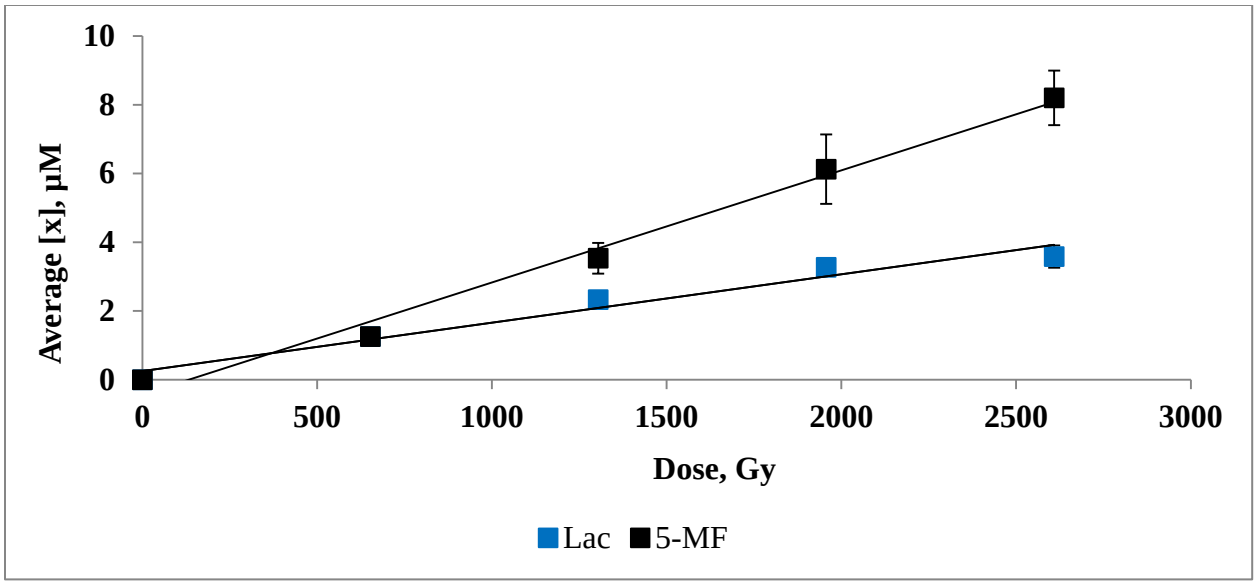

C.

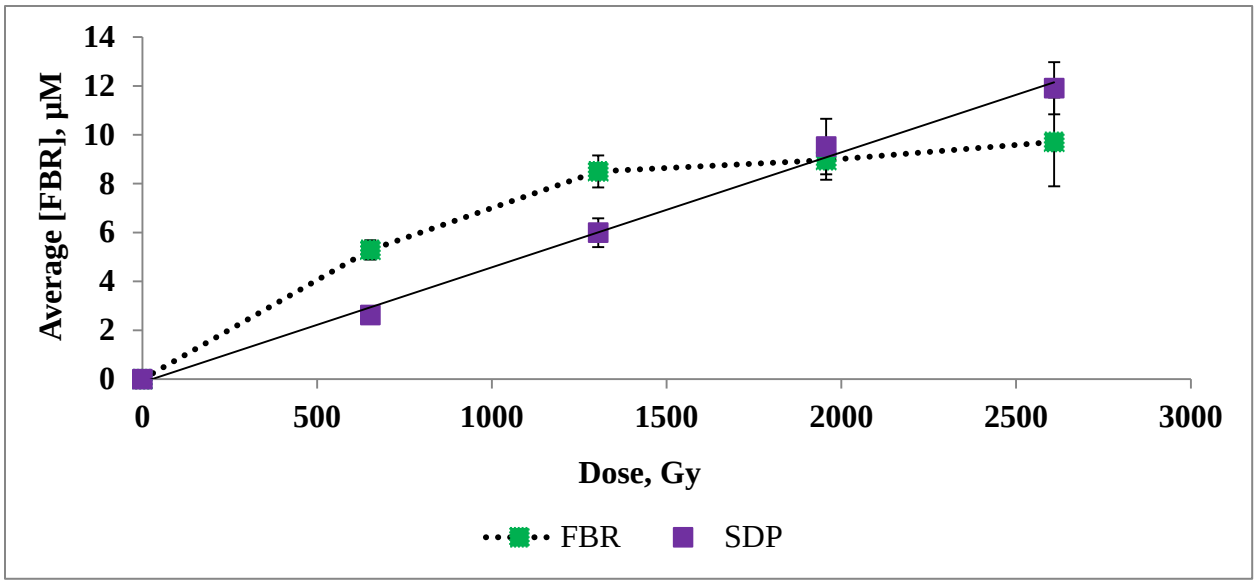

D.

Figure 27 (continued on the next page)

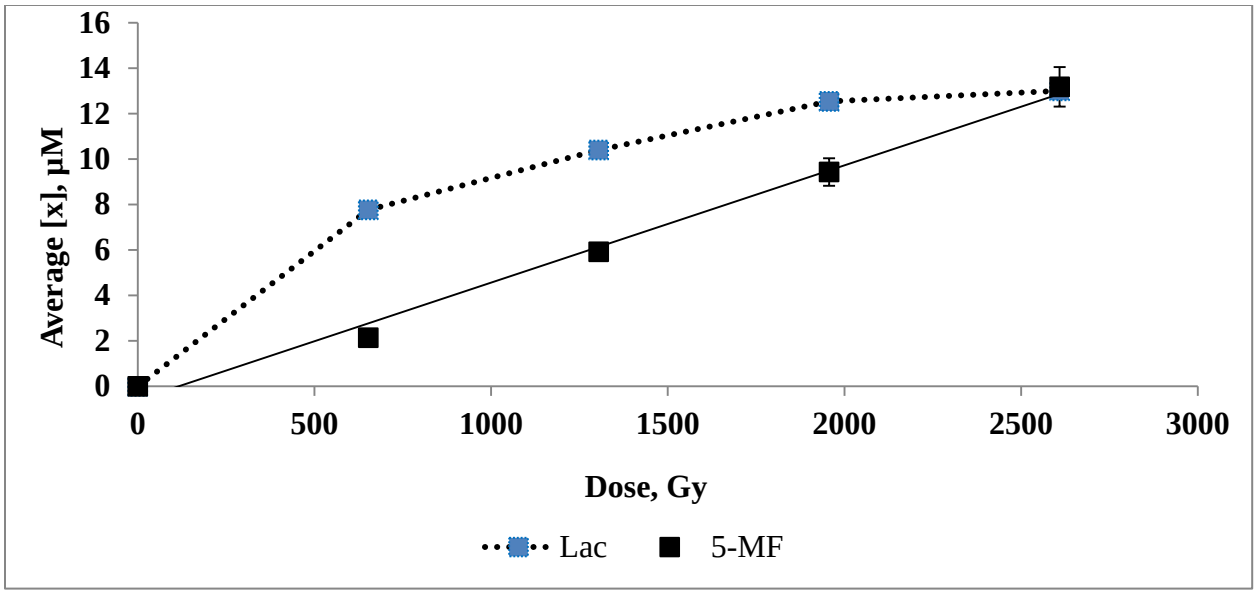

E.

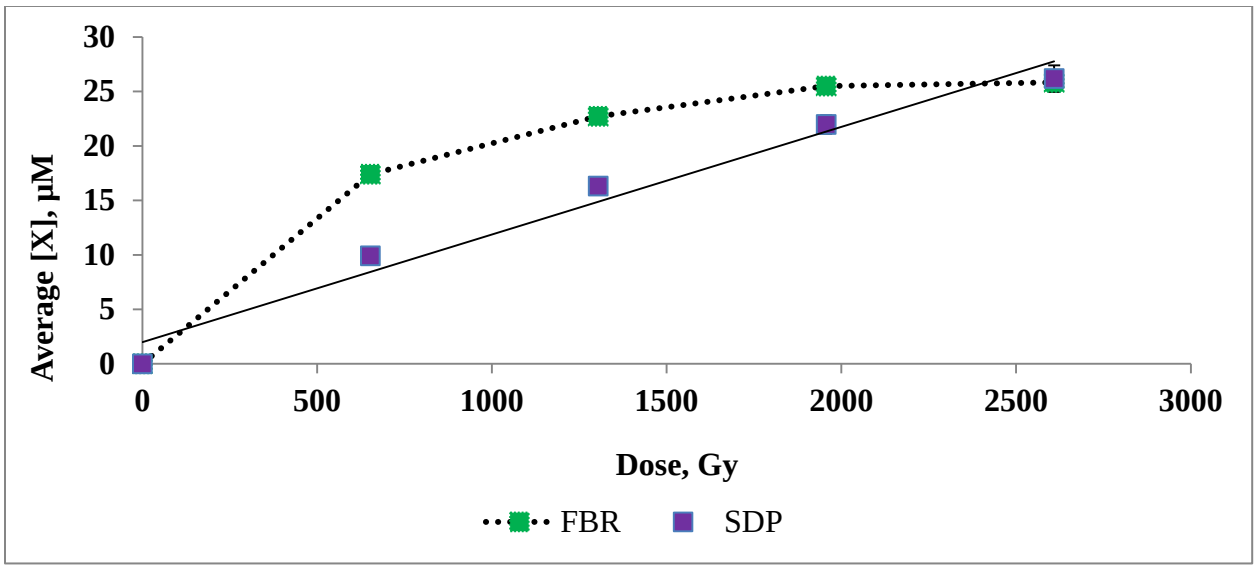

F.

Figure 27 (continued on the next page)

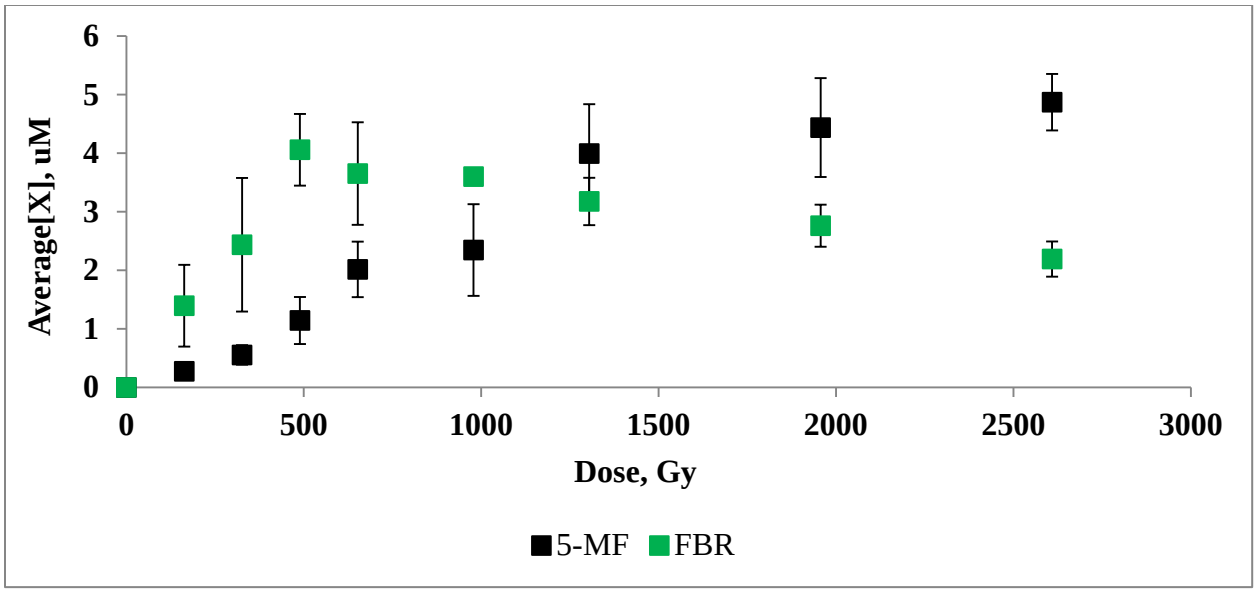

G.

Figure 27: Plots of average concentration of DNA damage products as a function of irradiation dose. Individual SDP for: (A) DNA-spermine suspension, (C) DNA-protamine suspension, and (E) DNA-polyLys suspension. Total SDP and FBR for: (B) DNA-spermine, (D) DNA-protamine, (F) DNA-polyLys, and (G) DNA-poly(Lys, Tyr).

It is noteworthy that FBR as a function of irradiation dose deviates from linearity for all DNA-polycation suspensions, as opposed to the linear dose dependence for DNA-polycation solutions. This nonlinearity likely indicates the occurrence of secondary side reactions with participation of the DNA free bases. The most straightforward explanation is that when free bases are released from DNA-polycation nanoparticles into the bulk, they act as scavengers of hydroxyl radicals, so that the effective concentration of free base in the solution is decreased. This phenomenon is not observed in homogeneous solutions of DNA, since in these solutions, DNA molecules efficiently compete for hydroxyl radicals. Table 8 summarizes the slopes of the

regression lines of individual SDP and total SDP and the percent contribution of each individual SDP to the total SDP for DNA-spermine, DNA-protamine, and DNA-polyLys.

Data for the samples of DNA-poly(Lys, Tyr) suspensions were not included in Table 8 because both 5-MF and FBR accumulate nonlinearly with dose. Lac also saturates in the sample of DNA-polyLys suspension, but the total SDP in this sample accumulates nearly linearly with irradiation dose. The slope of Lac was therefore estimated as the difference between the slope of total SDP and the slope of 5-MF. The resulting slope was used to evaluate a rough estimate of the percent contribution of Lac in this sample of DNA-polyLys suspension.

The percent contribution of each SDP to the total SDP for DNA (control), DNA-spermine, DNA-protamine, DNA-polyLys, and DNA-poly(Lys, Tyr) were plotted as column bars and the results are shown in Figure 28. Since it was not possible to prepare naked DNA suspensions, the results for DNA dilute solutions were used as a control in these experiments. Though the direct comparison of the absolute yields of SDP in these suspension samples with those observed with dilute solution of DNA is not possible, it is useful to compare relative contributions of individual SDP products.

Table 8: Slopes of the Regression Lines of Individual SDP and Total SDP and Percent Contributions of Individual SDP to the Total SDP for the DNA-Spermine, DNA-Protamine, and DNA-PolyLys Suspensions

	Slope (μM/Gy)				Percent contribution (%)		
DNA damage products	DNA dilute solution (control)	DNA-spermine	DNA-protamine	DNA-polyLys	DNA dilute solution (control)	DNA-spermine	DNA-protamine
Lac	2.9×10^{-2}	2.0×10^{-3}	1.4×10^{-3}	4.7×10^{-3} *	54.7	33.3	29.8
5-MF	1.4×10^{-2}	4×10^{-3}	3.3×10^{-3}	5.2×10^{-3}	26.4	66.7	70.2
Fur	1×10^{-2}	0	0	0	18.4	0	0
SDP	5.3×10^{-2}	6.0×10^{-3}	4.7×10^{-3}	9.9×10^{-3}	N/A	N/A	N/A

*Estimate of the percent contribution of Lac for the DNA-polyLys suspension based on the percent contribution of SDP.

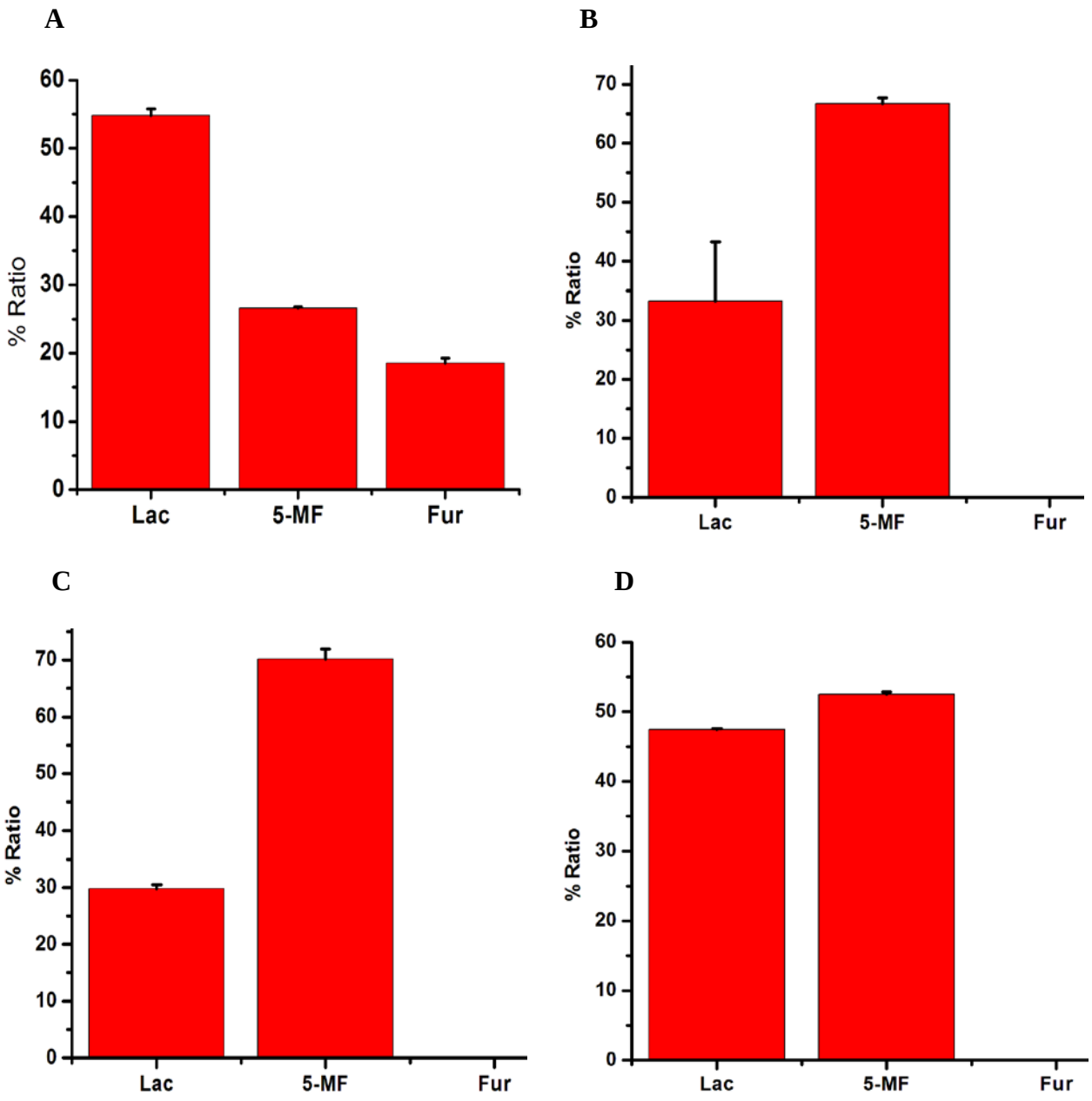

Figure 28 (continued on the next page)

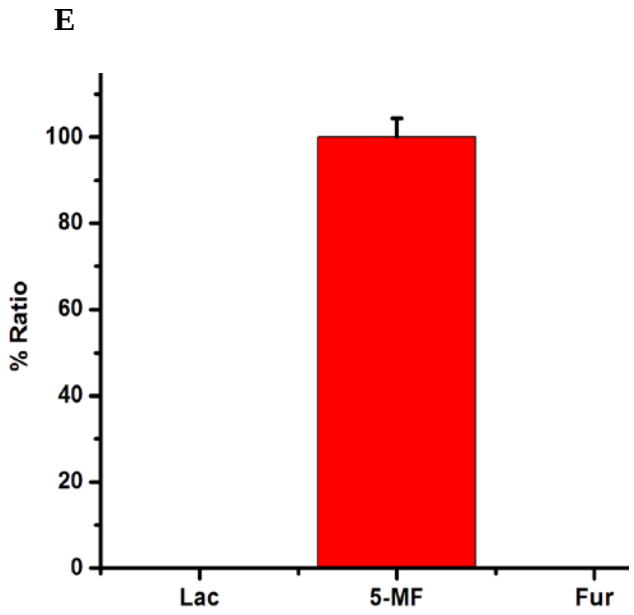

Figure 28: Bar plots of the percent contributions of individual SDP to the total SDP in (A) DNA dilute solution (control), (B) DNA-spermine suspension, (C) DNA-protamine suspension, (D) DNA-polyLys suspension, and (E) DNA-poly(Lys, Tyr) suspension

It is obvious from Figure 28 that there is a pronounced increase of the contribution of the C1„ pathway (based on the yields of 5-MF) on going from naked DNA (26.4 %) to DNA-polycation suspensions, with the growth of the percent contribution of the C1„ pathway in the order: DNA-polyLys (52.5%) < DNA-spermine (66.7 %) ~ DNA-protamine (70.2 %) < DNA-poly(Lys, Tyr) (100%). This growth of the role of the C1„ pathway is accompanied by the concomitant decrease of the role of the C4„ pathway (based on the yields of Lac). The percent contribution of the C5„ pathway (based on the yields of Fur) drops from 18.4% in naked DNA solution to practically 0% in all DNA-polycation suspensions. These results are in agreement with our general hypothesis that polycations tightly bound to DNA can repair DNA sugar radicals by hydrogen donation. C5„ radicals are the easiest to repair because of their surface accessibility and the highest energy of the C5„-H bond. This explains why production of Fur is

completely suppressed in DNA-polycation suspensions. C1„ radicals are the hardest to repair, because of their surface non-accessibility and the lowest energy of the C1„-H bond. So the percent contribution of the C1„ significantly increases in DNA-polycation suspensions. C4„ radicals are also sufficiently exposed and are relatively easy to repair thermodynamically, therefore the contribution of the C4„ pathway is decreased in DNA-polycation suspensions as compared to the C1„ pathway.

Lac and Fur were totally absent in the samples of DNA-poly(Lys, Tyr) suspensions (as shown in Figure 28, panel E), so 5-MF was the only SDP observed. The total disappearance of Lac in this case can be explained by the presence of an efficient hydrogen donor, tyrosine, in the polypeptide chain of poly(Lys, Tyr), so that the repair of C4„ and C5„ radicals is so efficient that the products of these two pathways become non-detectable by our HPLC analysis.

It was earlier predicted (in Chapter 1) that ±-hydrogens of peptide bond and possibly hydrogens from secondary C-H bonds of amino acid side chain in polypeptides or from secondary C-H bonds in spermine and putrescine can be used for the repair of DNA radical by polypeptides and polyamines. Donation of ±-hydrogens of peptide bonds is much more thermodynamically favorable than hydrogens of a secondary C-H bond. Polyamines do not have peptide bonds and hence lack easily abstractable ±-hydrogens of peptide bonds present in polypeptides. With this assumption, it is expected that, the relative yields of SDP in DNA-protamine and DNA-polyLys suspensions to be different from that observed with DNA-spermine suspensions. A more efficient repair of the C4„ radicals was expected in DNA-protamine and DNA-polyLys suspensions as compared to the DNA-spermine suspensions. The result of this more efficient repair would be a decrease in contribution of Lac than of 5-MF in DNA-polypeptide suspensions as compared to DNA-polyamine suspensions. However, this effect was

not observed when comparing the Lac-to-5-MF ratios in DNA-protamine and in DNA-spermine suspensions; they are approximately the same, though the data for DNA-spermine suspensions show a significant error bar (Figure 28 B), which makes these experimental data less reliable.

PolyLys and protamine, two similar peptides, do not show similar Lac-to-5-MF ratios as expected. PolyLys shows a lower efficiency in repair of C4„ radicals as compared to protamine (compare panels C and D in Figure 28). However, interpretation of results for DNA-polyLys suspensions is complicated by the nonlinear dose response of Lac (Figure 27 E). It is not clear why the accumulation of Lac is not linear for DNA-polyLys suspensions and why the results for DNA-protamine and DNA-polyLys suspensions are so different if one visualizes protamine and polyLys as polypeptide chains in which most of side chains (or all of them as in polyLys) are positively charged. However, one should consider differences between polyLys and protamine. Protamine is a polypeptide containing 89.8% of arginine, which has positively charged guanidinium groups[142] while polyLys has positively charged amine groups, $-NH_3^+$. It has been reported that the presence of neutral groups in protamine reduces the binding affinity of arginines residues to DNA as compared to polyarginine (polyArg).[151] PolyArg is such a stronger DNA binder that our attempts to make suspensions of DNA-polyArg were not successful: DNA-polyArg complex has a strong tendency to aggregate and to precipitate. PolyLys is a stronger DNA binder than protamine. It is possible that strong electrostatic interaction of $-NH_3^+$ of polyLys with the negatively charged phosphodiester group of DNA positions the polyLys side chain closer to DNA deoxyribose, which facilitates DNA sugar radical repair by hydrogen transfer from C-H groups of side chain and reduces the accessiblity of the ±-hydrogens of the peptide bond to DNA sugar radicals. Also, it cannot be excluded that a stronger interaction of

polyLys with DNA than protamine results in formation of larger particles of DNA-polyLys complexes and that these morphological changes affect the relative yields of DNA SDP .

In summary, the variation in the SDP on going from naked DNA to DNA-putrescine concentrated solution, DNA-spermine, DNA-protamine, DNA-polyLys, and DNA-poly(Lys, Tyr) is a good indication that hydrogen transfer may play a part in DNA repair processes in biological system.

CHAPTER 4

CONCLUSIONS

Histones and non-histone proteins, protamine, biogenic polyamines, and synthetic positively charged polypeptides have long been shown to protect DNA from hydroxyl radical-induced damage both *in vivo* and *in vitro.*[106-108] Understanding the mechanism of DNA protection by these DNA binders can greatly help in advancing preventive and treatment methods for diseases related to the accumulation of DNA damages. Mechanisms of DNA protection by DNA-binding polycations proposed in the literature include scavenging of hydroxyl radicals, DNA compaction and aggregation (PICA effect), and repair of DNA holes by electron transfer. Although a significant bulk of information exists in support of the first three mechanisms, until now there was no experimental evidence supporting one more plausible mechanism: repair of DNA free radicals by hydrogen donation from polycations. The aim of the present work was to obtain experimental evidences of this hydrogen transfer mechanism by HPLC-based analysis of relative ratios of DNA sugar damage products. Data presented in Chapter 3 led to the following conclusions:

1. The overall decrease in the yields of total SDP and FBR on going from naked DNA dilute solutions to DNA-putrescine dilute solutions was observed, though the relative ratios of individual products of DNA sugar damage remained unchanged. This indicates an insignificant, if any, contribution of the hydrogen transfer process in DNA radioprotection in these systems. Radioprotection of DNA by putrescine was attributed to scavenging of hydroxyl radicals by putrescine as the major mechanism, in agreement

with the observation of Newton *et al*.[114] This correlates with the low binding constant of putrescine to DNA.

2. In a search for an optimized method of preparing DNA-polycation complexes, concentrated solutions of DNA and DNA-putrescine were prepared by hydration of dry films. For the first time a shift in relative contributions of pathways of DNA sugar damage was observed for DNA-putrescine concentrated solutions, with the significant increase in the role of the C1„ pathway (from 26.3 % in naked DNA to 44.9 % in DNA-putrescine complexes). This increase may be attributed to preferential repair of more surface exposed C4„ and C5„ radicals by hydrogen donation from C-H bonds in putrescine as compared to much less surface accessible C1„ radicals. Aggregation of DNA molecules in concentrated solutions of naked DNA, even in the absence of putrescine, results in modification of the relative contributions of the pathways of DNA sugar damage as compared to dilute naked DNA solutions, with a decrease in the contribution of the C5„ pathway (from 18.9% in DNA dilute solutions to 5.30 % in DNA concentrated solutions) at the expense of the increase in the contribution of the C4„ pathway (from 54.7 % in DNA dilute solutions to 68.4 % in DNA concentrated solutions). This might be explained by the occurrence of the thermodynamically favorable process of intermolecular hydrogen transfer from a C4„ position of deoxyribose ring in one DNA molecule to the C5„ radical in the neighboring DNA molecule when DNA molecules are aggregated in concentrated solutions of naked DNA.
3. Nanoparticle suspensions of DNA-polycation complexes were prepared for the following polycations: protamine, spermine, polyLys, and poly(Lys, Tyr) using either dialysis with the gradual decrease of ionic strength of the solution or gradual dilution of DNA-

polycation mixtures. For all suspensions, significant modification of the relative contributions of the final products of DNA sugar damage was observed as compared to naked DNA, with the increase of the contribution of the C1„ pathway of DNA sugar in the order naked DNA (26.4%) < DNA-polyLys (52.5%) < DNA-spermine (66.7 %) < DNA-protamine (70.2 %) < DNA-poly(Lys, Tyr) (100%). This increase in the role of the C1„ pathway was accompanied by the concomitant decrease in the role of the C4„ pathway and complete disappearance of the C5„ pathway. For DNA-poly(Lys, Tyr) suspensions, even the C4„ pathway disappeared leaving the C1„ pathway as the only route of DNA sugar damage. These findings indicate that in DNA-polycation complexes there is significant protection of the surface-exposed C4„ and C5„ sites of DNA sugar, especially of the C5„ site, and the lack of protection of the C1„ sites hidden in the DNA minor groove. This protection is in agreement with the general hypothesis that DNA sugar radicals in complexes of DNA with polycations can be repaired by hydrogen transfer from polycations.

4. No correlation between the presence of easily abstractable alpha hydrogens in peptide bonds and the efficiency of repair of DNA sugar radicals was experimentally observed since spermine, a polyamine lacking peptide bonds, shows a level of protection of the C4„ comparable with polypeptides protamine and polyLys. However, it appears that the presence of an additional good hydrogen donor, the phenolic OH group in the tyrosine side chain of the poly(Lys, Tyr) copolymer, significantly facilitates repair of surface-accessible DNA sugar radicals, so that even the C4„ pathway is completely suppressed in DNA- poly(Lys, Tyr) suspensions.

To summarize, a significant modification of pathways of DNA sugar damage by hydroxyl radicals in complexes of DNA with polycations supports the hypothesis that hydrogen transfer from polycations to DNA may play a significant role in the DNA protection mechanism in biological systems.

REFERENCES

1. Cadet, J. D.; Pouget, J. P.; Ravanat, J. L.; Sauvaigo, S. *Curr. Prob. Dermatol.*, **2001**, *29*, 62-73.

2. Cook, J. A.; Gius, D.; Wink, D. A.; Krishna, M. C.; Russo, A.; Mitchell, J. B. *Semin. Radiat. Oncol.*, **2004**, *14*, 259-266.

3. Schmidt-Ullrich, R. K.; Dent, P.; Grant, S.; Mikkelsen, R. B.; Valerie, K. *Radiat. Res.*, **2000**, *153*, 245-257.

4. Valko, M. M. H.; Cronin, M. T. D. *Curr. Med. Chem*, **2005**, *12*, 1161-1208.

5. Shirley, R. O.; Work, L. *Antioxidants*, **2014**, *3*, 472-501.

6. Toyokuni, S. O. K.; Yodoi, J.; Hiai, H. *FEBS Lett*, **1995**, *358*, 1-3.

7. Xing, S. S.; Chen, C.; Wang, J.; Yu, Z. *Mol. Med. Rep*, **2014**, *10*, 599-604.

8. Toyokuni, S. O.; Yodoi, J.; Hiai, H. *FEBS Lett*, **1995**, *358*, 1-3.

9. Shirley, R. O.; Work, L. *Antioxidants*, **2014**, *3*, 472-501.

10. Aoshiba, K. Z.; Tsuji, T.; Nagai, A. *Eur. Respir. J.*, **2012**, *39*, 1368-1376.

11. Ishii, T.; Yasuda, K.; Akatsuka, A.; Hino, O.; Hartman, P. S.; Ishii, N. *Cancer Res*, **2005**, *65*, 203-209.

12. von Sonntag, C. *The Chemical Basis of Radiation Biology*; Taylor & Francis, London-New York-Philadelphia, **1987**.

13. Tao, N. J.; Lindsay, S. M.; Rupprecht, A. *Biopolymers*, **1989**, *28*, 1019-1030.

14. La Vere, T.; Becker, D.; Sevilla, M. D. *Radiat. Res.*, **1996**, *145*, 673.

15. Roginskaya, M.; Bernhard, W.; Razskazovskiy, Y. *Radiat. Res.*, **2006**, *166*, 9-18.

16. Wardman, P. *J. Phys. Chem.*, **1989**, *18*, 1637-1755.

17. von Sonntag, C. New York: Springer-Verlag Berlin Heidelberg, **2010**.

18. Motohashi, N.; Saito, Y. *Chem. Pharm. Bull.*, **1993**, *41*, 1842-1845.

19. Xu, Y. J.; Kim, E. Y.; Demple, B. *J. Biol. Chem.*, **1998**, *273*, 28837-28844.

20. Steenken, S.; Jovanovic, S. V. *J. Am. Chem. Soc.*, **1997**, *119*, 617.

21. Fukuzumi, K.; Miyao, H.; Ohkubo, K.; Suenobu, T. *J. Phys. Chem.*, **2005**, *109*, 3285-3294.

22. Reynisson, J.; Steenken, S. *Phys. Chem.*, **2002**, *4*, 5346-5352.

23. Steenken, S. *Free Radic. Res. Commun.*, **1992**, *16*, 349-379.

24. Close, D. M. *J. Phys. Chem.*, **2013**, *117*, 473-480.

25. Shafirovich, V. D.; Huang, W.; Geacintov, N. E. *J. Biol. Chem.*, **2001**, *276*, 24261-24626.

26. Wang, W. R.; Sevilla, M. D. *Int. J. Radiat. Biol.*, **1997**, *71*, 387-399.

27. Cai, Z.; Sevilla, M. D. *Radiat. Res.*, **2003**, *159*, 411-419.

28. Saito, I. N.; Nakatani, K.; Yoshioka, Y.; Yamaguchi, K.; Sugiyama, H. *J. Am. Chem. Soc.*, **1998**, *120*, 12686-12687.

29. Cadet, J.; Douki, T.; Gasparutto, D.; J-L., R. *Mutat. Res.*, **2003**, 531.

30. Douki, T. M.; Ravanat, J.-L.; Turesky, R. J.; Cadet, J. *Carcinogenesis*, **1997**, *18*, 2385-2391.

31. Burrows, C. J.; Muller, J. G. *Chem. Rev.*, **1998**, *98*, 1109-1151.

32. Cullis, P. M.; Malone, M. E.; Merson-Davies, L. A. *J. Am. Chem. Soc.*, **1996**, *118*, 2775-2781.

33. Doddridge, A. Z.; Cullis, P. M.; Jones, G. D. D.; Malone, M. E. *J. Am. Chem. Soc.*, **1998**, *120*, 10998-10999.

34. Asami, S. H.; Yamaguchi, R.; Tomioka, Y.; Itoh, H.; Kasai, H. *Cancer Res.*, **1996**, *56*, 2546-2549.

35. Kiyosawa, H. S.; Okudiara, H.; Murata , K.; Miyamoto, T.; Chung, M. H.; Kasai, H.; Nishimura, S. *Free Radic. Res. Commun.*, **1990**, *11*, 23-27.

36. Jackson, J. H.; Schraufstatter, I. U.; Hyslop, P. A.; Vosbeck, K.; Sauerheber, R.; Weitzman, S. A.; Cochrane, C. G. *J. Clin. Invest.*, **1987**, *80*, 1090-1095.

37. Chen, Q. M.; Ames, B.; Mossman, B. *Carcinogenesis*, **1996**, *17*, 2525-2527.

38. Valavandis, A.; Vlachogianni, T. *J. Environ. Sci. Health., Part C.*, **2009**, *27*, 120-139.

39. Pope III, C. A.; Burnett, R. T.; Thun, M. J.; Calle, E. E.; Krewski, D.; Ito, K.; Thurston, G. D. *JAMA-J. Am. Med. Assoc.*, **2002**, *287*, 1132-1141.

40. Kasprzak, K. S. *Free Radic. Biol. Med.*, **2002**, *32*, 958-967.

41. Marczynski, B. P.; Mensing, T.; Angerer, J.; Seidel, A.; El Mourabit, A.; Wilhem, M.; Bruning, T. *Int. Arch. Occup. Environ. Health*, **2005**, *78*, 97-108.

42. Marczynski, B.; Rihs, H.-P.; Rossbach, B.; Holzer, J.; Angerer, J.; Scherenberg, M.; Hoffman, G.; Bruning, T.; Wilhelm, M. *Carcinogenesis*, **2002**, *23*, 273-281.

43. Toraason, M.; Hayden, C.; Marlow, D.; Rinehart, R.; Mathias, P.; Werren, D.; Olsen, L. D.; Neumeister, C. E.; Mathews, E. S.; Cheever, K. L.; Marlow, K. L.; Debord, D. G.; Reid, T. M. *Int. Arch. Occup. Environ. Health*, **2001**, *74*, 396-404.

44. Steenken, S.; Jovanovic, S. V.; Bietti, M.; Bernhard, K., *J. Am. Chem. Soc.*, **2000**, *112*, 2373-2374.

45. Delaney, S.; Neeley, W. L.; Delaney, J. C.; Essigmann, J. M. *Biochemistry*, **2007**, ***46***, 1448-1455.

46. Rokhlenko, Y.; Geacintov, N. E.; Shafirovich, V. *J. Am. Chem. Soc.*, **2012**, *134*, 4955-4962.

47. Sheu, C. F.; Foote, C. S. *J. Am. Chem. Soc.*, **1995**, *117*, 474-477.

48. Sheu, C. F.; Foote, C. S. *J. Am. Chem. Soc.*, **1995**, *117*, 6439-6442.

49. Pogozelski, W. K.; Tullius, T. D. *Chem. Rev.*, **1998**, *98*, 1089-1107.

50. Colson, A.-O.; Sevilla, M. D. *J Phys. Chem*, **1995**, *99*, 3867-74.

51. Price, C. S.; Razskazovskiy, Y.; Bernhard, W.A. *Radiat. Res.*, **2010**, *174*, 645-649.

52. Roginskaya, M.; Razskazovskiy, Y.; Bernhard, W. A. *Angew. Chem. Int. Ed. (English)*, **2005**, *44*, 6210-6213.

53. Roginskaya, M.; Bernhard, W. A.; Marion, R. T.; Razskazovskiy, Y. *Radiat. Res.*, **2005**, *163*, 85-89.

54. Roginskaya, M.; Mohseni, R.; Moore, T. J.; Bernhard, W. A.; Razskazovskiy, Y. *Radiat. Res.*, **2014**, *181*, 131-137.

55. Roginskaya, M., Ph. D. Dissertation, University of Rochester: Rochester, NY, **2006**, pp 231.

56. Miaskiewicz, K.; Osman, R. *J. Am. Chem. Soc.*, **1994**, *116*, 232-238.

57. von Sonntag, C.; Hagen, U.; Schon-Bopp, A.; Schulte-Frohlinde, D. *Adv. in Rad. Biol.*, **1981**, *9*, 109-142.

58. Stelter, L.; von Sonntag, C.; Schulte-Frohlinde, D. *Int. J. Radiat. Biol.*, **1974**, *25*, 515.

59. Behrens, G.; Koltzenburg, G.; Ritler, A. *Int. J. Radiat. Biol.*, **1978**, *33*, 163.

60. Giese, B.; Burger, J.; Kang, T. W.; Kesselheim, C.; Wittmer, T. *J. Am. Chem. Soc.*, **1992**, 114.

61. von Sonntag, C., *The Chemical Basis of Radiation Biology*; Taylor & Francis: London–New York–Philadelphia,, **1987**.

62. Balasubramanian, B.; Pogozelski, W. K.; Tullius, T. D. *Proc. Natl. Acad. Sci. U.S.A.*, **1998**, *95(17)*, 9738-43.

63. Dizdaroglu, M.; von Sonntag, C.; Schulte-Frohlinde, D. *J. Am. Chem. Soc.*, **1975**, *97*, 2277-2228.

64. Dizdaroglu, M.; von Sonntag, C.; Schulte-Frohlinde, D. Z. *Naturforsch C*, **1975**, *30*, 826-828.

65. Wu, J. C.; Kozarich, J. W.; Stubbe, J. *J. Biol. Chem.*, **1983**, *258*, 4694-7.

66. Wu, J. C.; Kozarich, J. W.; Stubbe, J. *Biochemistry*, **1985**, *24*, 7562-8.

67. Wu, J. C.; Stubbe, J.; Kozarich, J. W. *Biochemistry*, **1985**, *24*, 7569-73.

68. Sugiyama, H.; Xu, C.; Murugesan, N.; Hecht, S. M. *J. Am. Chem. Soc.*, **1985**, *107*, 4104-5.

69. Rabow, L. E.; Stubbe, J.; Kozarich, J. W.; Gerlt, J. A. *J. Am. Chem. Soc.*, **1986**, *108*, 7130-1.

70. Sugiyama, H.; Xu, C.; Murugesan, N.; Hecht, S. M. *Biochemistry*, **1988**, *27*, 58-67.

71. Rabow, L. E.; Stubbe, J.; Kozarich, J. W. *J. Am. Chem. Soc.*, **1990**, *112*, 3196-203.

72. Regulus, P. D.; Bayle, P. A.; Favier, A.; Cadet, J.; Ravanat, J. L. *Proc. Natl. Acad. Sci. U.S.A.*, **2007**, *104*, 14037-14037.

73. Sczepanski, J. T.; Jacobs, A. C.; Majumdar, A.; Greenberg, M. M. *J. Am. Chem. Soc.*, **2009**, 131.

74. Sczepanski, J. T.; Hiemstra, C. N.; Greenberg, M. M. *Bioorg. Med. Chem.*, **2011**, 19.

75. Greenberg, M. M.; Weledji, Y. N.; Kim, J.; Bales, B. C. *Biochemistry*, **2004**, *43*, 8178-8183.

76. Jacobs, A. C.; Kreller, C. R. *Biochemistry*, **2011**, *50*, 136-143.

77. Dhar, S.; Kodama, T.; Greenberg, M. M. *J. Am. Chem. Soc.*, **2007**,*129*, 8702-8703.

78. Chen, B.; Zhou, X.; Taghizadeh, K.; Chen, J.; Strubbe, J. A.; Dedon, P. C. *Chem. Res.Toxicol.*, **2007**, *20*, 1701-1708.

79. Aso, M.; Kondo, M.; Suemune, H.; Hecht, S. M. *J. Am. Chem. Soc.*, **1999**, *121*, 9023-9033.

80. Aso, M.; Usui, K.; Fukuda, M.; Kakihara, Y.; Goromaru, T.; Suemune, H. *Org. Lett.*, **2006**, *8*, 3183-3186.

81. Usui, K.; Aso, M.; Fukuda, M.; Suemune, H. *J. Org. Chem.*, **2008**, *73*, 241-248.

82. Scheffold, R.; Dubs, P. *Helv. Chim. Acta*, **1967**, *50*, 798-808.

83. Daban, J. R. *Biochem. Cell. Biol.*, **2003**, *81*, 91-99.

84. Davey, C.A.; Sargent, D. F.; Luger, K.; Maeder, A. W.; Richmond,T. J. *J. Mol. Biol.*, **2002**, *319*, 1097–1113.

85. Widom, J. *Annu. Rev. Biophys. Biomol. Struct.*, **1998**, *27*, 285–327.

86. Wolffe, A. P. *Academic Press*, Inc., San Diego., **1992**.

87. Jeanne Kelly, Aardvark Design, and the National Cancer Institute, Obtained from: http://home.ccr.cancer.gov/connections/**2013**/Vol7_No1/news_7.asp (May 15- 2015). By permission.

88. Lewis, J. D.; Song, Y.; de Jong, M. E.; Bagha, S. M.; Ausio, J. *Chromosoma*, **2003**, *111*, 473–482.

89. Ward, W. S. *Mol. Hum. Reprod.*, **2010**, *16*, 30-6.

90. Hud, N. V.; Downing, K. H.; Balhorn, R. *Proc. Natl. Acad. Sci.*, U S A, **1995**, *92*, 3581–3585.

91. Adenot, P. G.; Mercier, Y.; Renard, J. P.; Thompson, E. M. *Development*, **1997**, *124*, 4615–4625.

92. Churikov, D. S.; Svetlova, M.; Zhang, K.; Gineitis, A.; Morton; Bradbury, E.; Zalensky, A. *Genomics*, **2004**, *84*, 745–756.

93. Gineitis, A. A.; Zalenskaya, I. A.; Yau, P. M.; Bradbury, E. M.; Zalensky, A. O. *J. Cell. Biol.*, **2000**, *151*, 1591–1598.

94. Hammoud, S. S.; Nix, D. A.; Zhang, H.; Purwar, J.; Carrell, D. T.; Cairns, B. R. *Nature*, **2009**, *460*, 473–478.

95. Pittoggi, C.; Renzi, L.; Zaccagnini, G.; Cimini, D.; Degrassi, F.; Giordano, R.; Magnano, A. R.; Lorenzini, R.; Lavia, P.; Spadafora, C. *J. Cell Sci*., **1999**, *112*, 3537–3548.

96. Martins, R. P.; Ostermeier, G. C.; Krawetz, S. A. *J. Biol. Chem*., **2004**, *279*, 51862–51868.

97. Nadel, B.; de Lara, J.; Finkernagel, S. W.; Ward, W. S. *Biol. Reprod*., **1995**, *53*, 1222–1228.

98. Singh, A.; Agarwal, A. *The Open Reproductive Science Journal*, **2011**, *3*, 65-71; this is an open access article licensed under the terms of the Creative Commons Attribution Non-Commercial License (http://creativecommons.org/licenses/by-nc/3.0/), which permits unrestricted, non-commercial use, distribution and reproduction in any medium, provided the work is properly cited.

99. Sarhan, S.; Seiler, N. *Biol. Chem. Hoppe. Seyler*, **1989**, *370*, 1279-1284.

100. Gerner, E. W.; Meyskens, F. L. *Nat. Rev. Cancer*, **2004**, *4*, 781-792.

101. Saminathan, M.; Thomas, T.; Shirahata, A.; Pillai, C. K.; Thomas, T. *J. Nucleic Acids Res.*, **2002**, *30*, 3722-3731.

102. Tabor, C. W.; Tabor, H. *Annu. Rev. Biochem*, **1984**, *53***,** 749-790.

103. Dittmann, K. H.; Mayer, C.; Rodemann, H. P. *Curr. Med. Chem. Anti-Canc. Agents*, **2003**, *3*, 360-363.

104. Ljungman, M.; Hanawalt, P. C. *Mol. Carcinog.*, **1992**, *5*, 264-269.

105. Chiu, S.; Oleinick, N. L. *Radiat. Res.*, **1997**, *148*, 188-192.

106. Ljungman, M. *Radiat. Res.*, **1991**, *126*, 58-64.

107. Elia, M. C.; Bradley, M. O. *Cancer Res.*, **1992**, *52*, 1580-1586.

108. Xue, L.-Y.; Friedman, L. R.; Oleinick, N. L.; Chiu, S-M. *Int. J. Radiat. Biol.*, **1994**, *66*, 11-21.

109. Newton, G. L.; Tran NQ, A. L; Ward, J. F.; Milligan, J. R., *Int. J. Radiat. Biol.*, **2004**, *80*, 643-651.

110. Newton, G. L.; Aguilera, J. A.; Ward, J. F.; Fahey, R. C. *Radiat. Res.*, **1997**, *148*(3), 272-284.

111. Warters, R. L.; Newton, G. L.; Olive, P. L.; Fahey, R. C. *Radiat. Res.*, **1999**, *151*, 354-362.

112. Chiu, S.; Oleinick, N. L. *Radiat. Res.*, **1998**, *149*, 543-549.

113. Spotheim-Maurizot, M.; Ruiz, S.; Sabattier, R.; Charlier, M. *Int. J. Radiat. Biol.*, **1995**, *68*, 571-577.

114. Newton, G. L.; Aguilera, J. A.; Ward, J. F.; Fahey, R. C. *Radiat. Res*., **1996**, *145*(6), 776-780.

115. Evans, M. D.; Dizdaroglu, M.; Cooke, M. S. *Mutat. Res*., **2004**, *567*, 1-61.

116. Newton, G. L.; Aguilera, J. A.; Ward, J. F.; Fahey, R. C. *Radiat. Res*., **1996**, *145*(6), 776-780.

117. Spotheim-Maurizot, M.; Ruiz, S.; Sabattier, R.; Charlier, M. *Int. J. Radiat. Biol*., **1995**, *68*(5), 571-7.

118. Manning, G. S. *Quar. Rev. Biophys*., **1978**, *11*, 179-246.

119. Gosule, L. C.; Schellman, J. A. *J. Mol. Biol*., **1978**, *121*, 311-326.

120. Chattoraj, D. K.; Gosule, L. C.; Schellman, J. A. *J. Mol. Biol*., **1978**, *121*, 327-337.

121. Porschke, D. *Biochemistry*, **1984**, *23*, 4821-4828.

122. Schuster, G. B. *Topics in Current Chemistry*, **2004**.

123. Silerme, S.; Bobyk, L.; Taverna-porro, M.; Cuier, C.; Saint-pierre, C.; Ravanat, J-L. *Chem. Res. Toxicol*., **2014**, *27*, 1011-1018.

124. Genereux, J. C.; Barton, J. K. *Chem. Rev*., **2010**, **110**, 1642-62.

125. Giese, B.; Amaudrut, J.; Kohler, A. K.; Spormann, M.; Wessely, S. *Nature*, **2001**, *412*, 318-320.

126. Genereux, J. C.; Boal, A. K.; Barton, J. K. *J. Am. Chem. Soc*., **2010**, *132*, 891-905.

127. Steenken, S.; Jovanovic, S. V. *J. Am. Chem. Soc*., **1997**, *119*, 617.

128. DeFelippis, M. R.; Murthy, C. P.; Broitman, F.; Weinraub, D.; Faraggi, M.; Klapper, M. H. *J. Phys. Chem*., **1991**, *95*, 3416.

129. Cullis, P. M.; Jones, G. D. D.; Symons, M. C. R. ; Lea, J. S. *Nature*, **1987**, *330*(6150), 773-774.

130. Milligan, J. R.; Aguilera, J. A.; Ly, A.; Tran, N. Q.; Hoang, O.; Ward, J. F. *Nucleic Acids Res*., **2003**, *31*, 6258-6263.

131. Pan, J.; Lin, W.; Wang, W.; Han, Z.; Lu, S.; Lin, N.; Zhu, D. *Biophys. Chem*., **2001**, *89*, 193-199.

132. Wagenknecht, H. A.; Stemp, E. D. A.; Barton, J. K. *Biochemistry*, **2000**, *39*, 5483-5491.

133. Wagenknecht, H. A.; Stemp, E. D. A.; Barton, J. K. *J. Am. Chem. Soc*., **2000**, *122*, 1-7.

134. Mayer-Enthart, E.; Kaden, P.; Wagenknecht, H.-A. *Biochemistry*, **2005**, *44*, 11749-11757.

135. Weiland, B.; Hüttermann, J. *Int. J. Radiat. Biol*., **2000**, *76*(8), 1075-1084.

136. Rauk, A.; Yu, D.; Taylor, J.; Shustov , G. V.; Block, D. A.; Armstrong, D. A. *Biochemistry*, **1999**, *38*, 9089-9096.

137. Miaskiewicz, K.; Osman, R. *J. Am. Chem. Soc*., **1994**, *116*, 232-238.

138. Berkowiwitz, J.; Ellison, G. B.; Gutman, D. *J. Phys. Chem*., **1994**, *98*, 2744-2765.

139. van Holde, K. E. *Chromatin; Springer-verlag New York*, **1988**.

140. Borges dos Santos, R. M.; Martinho Simões, J. A. *J. Phys. Chem*. Ref Data, **1998**, *27*, 707.

141. Greenling, J. R. *Fundamentals of Radiation Dosimetry*; 2nd ed.; Taylor & Francis Group: New York, **1985**.

142. Corfield, M. C.; Robson, A. *Wool Industries Research Association*, Torridon, Headingley, Leeds, **1953**, *55*, 517-522.

143. Braunlin, W. H.; Strick, A.; Record, M. T. *Biopolymers*, **1982**, *21*, 1301-1314.

144. Wyszko, E.; Barciszewska, M. Z.; Markiewicz, M. S.; Markiewicz, W. T.; Clark, F. C. B.; Barciszewski, J. *Biochimica et Biophysica*, **2003**, *1625*, 239-245.

145. Nayvelt, I.; Thomas, T.; Thomas, T. J. *Biomacromolecules*, **2007**, *8*, 477-484.

146. Gosule, L. C.; Schellman, J. A. *J. Mol. Biol*., **1978**, *121*, 311.

147. Widom, J.; Baldwin, R. L. *J. Mol. Biol*., **1980**, *144*, 431.

148. Thomas, T. J.; Bloomfield, V. A. *Biochemistry*, **1985**, *24*, 713.

149. Leng, M.; Gary, F. *Biochemistry*, **1966**, *56*, 1325-1332.

150. Santella, M. R.; Li, J. H. *Biopolymers*, **1974**, *13*, 1909-1926.

151. Wehling, K.; Arfmann, H.-A.; Standke, C. K.-H.; Wagner, G. K. *Nucleic Acids Res.*, **1975**, *2*, 799-807.

APPENDIX

COPYRIGHT RELEASE

Below is the copy right release for Figure 13: Structural features of DNA-histones and non-histones proteins complex; page 40.

Boersma, Brenda (NIH/NCI) [E] <**boersmab@mail.nih.gov**> Sep 30

to me

The image should be created to: Jeanne Kelly, Aardvark Designs, and the National Cancer Institute.

Thanks,
Brenda

Brenda Boersma-Maland, Ph.D.
Scientific Program Specialist
NCI/CCR/OD
31 Center Drive
Bldg 31 Room 3A11
Bethesda, MD 20892
Phone: (301) 402-5055
Fax: (301) 496-0775

VITA

MODESTE N'NECKEMDEM TEGOMOH

Education:	B.S. Chemistry, University of Buea, Buea, Cameroon, 2011 M.S. Chemistry, East Tennessee State University, Johnson City, Tennessee, 2015
Professional Experience:	Graduate Assistant, East Tennessee State University, College of Arts and Sciences, 2013-2014 Teaching Assistant, East Tennessee State University, College of Arts and Sciences, 2014-2015
Honors and Awards:	Golden Key International Honour Society Dean's List, 2014-2015